Federal University of Ceará
Department of Teleinformatics Engineering
Postgraduate Program in Teleinformatics Engineering

Spatial Interference Alignment under Realistic Scenarios

Master of Science Thesis

Author
Paulo Garcia Normando

Advisor
Prof. Dr. Yuri Carvalho Barbosa Silva

Co-Advisor
Prof. Dr. Walter Cruz Freitas Junior

Fortaleza – Ceará
August 2013

Universidade Federal do Ceará
Departamento de Engenharia de Teleinformática
Programa de Pós-graduação em Engenharia de Teleinformática

Alinhamento de Interferência Espacial em Cenários Realistas

Autor
Paulo Garcia Normando

Orientador
Prof. Dr. Yuri Carvalho Barbosa Silva

Co-orientador
Prof. Dr. Walter Cruz Freitas Junior

Dissertação apresentada à Coordenação do Programa de Pós-graduação em Engenharia de Teleinformática da Universidade Federal do Ceará como parte dos requisitos para obtenção do grau de ***Mestre em Engenharia de Teleinformática****. Área de concentração: Sinais e sistemas.*

Fortaleza – Ceará
Agosto 2013

This page was intentionally left blank

Abstract

Due to the rapid growth and the aggressive throughput requirements of current wireless networks, such as the 4th Generation (4G) cellular systems, the interference has become an issue that cannot be neglected anymore. In this context, the Interference Alignment (IA) arises as a promising technique that enables transmissions free of interference with high-spectral efficiency. However, while recent works have focused mainly on the theoretical gains that the technique could provide, this dissertation aims to go a step further and clarify some of the practical issues on the implementation of this technique in a cellular network, as well as compare it to other well-established techniques.

As an initial evaluation scenario, a 3-cell network was considered, for which several realistic factors were taken into account in order to perform different analyses. The first analysis was based on channel imperfections, for which the results showed that IA is more robust than Block Diagonalization (BD) regarding the Channel State Information (CSI) errors, but both are similarly affected by the correlation among transmit antennas. The impact of uncoordinated interference was also evaluated, by modeling this interference with different covariance matrices in order to mimic several scenarios. The results showed that modifications on the IA algorithms can boost their performance, with an advantage to the approach that suppresses one stream, when the Bit Error Rate (BER) is compared. To combine both factors, the temporal channel variations were taken into account. At these set of simulations, besides the presence of an external interference, the precoders were calculated using a delayed CSI, leading to results that corroborate with the previous analyses.

A recurring fact on the herein considered analyses was the dilemma of weather to apply the Joint Processing (JP)-based algorithms in order to achieve higher sum capacities or to send the information through a more reliable link by using IA. A reasonable step towards solving this dilemma is to actually perform the packet transmissions, which was accomplished by employing a system-level simulator composed by a large number of Transmission Points (TPs). As a result, all analyses conducted with this simulator showed that the IA technique can provide an intermediate performance between the non-cooperation and the full cooperation scheme.

Concluding, one of the main contributions of this work has been to show some scenarios/cases where the IA technique can be applied. For instance, when the CSI is not reliable it can be better to use IA than a JP-based scheme. Also, the modifications on the algorithms to take into account the external interference can boost their performance. Finally, the IA technique finds itself in-between the conventional transmissions and Coordinated Multi-Point (CoMP). IA achieves an intermediate performance, while requiring a certain degree of cooperation among the neighboring sectors, but demanding less infrastructure than the JP-based schemes.

Keywords: Interference alignment, wireless communications, multi-antenna systems.

Resumo

Devido ao rápido crescimento e os agressivos requisitos de vazão nas atuais redes sem fio, como os sistemas celulares de 4^a Geração, a interferência se tornou um problema que não pode mais ser negligenciado. Neste contexto, o Alinhamento de Interferência (IA) tem surgido como uma técnica promissora que possibilita transmissões livres de interferência com elevada eficiência espectral. No entanto, trabalhos recentes têm focado principalmente nos ganhos teóricos que esta técnica pode prover, enquanto esta dissertação visa dar um passo na direção de esclarecer alguns dos problemas práticos de implementação da técnica em redes celulares, bem como compará-la com outras técnicas bem estabelecidas.

Uma rede composta por três células foi escolhida como cenário inicial de avaliação, para o qual diversos fatores realistas foram considerados de modo a realizar diferentes análises. A primeira análise foi baseada em imperfeições de canal, cujos resultados mostraram que o IA é mais robusto aos erros de estimação de canal que o BD (do inglês, *Block Diagonalization*), enquanto as duas abordagens são igualmente afetadas pela correlação entre as antenas. O impacto de uma interferência externa não-coordenada, que foi modelada por diferentes matrizes de covariância de modo a emular vários cenários, também foi avaliado. Os resultados mostraram que as modificações feitas nos algoritmos de IA podem melhorar bastante seus desempenho, com uma vantagem para o algoritmo que suprime um único fluxo de dados, quando são comparadas as taxas de erro de bit alcançadas por cada um. Para combinar os fatores das análises anteriores, as variações temporais de canal foram consideradas. Neste conjunto de simulações, além da presença da interferência externa, os pré-codificadores são calculados através de medidas atrasadas de canal, levando a resultados que corroboraram com as análises anteriores.

Um fato recorrente percebido em todas as análises anteriores é o dilema entre aplicar os algoritmos baseados em BD, para que se consiga alcançar maiores capacidades, ou enviar a informação através de um enlace mais confiável utilizando o IA. Uma maneira de esclarecer este dilema é efetivamente realizar simulações a nível sistêmico, para isto foi aplicado um simulador sistêmico composto por um grande número de setores. Como resultado, todas as análises realizadas neste simulador mostraram que a técnica de IA atinge desempenhos intermediários entre a não cooperação e os algoritmos baseados na pré-codificação conjunta.

Uma das principais contribuições deste trabalho foi mostrar alguns cenários em que a técnica do IA pode ser aplicada. Por exemplo, quando as estimações dos canais não são tão confiáveis é melhor aplicar o IA do que os esquemas baseados no processamento conjunto. Também mostrou-se que as modificações nos algoritmos de IA, que levam em consideração a interferência externa, podem melhorar consideravelmente o desempenho dos algoritmos. Finalmente, o IA se mostrou uma técnica adequada para ser aplicada em cenários em que a interferência é alta e não é possível ter um alto grau de cooperação entre os setores vizinhos.

Palavras-chave: Alinhamento de interferência, comunicações sem fio e multi-antena.

Contents

Abstract i

Resumo ii

List of Figures v

List of Tables vii

List of Algorithms viii

Notation ix

---

1 Introduction 1

1.1 Motivation . . . 1
1.2 State-of-the-art . . . 2
1.3 Open problems . . . 4
1.4 Objectives and contributions . . . 6
1.5 Outline . . . 6

2 Interference Alignment 8

2.1 System Model . . . 8
2.2 Interference Alignment Concept . . . 9
2.2.1 Degree of Freedom . . . 9
2.2.2 Feasibility . . . 11
2.3 Interference Alignment Algorithms . . . 12
2.3.1 Closed-Form Solution . . . 12
2.3.2 Interference Alignment via Alternating Minimization . . . 13
2.3.3 IA-MMSE . . . 15
2.4 Block Diagonalization . . . 17
2.5 Simulation framework . . . 19

3 Channel Imperfection Analysis 21

3.1 Imperfection Models . . . 21
3.2 Channel Imperfection Results . . . 22

4 External Interference Analysis **30**
4.1 External Interference Model 30
4.2 Modification on Interference Alignment algorithms 31
4.2.1 Whitening Block Diagonalization (BD) 33
4.3 External Interference Analysis 34
4.3.1 Two antennas per node case 34
4.3.2 Four antennas per node case 39
4.4 Jakes model 45
4.4.1 Channel Variation Modeling 45
4.4.2 Simulation Results with Jakes Model 45

5 System Level Interference Alignment **50**
5.1 Simulation Scenario 50
5.1.1 Full Joint Processing 52
5.1.2 Conventional 52
5.1.3 Interference Alignment 52
5.1.4 Partial Joint Processing 53
5.2 Results and Analyses 53
5.3 Scheduler Analysis 57

6 Conclusions and Future Work **60**

Bibliography **63**

List of Figures

2.1 K-user MIMO Interference Channel. 9
2.2 3-user MIMO Interference Channel when Interference Alignment (IA) is applied. . 10
2.3 Basic simulation scenario composed by a 3-cell cluster. 19

3.1 Simulation scenarios of channel imperfection analysis. Cluster with 3 cells with one mobile at each cell. 22
3.2 Sum Capacity as a function of the SNR for different combinations of α and β. . . 24
3.3 BER as a function of the SNR for different combinations of α and β. 25
3.4 Impact of α parameter on the algorithms performance for SNR $= 15$ dB. 26
3.5 Impact of β parameter on the algorithms performance for SNR $= 15$ dB. 27
3.6 Impact of α parameter on the algorithms performance for SNR $= 0$ dB. 28
3.7 Impact of β parameter on the algorithms performance for SNR $= 0$ dB. 29

4.1 Receives inside the cluster perceiving an external interference, modeled as colored noise. 30
4.2 Simulation scenarios of external interference analysis. Cluster with 3 cells with one mobile at each cell. 34
4.3 Sum Capacity achieved by the algorithms versus External Interference level for different Signal to Noise Ratio (SNR) values at the border of the cell. 35
4.4 Sum Capacity versus SNR for different external interference values at the border of the cluster. At the left side, the results relate to the case in which users are distributed over all cells and at the right side, users are distributed respecting a distance of 2/3 of the cluster radius. 37
4.5 Bit Error Rate (BER) versus SNR for different external interference values at the border of the cluster. At the left side, the results relate to the case in which users are distributed over all cells and at the right side, users are distributed respecting a distance of 2/3 of the cluster radius. 38
4.6 Simulation with a Rank-1 external interference and nodes equipped with 4 antennas. The left side presents the Sum Capacity versus SNR while the right side presents the BER versus SNR, both for different external interference values at the border of the cluster. 41
4.7 Simulation with a Rank-2 external interference and nodes equipped with 4 antennas. The left side presents the Sum Capacity versus SNR while the right side presents the BER versus SNR, both for different external interference values at the border of the cluster. 42

4.8 Simulation with a Rank-4 external interference and nodes equipped with 4 antennas. The left side presents the Sum Capacity versus SNR while the right side presents the BER versus SNR, both for different external interference values at the border of the cluster. 43
4.9 Sum Capacity achieved by IA and BD algorithms as a function of the interference level at the border of the cluster, with the external interference modeled with covariance matrices of different ranks. 44
4.10 Comparison of Sum Capacity achieved by IA, BD with users placed closer to the edge of the cluster for different values of mobile speed. At the left side, the results concern the interference of 0 dBm at the cluster edge, while at the right side, the results are obtained considering 20 dBm of external interference. 48
4.11 Sum Capacity achieved by IA, BD with users placed closer to the edge of the cluster for different values of external interference. At the left side the external interference was modeled with a rank-1 covariance matrix, while at the right side it was modeled with rank-4 covariance matrix. Considering the outdated channel with the solid lines and updated with dashed lines. 49

5.1 Multicell scenario composed by seven CoMP-cells. 51
5.2 CoMP-cell with its subregions for a hypothetic combination: core and periphery. 53
5.3 CoMP-cell with its subregions core and periphery for three different combinations. 53
5.4 Average throughput of the User Equipments (UEs) when each algorithm is applied. 55
5.5 Average throughput of the core UEs when each algorithm is applied for different combinations of sectors performing the cooperation. 56
5.6 Average throughput of UEs when each algorithm is applied for different combinations of sectors performing the cooperation. 57
5.7 Average throughput achieved by users in the core of the Coordinated Multi-Point (CoMP) cell versus the load of the system for different schedulers and transmission schemes. 59

List of Tables

2.1 Simulation parameters of the 3-cell scenario 19

4.1 Jakes' channel parameters. 46

5.1 Simulation parameters of the multicell scenario. 51

List of Algorithms

2.1 Interference Alignment Closed-Form solution. 13
2.2 Interference Alignment via Alternating Minimization. 15
2.3 Interference Alignment with MMSE criterion. 17

Notation

Acronyms

3G	3rd Generation
3GPP	3rd Generation Partnership Project
4G	4th Generation
4-PSK	4-Phase Shift Keying
AWGN	Additive White Gaussian Noise
BD	Block Diagonalization
BER	Bit Error Rate
BS	Base Station
CoMP	Coordinated Multi-Point
CPU	Central Processing Unit
CSI	Channel State Information
DoF	Degree of Freedom
FDD	Frequency Division Duplexing
FDMA	Frequency Division Multiple Access
FJP	Full Joint Processing
IC	Interference Channel
JP	Joint Processing
IA	Interference Alignment
LAN	Local Area Network
LTE	Long Term Evolution
KKT	Karush-Kuhn-Tucker
MCS	Modulation and Coding Scheme
MIMO	Multiple Input Multiple Output
MIMO-IC	MIMO-Interference Channel
MIMO-X	MIMO-Cross Channel
MMSE	Minimum Mean Square Error
MSE	Mean Square Error
MRC	Maximal Ratio Combining
OFDMA	Orthogonal Frequency Division Multiple Access
PJP	Partial Joint Processing
PSK	Phase Shift Keying
PRB	Physical Resource Block
QAM	Quadrature Amplitude Modulation

QoS	Quality of Service
SCM	Spatial Channel Model
SER	Symbol Error Rate
SNR	Signal to Noise Ratio
SINR	Signal to Interference-plus-Noise Ratio
SISO-IC	SISO-Interference Channel
SVD	Singular Value Decomposition
TDMA	Time Division Multiple Access
TP	Transmission Point
TTI	Transmission Time Interval
UE	User Equipment
ZF	Zero-Forcing

Chapter 1

Introduction

1.1 Motivation

In the last decades the broadband services, bonded with multimedia applications, experienced a large growth and popularization. This increased the demand for very high data rates and Quality of Service (QoS). Associated to that, the people's need to be connected every time and everywhere also increased. One of the keys to satisfy this necessity is through the employment of wireless communications systems, especially via the cellular based networks, since they allow the users' mobility. In this context, these systems have undergone a fast expansion.

On another side, research on these communication networks has been focused on improving the transmission rates and creating systems with high spectral efficiency. Mainly guided by Shannon's publication [1], that calculates the achievable channel capacity through some parameters of the systems, such as the transmission power and bandwidth. This chase for increasing the systems rate was intensified in the last decades. A good example is that the incoming 4th Generation (4G) systems must at least double the cell-edge throughput over the previous 3rd Generation (3G) networks [2]. Thus, seeking the performance improvement, systems have changed their architecture, such as considering the Multiple Input Multiple Output (MIMO) approach.

However, a factor that has always limited the wireless communication systems performance is the interference. In these systems, all transmitters share the same medium to send the desired information to the receivers, which is an intrinsic wireless characteristic. Moreover, with the densification of these networks and the increasing demand for higher rates the importance of managing the interference has grown. Traditionally, the interference has been handled using basically three different approaches [3]:

i. Decoding the interference;

ii. Treating the interference as a noise;

iii. Interference avoidance.

The first two approaches are considered when the interference level is much greater or much weaker than the desired signal, respectively. When the interference is strong, it can be decoded and subtracted from the received signal, yielding, in this manner, the desired signal. On weak interference cases, usually, nothing is done to mitigate the interference. Besides, this is a case that is getting even more rare due to the expansion of wireless systems. Both

methods limit the system performance. For the decoding case, there is a trade-off between improving the decode quality or the users' data rate [3]. When the interference is neglected, it will clearly burden the data reception.

Nevertheless, the most common and important case of interference is when the interference has a similar strength to the desired signal. In this situation, the transmitters agree on transmitting through orthogonal resources, and in this manner the interference is avoided. So, a portion of the frequency or time, for instance, is divided among the neighboring transmitters, these methods are called Frequency Division Multiple Access (FDMA) and Time Division Multiple Access (TDMA), respectively. This method not only limits each transmitter performance but it also divides the available resources by the number of considered partitions. In order to reduce this performance loss, an approach similar to the frequency reuse can be applied, which performs the partition only for the closest transmitters [4]. However, this method may not be sufficient to provide the new throughput requirements, so, more refined techniques must be considered to handle the interference.

Therefore, combining the MIMO technology and the cooperation among the neighboring transmitters is a key to manage the interference and enable the system meet the required data rates. Aligned with this combination, the Coordinated Multi-Point (CoMP) architecture has been applied to achieve the aforementioned goals. One of the techniques that can be applied in this scenario is the Interference Alignment (IA), which is a novel method that claims that pairs of transmitters and receivers can perform transmissions free of interference and achieve the optimal multiplexing gain on MIMO systems [5]. Also, it was proven that by applying the IA technique, transmitters are able to send data with half of their channel capacity to his desired receiver, regardless of the number of users in a K-user Interference Channel (IC) network [6].

An example to perceive this gain is to consider the IC network composed by K pairs of transmitters and receivers. With a resource orthogonalization method, each pair is able to transmit at a rate equal to $1/K$ of the channel capacity. However, suppose that the medium adds a delay of one symbol duration to the interfering signals and two symbols to the desired signal. Then, if the transmitters send useful information and the receivers listen the channel just in the even time slots, then the communication of all pairs will become free of interference. This shows that in these networks, by applying a proper transmission method, the interference can be confined (aligned) in half of the dimension, remaining the other half to accomplish the transmissions free of interference. This, somehow, challenged the conventional wisdom about the throughput limits of wireless networks and made the technique arise as an important object of study in recent years. The following section briefly covers the state of the art in IA, but with no intention to exhaust the theme.

1.2 State-of-the-art

There are mainly two versions of interference alignment in the literature: *signal space alignment* and *signal scale alignment*. The signal space alignment is accomplished by a linear combination of some precoding vectors and the data that will be transmitted. This approach is applicable on the interference channels with multiple antennas or with time varying/frequency selective channel coefficients. Regarding the signal scale approach, it uses structured coding, e.g. lattice codes, to align interference in the signal level and are especially useful in the case of constant channels [7]. Since the range of applications of the signal space approach is larger and it is easier to execute, most efforts have been focused on it. Hence, this trend is also followed in this dissertation, and, hereafter the signal space alignment approach

is just referred as IA.

The signal space alignment was introduced in [8], in which the impact of the interference on wireless networks was attempted to be characterized. This work showed that, when IA is applied, the achievable Degree of Freedom (DoF) of a MIMO-Cross Channel (MIMO-X) network, composed by two pairs of transmitters and receivers equipped with two antennas, are able to achieve four DoF, while the conventional methods achieve just three DoF. This gain could only be achieved by setting aside a part of the available dimension (time, frequency or space) at each receiver and forcing the interfering terms to be received in that partition.

Since this initial work, the interest on the characterization of other different networks via the DoF has increased, especially when the the IA technique is applied. Cadambe and Jafar (2008) [6] introduced the IA for the K-user IC with equal number of antennas at all transmitters and receivers, showing that this network can achieve up to $K/2$ DoF. Later this work was extend for an unequal number of antennas at each network node [9]. Similar IA schemes were proposed for X networks, where the useful signal is also transmitted in the crossed links for an arbitrary number of users [6].

Afterwards, some different algorithms were proposed to perform IA, some aiming at the perfect alignment, and others relaxing a little this constraint in order to obtain higher sum rates. The precoding design algorithm presented in [6] was extended to be accomplished in a distributed manner, and its convergence was proven in [10]. Results from these works established that these algorithms achieve the optimal Shannon capacity only at high Signal to Noise Ratios (SNRs) cases. In order to overcome this issue, an algorithm that tries to maximize the Signal to Interference-plus-Noise Ratio (SINR) instead of just performing the alignment was introduced in [11]. Both algorithms present a similar iterative framework, which enables them to find the appropriate precoder in different network configurations.

Still considering the objective of achieving the optimal gain on cases of finite SNRs values, an algorithm that minimizes the sum Mean Square Error (MSE) was introduced in [12]. By using the pricing concept, similarly as [13], these algorithms are also able to maximize several sum utilities, with different objectives, which enables the precoding design to follow a more egoistic approach (minimizing the interference that its own receiver perceives) or a more altruistic one (trying to avoid the interference that its transmitter causes on the unintended receivers). This precoding designing dilemma of compromising the beamforming gain at each intended receiver or mitigating the interference on the other receivers is also tackled in [14].

Several other works performed comparisons of the different proposed algorithms in several scenarios. The closed-form solution, an Minimum Mean Square Error (MMSE)-based algorithm, and another one that tries to minimize the interference that leaks at the receiver, had their performances compared within a two user X-network in [15]. The application of the technique in cellular networks was addressed by Suh and Tse (2008) [16] and by Sun, Liu, and Zhu (2010) [17], while [18] showed that IA almost doubles the throughput of MIMO Local Area Networks (LANs).

Nevertheless, the scenarios or system configurations on which the alignment is possible or feasible are not entirely clear yet. In [19], the feasibility conditions under which IA could be applied are addressed. These conditions were demonstrated by simply counting the number of equations and variables of the problem, since the IA problem can be seen as a mere system of equations. This work was limited to demonstrate the conditions to achieve the interference alignment, but closed-form solutions of several scenarios are still unknown. Another interesting result from this paper is that the number of antennas required at each node can easily become impracticable as the number of coordinated transmitters

increases. For instance, consider three transmitter-receiver pairs and let us assume each node is equipped with two antennas, then they can communicate with each other free of interference through IA. However, if the cooperation was performed with four pairs, the number of required antennas goes up to three, restricting the kind of devices that could be used.

At this point, IA has been shown to be a technique capable to mitigate the interference on several network configurations. Nevertheless, few works have approached the challenges of implementation in more realistic conditions. Most of the previous results on the literature were obtained considering ideal channels. One work that deviates from this focus is [20], which proposes an IA-based algorithm robust to Channel State Information (CSI) errors. The existence of an uncoordinated interference is considered in [21], however it limits itself to model the interference with just one dominant source.

The paper of Suh et. al. [2] is a relevant work that tackles some challenges of implementation, especially the extensive requirement of CSI to be exchanged over the network backhaul. Its main contribution was a new IA algorithm for downlink cellular systems that requires only intra-cell feedback. Furthermore, the work evaluates the proposed algorithms through a system level simulator that effectively performs the transmission between two cells while the surrounding cells are modeled as white Gaussian noise. This considered simulator could be improved, since even when IA is employed there is still uncoordinated interference, and more details are required for a more thorough systemic analysis. Nevertheless, the results of the paper aggregate relevant new information when compared with previous works.

Another work that tries to evaluate the technique in a more realistic scenario is [22], which analyzes some IA algorithms by using measurements of a real channel. Thus, by using the measurements, a 3-user frequency-selective SISO-Interference Channel (SISO-IC) is emulated, and the performance of IA schemes are compared with the method of interference avoidance that orthogonalizes the radio resource through frequency planning. This work provides pertinent results, however the presence of an external or uncoordinated interference can have a different impact on these two techniques, which is not taken into account in its isolated scenario.

Aiming to have a good picture of the IA technique behavior in real systems, recent works have focused on the system level performance evaluation. One example is the work that evaluates IA under different receive strategies through a 3rd Generation Partnership Project (3GPP) compliant downlink Long Term Evolution (LTE) simulator [23]. The referred paper combines IA and other well established transmissions with a set of linear receivers, not worrying whether their design matches or not. For instance, the simulator can use the IA precoders with an Maximal Ratio Combining (MRC) reception, hence, in this case, the interference cancellation cannot be accomplished. This is a case in which the receivers are not able to perform complex computations.

Finally, it can be perceived that there are several research directions, but there are still some gaps on the discussed topics and some unresolved questions.

1.3 Open problems

Based on this brief review on the IA topic, it can be noticed that the research in this field has tackled different points and experienced a great advance. However several points are still unclear and deserve further investigations.

The initial research has been focused on the theoretical gains that the technique could deliver, through the DoF characterization of several networks. These works were followed by

those that proposed several precoding design algorithms, whose performances were evaluated basically in terms of the sum capacity, which translates the multiplexing gain, as well as the achievable DoF. Since the sum capacity achieved by the system is calculated just via the SINR perceived in each receiver, the transmissions are not effectively performed on the simulations of these works. Therefore, by simulating the transmission with different modulations and coding schemes the algorithms' performances could also be analyzed through the Symbol Error Rate (SER) or Bit Error Rate (BER) results, which are metrics that can provide useful information on the reliability of the transmission links.

Besides IA, there exist other techniques that are able to mitigate the interference among cooperating transmitters. Most of them are based on the Joint Processing (JP) architecture, that requires coordination among all transmitters, which results on strong infrastructure requirements. In spite of this, these schemes are already considered on the new 4G networks. Therefore, another gap on the algorithms' evaluation is that they have not been compared with other well-established techniques, such as the JP schemes.

Another issue on the evaluation of the technique is that the majority of the works considered perfect CSI knowledge at the transmitters to design the precoders. Nevertheless, there are basically two ways of gathering this information, namely by channel reciprocity and through feedback. The first one is based on the reciprocity principle that states that the transfer function of the direct channel (from transmitter to the receiver) at an instant is equal to the transpose of the reverse channel (from receiver to the transmitter). This is not valid, however, for Frequency Division Duplexing (FDD) systems, because these channels do not use the same frequency. The error can be minimized by using close frequencies in the downlink and in the uplink, but it cannot be avoided. The second manner is via feedback from the receivers, since they are able to easily estimate the channel. However the feedback transmissions are also susceptible to errors and delay, which may cause a significant impact on the final system performance. Thus, the consideration of perfect CSI knowledge for the precoding design may be not realistic.

On wireless communications, the obstacles are not equally distributed around the receivers, thus, the signal does not arrive from all directions, and some spatial directions may be enhanced. Also, at many receivers the space is insufficient to guarantee that the arriving signals are orthogonal at each antenna. Hence, another channel imperfection problem that was poorly addressed by past works is the correlation among antennas.

All the referred non-traditional methods to handle the interference require some kind of cooperation to mitigate it. Also, with the growth of the number of wireless systems, it can be difficult to employ such cooperation among a large number of transmitters. Hence, it is common to have coexisting networks that interfere with each other. Therefore, the consideration of the presence of an external interference is another realistic assumption, which was tackled in [2, 21]. However, due to the rather simple models that were used, there are some further unresolved issues in this topic.

The cellular network largely contributes to the ubiquity of communication systems, what makes it one of the most important kinds of wireless networks. This network also aggregates the previously related issues regarding the realistic conditions. Thus, knowing how the IA techniques will perform in such scenario is indispensable. However, only few works focused on this, such as [2], that proposed its own algorithm, but performed evaluations under simplistic configurations. So, this is still an open problem.

1.4 Objectives and contributions

The last two sections addressed the already studied and some unresolved issues on the IA topic. Thus, this work aims to provide useful evaluations of some algorithms, seeking to clarify how the technique will work in practical systems.

For this work, the cellular network is adopted as the main scenario where the IA algorithms will be employed and assessed. So, the first contribution of this work is the evaluation of the IA technique in this scenario. However, this evaluation is taken not just in terms of the sum capacity achieved by the system, but also through the BER results. Also, the comparison with one JP-based transmission scheme is accomplished, in order to better understand the actual gain that the technique could provide. In this manner, the assessment of the algorithms is not limited to the theoretical gains and it could provide more useful insights into how the IA technique could really perform in practice.

Therefore, aiming to go a step further on the comprehension of how realistic conditions will affect the technique's performance, some channel imperfections are added in the simulator. First, an additive error in the CSI is considered for the precoding design. Then, correlation among the transmitter antennas is assumed. The JP-based transmission scheme is also compared with the IA algorithms.

Parallel to that, the presence of an uncoordinated interference is considered in the same simulator. This interference is modeled as a colored noise, and the rank of its covariance matrix is changed to mimic different kinds of interference. If there is just one dominant interference, the rank of the covariance matrix must be one, if there are two the rank must be two, and so on. This model can embrace several kinds of interference. In this scenario, some changes were made to the IA algorithm in order to take into account this external interference. Also, a modification of one IA algorithm is proposed, in order to try a better alignment of the internal and external interference. As a matter of fairness, the JP-based algorithm is also modified to account for the uncoordinated interference at the precoding design.

In order to also evaluate the impact of temporal channel variations on the IA technique, the channel is generated using the Jakes' model, which allows to assess the impact of the delayed channel on the algorithms' performances. So, this channel imperfection and the uncoordinated interference can be combined in this set of simulations.

Although the previous analyses tackle some important factors that are present in real systems, the analysis was performed at a not too realistic scenario, assuming a simulated system composed of just three transmitters, while in practice this number is much larger. Furthermore, the transmission considered only one modulation scheme and no coding. For the purpose of assessing IA in a scenario closer to practice, this work additionally performs system level simulations in a larger network. In this scenario, not only the IA algorithms are compared but some schedulers are evaluated as well.

1.5 Outline

After briefly presenting the current context of Interference Alignment research, this dissertation is further divided into five chapters, whose contents are as follows:

- **Chapter 2**: In this chapter, the main idea and some basic concepts of the IA technique are addressed, focusing on the spatial dimension. In the sequence, the algorithms applied in this work are presented, including the JP-based algorithm. And it ends by showing the framework used in the simulations considered along the whole work;
- **Chapter 3**: In this chapter, the impact of the channel imperfections on the IA technique

is analyzed. So, it starts by presenting the model of the additive error in the CSI and the correlation among transmission antennas. It finishes by presenting the analyses of the simulations results;

- **Chapter 4**: The analyses of how the external interference affects the IA algorithms are performed in this chapter, so, the model of the uncoordinated interference is shown and some algorithms' modifications are presented. The channel variations are also considered in this chapter, then the Jakes' model is discussed and the impact of the delayed channel knowledge is studied here;
- **Chapter 5**: The IA technique evaluation ends in this chapter by performing the assessment in a system level simulator. Similar to the previous analysis the IA algorithms are compared with JP-schemes of transmission in a more elaborated simulator. In this simulator, some scheduling policies are also evaluated.
- **Chapter 6**: Finally, the conclusions of the analyses are drawn and the next steps the research can take are discussed.

Chapter 2

Interference Alignment

This chapter begins presenting the system model used through almost all the work. From this system model the basic concepts of Interference Alignment (IA) are discussed, followed by the presentation of the algorithms based on the technique. And the chapter is closed by showing the simulator framework used in the forthcoming analysis.

2.1 System Model

The MIMO-Interference Channel (MIMO-IC) is composed by a set of transmitters and receivers that are organized in pairs, meaning that each transmitter desires to send information to its respective receiver, as illustrated in Figure 2.1. Thus, the interference is composed by the union of all signals arriving at the receivers that were not sent by their correspondent transmitter. This model can perfectly emulate the scenario chosen to evaluate the IA technique, a cellular network, since there is a link between each user and Base Stations (BSs).

So, hereafter the K-User MIMO-IC network is considered, where each of the K transmitters is equipped with N_T antennas and wants to send S streams to a specific receiver that is equipped with N_R antennas. Then, data is precoded and transmitted, resulting in the following received signal:

$$\mathbf{y}_k = \mathbf{H}_{kk}\mathbf{V}_k\mathbf{d}_k + \sum_{j=1, j\neq k}^{K} \mathbf{H}_{kj}\mathbf{V}_j\mathbf{d}_j + \mathbf{n}_k, \tag{2.1}$$

where $\mathbf{H}_{kj} \in \mathbb{C}^{N_R \times N_T}$ denotes the channel between transmitter j and receiver k, $\mathbf{V}_k \in \mathbb{C}^{N_T \times S}$ and $\mathbf{d}_k \in \mathbb{C}^{S \times 1}$ denote, respectively, the precoder and the vector of symbols of the k-th transmitter, finally, $\mathbf{n}_k \in \mathbb{C}^{N_R \times 1}$ is the white Gaussian noise vector with variance σ_n^2. In order to recover the original data streams, the received signal $\mathbf{y}_k \in \mathbb{C}^{N_R \times 1}$ is processed by applying the receive filter $\mathbf{U}_k^H \in \mathbb{C}^{S \times N_R}$ at the receiver side.

Given the system variables, the Signal to Interference-plus-Noise Ratio (SINR) of the j-th stream of the k-th user in the network is given by:

$$\text{SINR} = \gamma_k^{[j]} = \frac{|\mathbf{u}_k^{[j]H}\mathbf{H}_{kk}\mathbf{v}_k^{[j]}|^2}{\sum_{d=1}^{S}\sum_{i=1}^{K} |\mathbf{u}_k^{[d]H}\mathbf{H}_{ki}\mathbf{v}_i^{[d]}|^2 - |\mathbf{u}_k^{[j]H}\mathbf{H}_{kk}\mathbf{v}_k^{[j]}|^2 + ||\mathbf{u}_k^{[j]H}||^2\sigma_n^2}, \tag{2.2}$$

where $\mathbf{v}_k^{[j]}$ and $\mathbf{u}_k^{[j]}$ are the j-th column of the k-th precoder and receive filter, respectively.

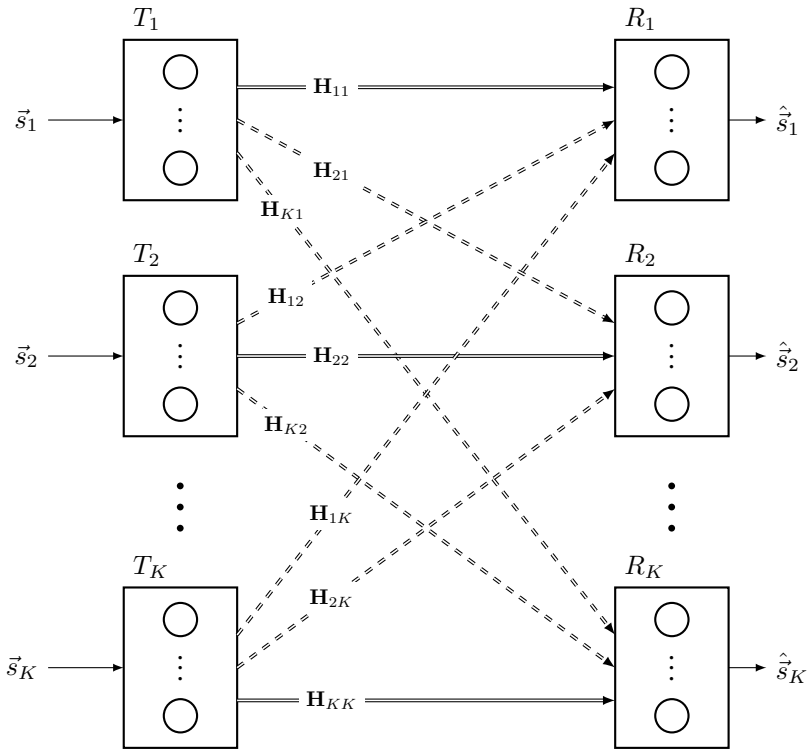

Figure 2.1: K-user MIMO Interference Channel.

2.2 Interference Alignment Concept

The main idea behind this novel technique is to align, at each receiver, multiple interference signals in a subspace with dimension smaller than the number of interferers [2]. This is a very general idea, in the sense that the signals can be aligned in any dimension, including time, frequency, or space. Also, it can be viewed as a cooperative and altruistic approach since the transmitters may neglect the performance of their own link to allow other users to perfectly cancel interference [21].

Thus, what the IA technique does is to design the precoders and the receiver filters so that the interference can be canceled at every receiver. Hence, the generic IA problem can be written as:

$$\mathbf{U}_k^H \mathbf{H}_{kj} \mathbf{V}_j = 0, \forall j \neq k \tag{2.3}$$

$$\operatorname{rank}\left(\mathbf{U}_k^H \mathbf{H}_{kk} \mathbf{V}_k\right) = S. \tag{2.4}$$

Note that a space of dimension S is required to confine the interference at each receiver. Nevertheless the analytical solution of this system of equations is known for just a few scenarios. In the following two very important concepts are addressed, which help to understand how the technique works and its possibles gains.

2.2.1 Degree of Freedom

In the context of communication networks, capacity is a measurement of the maximum amount of data that may be transferred on the network. The exact capacity for most wireless networks is unknown, thus, the best way to assess the capacity limit is through approximations. Specifically, for a single Multiple Input Multiple Output (MIMO) transmitter-receiver pair, it can be described as a function of the Signal to Noise Ratio (SNR) as:

$$C\left(SNR\right) = \eta \log(SNR) + o\left(\log(SNR)\right), \tag{2.5}$$

where η is called multiplexing gain, which represents the number of streams that can be sent in (almost) parallel channels. In [5] it was shown that this gain can achieve, with the right processing, a multiplexing gain equal to the minimum between the number of transmit and receive antennas.

The term $o\left(\log(SNR)\right)$ becomes negligible at high SNR in relation to the $\log(SNR)$, thus the following relation can be defined:

$$\eta \triangleq \lim_{\mathrm{SNR}\to\infty} \frac{C(\mathrm{SNR})}{\log(\mathrm{SNR})}, \tag{2.6}$$

which represents the ratio between the linear scale of the capacity and the logarithm of the SNR. For the multiuser case this increasing factor is called Degree of Freedom (DoF). When a network presents such behavior it is common to say that it achieved the optimal multiplexing gain.

This concept was the main study object of the first IA works, and before them it was shown that a fully connected K-user Interference Channel (IC) network achieves only one DoF [6]. However, by applying the IA technique, $K/2$ DoF can be reached. Therefore, most works focused on finding the achievable DoF of several network configurations, which made this concept very important on IA studies. Consequently, it is worth to highlight three points of view about this concept:

i. A network has η degrees of freedom if and only if the sum capacity of the network can be expressed as $\eta \log \mathrm{SNR} + o(\log \mathrm{SNR})$;

ii. It provides a good capacity approximation at the high SNR regime;

iii. The degrees of freedom of a network may be interpreted as the number of resolvable (interference-free) signal space dimensions.

This last interpretation is illustrated by the example exposed in Figure 2.2, which shows the application of IA in a 3-user MIMO-IC network. In this example, the interferences signals are aligned in one direction, at each receiver. Therefore, each user has one dimension free of interference for the transmission of the desired signal. Thus, it is said that this system can achieve $3/2$ DoFs.

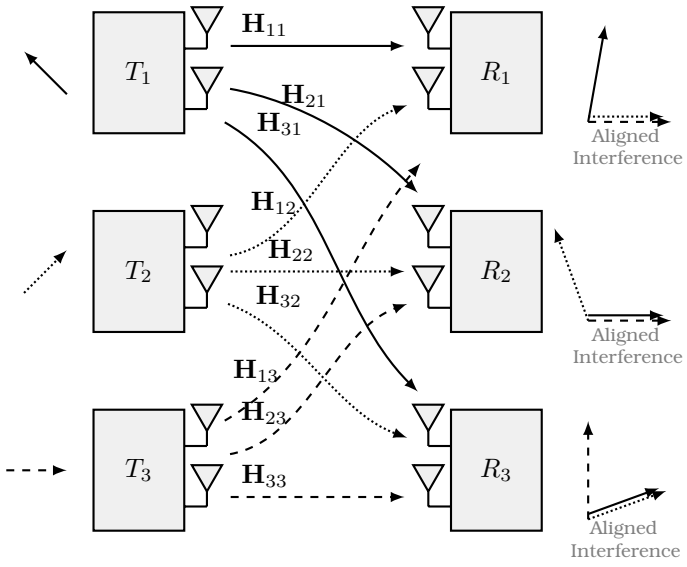

Figure 2.2: 3-user MIMO Interference Channel when IA is applied.

2.2.2 Feasibility

From the DoF concept, lots of works derived the theoretical gains that IA could provide on different kinds of networks. However, the technique cannot be randomly applied in a network and expect that the interference will be completely eliminated. There are some conditions regarding the configurations (number of antennas, streams transmitted, etc.) that must be respected. As an example, considering IA along the spatial domain, as the number of cooperating transmitters increases, the number of antennas required to accomplish the alignment also increases. In this regard, the relation between the number of users, antennas and transmitted streams was derived in [19], which is referred to as the feasibility conditions to achieve IA. These conditions play an important role on the choice of scenario to which the technique can be applied.

From the generic IA problem in (2.3), it can be perceived that the interference is eliminated by choosing the right precoders and receiver filters, through the solution of the system of equations. These systems can present one solution, infinite solutions and no consistent solution, but how they are classified depends on the number of variables and equations involved. If there are more independent equations than variables, the system has one or more solutions. So, to know if the IA problem has any solution it is just necessary to count the number of independent equations and variables involved. These numbers are intrinsically dependent on the configuration of the network, how many antennas each node is equipped with, how many pairs are cooperating to accomplish the alignment and etc. Then, in order to determine for each scenario whether the IA algorithms could be applied, the number of equations and variables are accounted for as follows.

Considering the system model adopted in this work, both the equations and variables involved in the system can be counted. Thus, in order to know the number of equations that effectively participate of the solution, the IA problem can be rewritten as:

$$\mathbf{u}_k^{[m]H}\mathbf{H}_{kj}\mathbf{v}_j^{[n]} = 0, \forall j \neq k \text{ and } \forall m, n \in \{1, 2, \cdots, S\} \tag{2.7}$$

where $\mathbf{v}_j^{[n]}$ and $\mathbf{u}_j^{[n]}$ are the n-th column of the j-th precoder and receive filter, respectively.

Consequently, assuming that each user has the same number of streams $s_i = S$, the number of equations present in the system is:

$$N_e = \sum_{\substack{j,k=1 \\ j\neq k}}^{K} s_i s_j = \sum_{\substack{j,k=1 \\ j\neq k}}^{K} S^2 = (K^2 - K)S^2. \tag{2.8}$$

Counting the number of variables is not as direct as the number of equations. Some of the variables are not useful on the solution of the problem and it is necessary to be careful not to include them into the count. For instance, considering the transmitter k that applies the $\mathbf{V}_k \in \mathbb{C}^{N_T \times S}$ precoder, the first thought is to consider its dimension as the number of variables. However, consider a square matrix $\mathbf{B}$, obtained from removing the $N_T - S$ last lines of the $\mathbf{V}_k$ matrix. Then, the vector space generated by $\mathbf{V}_k\mathbf{B}$ is the same spanned by $\mathbf{V}_k$. Consequently, there are only $N_T - S$ useful variables in each precoding filter. If the same process was applied, then the same conclusion can be taken for the receiver filter, thus only $N_R - S$ useful variables are counted for each receiver. Therefore the total number of useful variables in the problem

is given by:

$$N_v = \sum_{i=1}^{K} s_i \left(N_T + N_R - 2s_i\right) = \sum_{i=1}^{K} S \left(N_T + N_R - 2S\right) = KS \left(N_T + N_R - 2S\right). \tag{2.9}$$

Finally, in order to know if the network configuration is feasible for the IA technique, considering a symmetric system, the number of variables has to be equal or greater than the number of equations. Thus, the following rule can be derived:

$$N_T + N_R - (K+1)\, S \geq 0 \tag{2.10}$$

The most analyzed configuration is the 3-user channel, where the nodes are equipped with two or four MIMO antennas. Considering the 2×2 case, the feasibility rule in (2.10) will show that each user is able to send just one stream. Also, this rule shows that if four users are considered then two antennas per node are not sufficient to solve the IA problem. If the number of antennas is increased by two, i.e. 4×4 case, the number of streams each user is able to send increases just by one. So, this shows that, as the number of interferers increases, the number of antennas required to perform the technique grows faster, which can be a problem for the technique.

2.3 Interference Alignment Algorithms

This section presents the algorithms based on IA that will be evaluated in this work. All of them enable the network to achieve the previously mentioned DoF if the feasibility conditions are respected. Also, the first two algorithms aim at the perfect/pure interference alignment, while the last one relaxes this constraint in order to improve the direct channel.

2.3.1 Closed-Form Solution

The first algorithm presented here is the IA closed-form solution for the 3-user case of MIMO-IC. This algorithm can be very useful for the comprehension of the IA concept, since the alignment can be seen in a more explicit way than in the other algorithms. The 3-user case solution is calculated by solving the following system of equations, that represents the alignment of the interfering signals at each receiver:

$$\text{span}(\mathbf{H}_{12}\mathbf{V}_2) = \text{span}(\mathbf{H}_{13}\mathbf{V}_3), \tag{2.11}$$

$$\text{span}(\mathbf{H}_{21}\mathbf{V}_1) = \text{span}(\mathbf{H}_{23}\mathbf{V}_3), \tag{2.12}$$

$$\text{span}(\mathbf{H}_{32}\mathbf{V}_2) = \text{span}(\mathbf{H}_{31}\mathbf{V}_1), \tag{2.13}$$

where $\text{span}(A)$ corresponds to the subspace generated by the columns of A.

These conditions can be even more restrictive when rewritten as:

$$\text{span}(\mathbf{H}_{12}\mathbf{V}_2) = \text{span}(\mathbf{H}_{13}\mathbf{V}_3), \tag{2.14}$$

$$\mathbf{H}_{32}\mathbf{V}_2 = \mathbf{H}_{31}\mathbf{V}_1, \tag{2.15}$$

$$\mathbf{H}_{21}\mathbf{V}_1 = \mathbf{H}_{23}\mathbf{V}_3. \tag{2.16}$$

So, if $\mathbf{V}_2$ and $\mathbf{V}_3$ were written as function of $\mathbf{V}_1$, then the system is given by:

$$\text{span}(\mathbf{H}_{12}\mathbf{H}_{32}^{-1}\mathbf{H}_{31}\mathbf{V}_1) = \text{span}(\mathbf{H}_{13}\mathbf{H}_{23}^{-1}\mathbf{H}_{21}\mathbf{V}_1), \tag{2.17}$$

$$\mathbf{V}_2 = \mathbf{H}_{32}^{-1}\mathbf{H}_{31}\mathbf{V}_1, \tag{2.18}$$

$$\mathbf{V}_3 = \mathbf{H}_{23}^{-1}\mathbf{H}_{21}\mathbf{V}_1. \tag{2.19}$$

Then, the solution for $\mathbf{V}_1$ is any subset of S eigenvectors of the following matrix:

$$\mathbf{E} = \mathbf{H}_{31}^{-1}\mathbf{H}_{32}\mathbf{H}_{12}^{-1}\mathbf{H}_{13}\mathbf{H}_{23}^{-1}\mathbf{H}_{21}. \tag{2.20}$$

This way there are $C_{2S}^{S} = \binom{2S}{S}$ ways to choose the precoder of the first transmitter, and all of the solutions accomplish the perfect interference alignment at each receiver. It turns out that this precoding design guarantees that the interference is aligned for each user. Hence, in order to completely eliminate the interference and revert the channel effect, then a Zero-Forcing (ZF) receiving filter may be applied at each receiver. Therefore, the receiver matrices must be calculated respecting the following relation:

$$\begin{aligned} \mathbf{U}_1^H[\mathbf{H}_{12}\mathbf{V}_2\ \mathbf{H}_{13}\mathbf{V}_3] &= 0, \\ \mathbf{U}_2^H[\mathbf{H}_{21}\mathbf{V}_1\ \mathbf{H}_{23}\mathbf{V}_3] &= 0, \\ \mathbf{U}_3^H[\mathbf{H}_{31}\mathbf{V}_1\ \mathbf{H}_{32}\mathbf{V}_2] &= 0, \end{aligned} \tag{2.21}$$

since the precoders already aligned the interferences, then the relation becomes:

$$\begin{aligned} \mathbf{U}_1^H[\mathbf{H}_{12}\mathbf{V}_2] &= 0, \\ \mathbf{U}_2^H[\mathbf{H}_{21}\mathbf{V}_1] &= 0, \\ \mathbf{U}_3^H[\mathbf{H}_{31}\mathbf{V}_1] &= 0. \end{aligned} \tag{2.22}$$

Note that the direct channels are never used in this algorithm, and thus how much the direct signal lies inside the null space cannot be controlled. Also, if a different subset of precoders are chosen, then the algorithm may perform differently. So, each different subset of the eigenvectors of $\mathbf{E}$ yields a distinct IA solution. Hence, in order to boost the closed-form solution performance, the set of precoders that maximizes the minimum of the SINRs may be used. For a reasonable number of antennas (e.g. , 2 or 4), performing this choice is not too costly, since the exhaustive search will be done among two or four choices. This algorithm is labeled as IA closed-form strategy and it is summarized in Algorithm 2.1.

Algorithm 2.1 Interference Alignment Closed-Form solution.

i. Using (2.20) calculate the $\mathbf{E}$ matrix;

ii. Assign S eigenvectors of $\mathbf{E}$ for $\mathbf{V}_1$;

iii. Use (2.18) and (2.19) to obtain $\mathbf{V}_2$ and $\mathbf{V}_3$;

iv. Calculate the receiver matrices of each user, $\mathbf{U}_k^H$, according to (2.22) .

2.3.2 Interference Alignment via Alternating Minimization

The previous algorithm could provide an idea of how IA is accomplished, however it limits the scenarios where the technique can be applied. An alternative algorithm that also seeks the pure IA goal specified in (2.3), is the IA via alternating minimization, which was first proposed

in [6] and presents a lot of advantages over the closed-form solution. First, it can be applied to several network configurations, as long as the feasibility conditions are respected, which provides more flexibility to the technique. Also, it can be performed in a distributed manner, i.e., it is not necessary to have a Central Processing Unit (CPU) where all the estimates of the network are concentrated to design the precoders. So, this is an indispensable algorithm to the analyses performed in this work.

The IA via alternating minimization is not accomplished by directly solving that system of equations. It is based on the concept of subspaces, for which the available dimension at each receiver can be split in two subspaces. The first one is where the desired signal is decoded and the other is where the interference must be confined. Thus, what this algorithms makes is to adapt the interference subspaces and the precoders to accomplish the interference alignment. Thus, considering this subspace approach, the function that translates the IA objective and must be minimized is:

$$J_{IA} = \sum_{k=1}^{K} \mathbb{E} \left\| \mathbf{\Phi}_k^H \sum_{j=1, j\neq k}^{K} \mathbf{H}_{ki} \mathbf{V}_i \mathbf{s}_i \right\|_F^2 . \tag{2.23}$$

where $\mathbf{\Phi}_k$ is an orthonormal basis for the interference subspace.

Considering the independence of the signals, the instantaneous objective function is:

$$J_{IA} = \sum_{k=1}^{K} \sum_{\substack{j=1 \\ j\neq k}}^{K} \mathrm{tr}\left(\mathbf{\Phi}_k^H \mathbf{H}_{kj} \mathbf{V}_j \mathbf{V}_j^H \mathbf{H}_{kj}^H \mathbf{\Phi}_k\right), \tag{2.24}$$

which can be seen as the power of the leaked interference. Also, the precoders must satisfy the power constraints.

This function can be minimized through an alternating optimization approach, by choosing the precoders and interference subspace as:

$$\mathbf{\Phi}_k^{opt} = \nu_{min}^S \left(\sum_{\substack{j=1 \\ j\neq k}}^{K} \mathbf{H}_{kj} \mathbf{V}_j \mathbf{V}_j^H \mathbf{H}_{kj}^H \right), \tag{2.25}$$

and

$$\mathbf{V}_k^{opt} = \nu_{min}^S \left(\sum_{\substack{j=1 \\ j\neq k}}^{K} \mathbf{H}_{kj}^H \mathbf{\Phi}_j \mathbf{\Phi}_j^H \mathbf{H}_{kj} \right), \tag{2.26}$$

where $\nu(\cdot)_{min}^S$ is a function that returns a matrix whose columns are the eigenvectors corresponding to the S smallest eigenvalues of the input matrix.

Translating into words, at the first step, users try to adapt their interference subspace towards the direction of interference caused by the other transmitters. On the second step, by knowing the subspaces of all users, each transmitter tries to change its precoder to project, onto these subspaces, the interference caused at the other users. Thus, these two steps are alternately performed until the algorithm converges. Convergence that can be proved by showing that at each iteration the objective function decreases. It is important to remember that although the convergence to a minimum can be proved, the interference alignment is just accomplished when the feasibility conditions are respected.

After several iterations, the ZF receiving filters may be applied to eliminate the interference. This algorithm is hereafter called “Alternating” and is presented in Algorithm 2.2. Please note

that the initial precoders can be randomly initialized. It is important to highlight that a maximum number of 60 iterations is considered for the simulations, which was verified to be almost always enough to provide good alignment in the 3-user case, while for 5 or 7-user scenarios 260 and 800 iterations are required, respectively.

Algorithm 2.2 Interference Alignment via Alternating Minimization.

i. Initialize the set of precoders;

ii. Find the interference subspace, $\sum_{j=1,j\neq k}^{K} \mathbf{H}_{kj}\mathbf{V}_j\mathbf{V}_j^H\mathbf{H}_{kj}^H$, of each user;

iii. Assign the orthonormal basis of the interference subspace as the S dominant eigenvectors of the interference subspace, according to (2.25);

iv. Calculate $\sum_{j=1,j\neq k}^{K} \mathbf{H}_{kj}^H\mathbf{\Phi}_j\mathbf{\Phi}_j^H\mathbf{H}_{kj}$ for each user;

v. Assign the precoders as the S dominant eigenvectors of the matrix calculated in the previous step, according to (2.26);

vi. Repeat from step **ii** until convergence.

Besides the already mentioned flexibility of this algorithm, another interesting feature is that it provides orthogonal precoders, which are especially attractive when the Channel State Information (CSI) is quantized.

2.3.3 IA-MMSE

In order to have a broader picture of the IA technique, here an IA algorithm that uses the Minimum Mean Square Error (MMSE) criterion at the reception is presented. Its solution tries to balance the goals of aligning and eliminating the interference at the receivers with the need of keeping the signal level well above the circuit noise [21]. Similar to the IA alternating algorithm, the IA MMSE uses an alternating optimization framework to find the precoders and receive filters. Also, the MMSE approach is flexible in the same manner of the alternating algorithm, and it must still satisfy the feasibility conditions.

The MMSE criterion seeks to minimize the error in the reception, thus, the Mean Square Error (MSE) is related to the difference between the decoded and transmitted symbols, which can be written as:

$$\text{MSE}_k = \sum_{k=1}^{K} \mathbb{E}\|\mathbf{U}_k^H\mathbf{y}_k - \mathbf{d}_k\|^2. \tag{2.27}$$

Replacing the received signal $\mathbf{y}_k$ from (2.1) in (2.27) yields:

$$\text{MSE}_k = \sum_{k=1}^{K} \mathbb{E}\left\|\mathbf{U}_k^H\left(\mathbf{H}_{kk}\mathbf{V}_k\mathbf{d}_k + \sum_{j=1,j\neq k}^{K}\mathbf{H}_{kj}\mathbf{V}_j\mathbf{d}_j + \mathbf{n}_k\right) - \mathbf{d}_k\right\|^2. \tag{2.28}$$

Hence the MMSE optimization problem to be solved is given by:

$$\min_{\{\mathbf{V}_k\};\{\mathbf{U}_k\}} \sum_{k=1}^{K} \text{tr}\left(\mathbf{U}_k^H\left(\sum_{j=1}^{K}\mathbf{H}_{kj}\mathbf{V}_j\mathbf{V}_j^H\mathbf{H}_{kj}^H + \sigma_k\mathbf{I}\right)\mathbf{U}_k\right) - 2\mathbb{R}\left\{\text{tr}\left(\mathbf{U}_k^H\mathbf{H}_{kk}\mathbf{V}_k\right)\right\} \tag{2.29}$$

$$\text{subject to } \text{tr}(\mathbf{V}_j^H\mathbf{V}_j) \leq P_j; \qquad \forall j = \{1,\ldots,L\}, \tag{2.30}$$

where $\mathbb{R}\{\cdot\}$ corresponds to the real part of a number.

Due to the convexity characteristic of this problem, the Lagrange method can be employed

to find a solution. The Lagrangian of this optimization problem is written as:

$$\begin{aligned}\mathfrak{L} = \sum_{k=1}^{K} \mathrm{tr}\left(\mathbf{U}_k^H \left(\sum_{j=1}^{K} \mathbf{H}_{kj}\mathbf{V}_j\mathbf{V}_j^H\mathbf{H}_{kj}^H + \sigma_k\mathbf{I}\right)\mathbf{U}_k\right) - 2\mathbb{R}\left\{\mathrm{tr}\left(\mathbf{U}_k^H\mathbf{H}_{kk}\mathbf{V}_k\right)\right\} \\ + \sum_{j=1}^{K} \mu_j\left(\mathrm{tr}\left(\mathbf{V}_j^H\mathbf{V}_j\right) - P_j\right),\end{aligned} \tag{2.31}$$

where μ_j is the Lagrangian multiplier for the precoder j. Hence, the Karush-Kuhn-Tucker (KKT) conditions are:

$$\nabla\mathfrak{L} = \mathbf{0} \tag{2.32a}$$

$$\mu_j\left(\mathrm{tr}\left(\mathbf{V}_j^H\mathbf{V}_j\right) - P_j\right) = 0,\ \forall j \tag{2.32b}$$

$$\mathrm{tr}\left(\mathbf{V}_j^H\mathbf{V}_j\right) \leq P_j,\ \forall j \tag{2.32c}$$

$$\mu_j \geq 0, \forall j \tag{2.32d}$$

In order to solve this problem, it is assumed that the set of precoders $\mathbf{V}_j$ is initially fixed and $\mu_j \geq 0$, which satisfies the KKT conditions (2.32b)-(2.32d). The gradient of the receiver filter, $\mathbf{U}_k$, can be calculated from the first KKT condition, resulting in:

$$\mathbf{U}_k = \left(\sum_{j=1}^{K} \mathbf{H}_{kj}\mathbf{V}_j\mathbf{V}_j^H\mathbf{H}_{kj}^H + \sigma_n^2\mathbf{I}\right)^{-1} \mathbf{H}_{kk}\mathbf{V}_k. \tag{2.33}$$

Likewise, fixing the receive filters allows the derivation of the precoders from the first KKT condition. The precoder $\mathbf{V}_j$ is then given by

$$\mathbf{V}_j = \left(\sum_{k=1}^{K} \mathbf{H}_{kj}^H\mathbf{U}_k^H\mathbf{U}_k\mathbf{H}_{kj} + \mu_j\mathbf{I}\right)^{-1} \mathbf{H}_{jj}^H\mathbf{U}_j^H. \tag{2.34}$$

However, unlike the receive filters, the other KKT conditions are not automatically satisfied. Hence, the equality and inequality cases in (2.32d) must be checked. First, if $\mu_j = 0$, then the other conditions are satisfied and the optimal precoder is directly found from (2.34). If $\mu_j > 0$, it implicates that $\mathrm{tr}\left(\mathbf{V}_j^H\mathbf{V}_j\right) = P_j$, and the Lagrange multipliers μ_j must be found. Unfortunately, even if $\mathbf{V}_j$ were replaced from (2.34) in (2.32b), a closed form solution for μ_j cannot be found. On the other hand, it can be observed that the power of the precoder is monotonically decreasing as a function of the Lagrangian multiplier. Therefore, the bisection method can be applied to find the Lagrange multiplier and finally calculate the precoder from (2.34).

Note that, similarly to the Alternating Minimization algorithm in Section 2.3.2, this non-trivial coupled optimization problem can be solved by an iterative framework where a set of variables are fixed while the other one is calculated, repeating the process for each variable. The MMSE-based IA algorithm is summarized in Algorithm 2.3.

It is expected that the MMSE-based algorithm outperform the Alternating Minimization algorithm, since it accounts for the impact of the thermal noise. On the other hand, the IA MMSE algorithm does not provide orthogonal precoders as the Alternating Minimization algorithm. Moreover, the MMSE-based algorithm is much more complex because it requires solving two optimization problems at every iteration.

As previously discussed, the IA MMSE algorithm uses an alternating approach, where

Algorithm 2.3 Interference Alignment with MMSE criterion.

i. Initialize the precoder matrices $\mathbf{V}_j$ with the closed-form solution;

ii. Calculate the receive vectors, $\mathbf{U}_k$,using (2.33);

iii. Solve μ_j by replacing (2.34) on the power constraint of transmitter j, then update $\mathbf{V}_j$ according to (2.34) with solved μ_j;

iv. Repeat from step **ii** until convergence.

the precoder is fixed, then the received filter is calculated and vice-versa. At each iteration the MSE always decreases, which ensures that the algorithm will converge to at least a local minimum. Some preliminary simulations were performed and the IA MMSE algorithm achieves a very good performance with only 32 iterations, assuming it is initialized with the closed-form solution.

This initialization method has a large impact on the complexity of the algorithm, since if the precoders are randomly initialized, the algorithm needs more than 100 iterations to converge. On the other hand, this initialization can be performed just for the three-user case, since the closed-form solution is only known for this case. Also, the distributed manner that this algorithm may be applied is no longer possible.

2.4 Block Diagonalization

Previously, the algorithm discussion was started by describing the closed-form solution of IA, which is the purest form to achieve the interference alignment goal. Then, a more flexible algorithm was introduced that can be implemented in a distributed form. Finally, the IA goal is relaxed and an MMSE-based algorithm is applied. All these three algorithms cover some relevant issues regarding wireless networks, and assessing them could provide some insights on the IA performance. Nevertheless, with the purpose of grasping how good the IA technique can perform, it is still necessary to have a benchmark for them.

On current cellular networks, Joint Processing (JP)-based transmission schemes are already considered. These schemes presume a cooperation among the transmitters to avoid the interference, similarly to the IA technique. However, they require not only the information about the channel matrices of the network, but they also need the knowledge of all the data that will be sent at each transmitter. This demands much more from the infrastructure than the IA technique. Hence, it is most likely that these schemes are able to achieve better performance than IA, which can be considered as a goal for IA performance.

At the JP-based schemes there is cooperation among the different transmitters, where each one participates on the transmission of all users of the network. Then the network can be treated as if there were just a single virtual MIMO transmitter. So, as all transmitters will send useful information to all receivers, the channel model shown in Section 2.1 can be rewritten as:

$$\begin{aligned}\mathbf{y}_k &= \sum_{j=1}^{K} \mathbf{H}_k \mathbf{M}_j \mathbf{d}_j + \mathbf{n}_k \\ &= \mathbf{H}_k \mathbf{M}_k \mathbf{d}_k + \underbrace{\sum_{j=1, j\neq k}^{K} \mathbf{H}_k \mathbf{M}_j \mathbf{d}_j}_{\text{Interference}} + \mathbf{n}_k,\end{aligned} \tag{2.35}$$

where $\mathbf{H}_k = [\mathbf{H}_{k1}\ \mathbf{H}_{k2}\ \cdots\ \mathbf{H}_{kK}]$ is the matrix comprised by concatenation of the channel matrices of all transmitters to the desired user k. And $\mathbf{M}_k$ is the modulation matrix associated to user k. One of the JP-based algorithms chosen to be applied at this work was the Block

Diagonalization (BD) [24].

Accordingly, the block diagonalization process is accomplished with a cascade of two precoding matrices, $\mathbf{B}_k$, that removes the intra-cell interference, and $\mathbf{D}_k$, which is responsible for parallelizing the transmission. Hence, the block diagonalization precoding matrix is $\mathbf{M}_k = \mathbf{B}_k\mathbf{D}_k$.

The first step to accomplish Block Diagonalization is to eliminate all multi-user interference, hence the constraint $\mathbf{H}_k\mathbf{M}_j = \mathbf{0}$ for $k \neq j$ is imposed. This means that the interference parcel of (2.35) will be forced to zero. Thus, consider the matrix $\widetilde{\mathbf{H}}_k$, formed by the concatenation of the interfering channel matrices, that spans the interference subspace of user k and is written as:

$$\widetilde{\mathbf{H}}_k = \left[\mathbf{H}_1 \cdots \mathbf{H}_{k-1}\ \mathbf{H}_{k+1} \cdots \mathbf{H}_K\right]. \tag{2.36}$$

and its Singular Value Decomposition (SVD) is defined as:

$$\widetilde{\mathbf{H}}_k = \widetilde{\mathbf{U}}_k \left[\widetilde{\mathbf{\Lambda}}_k\ \mathbf{0}\right] \left[\widetilde{\mathbf{V}}_k^{(1)}\ \widetilde{\mathbf{V}}_k^{(0)}\right]^H, \tag{2.37}$$

then, $\mathbf{B}_k$ is constructed by choosing the L_k columns of $\widetilde{\mathbf{V}}_k^{(0)}$, which form the orthogonal basis for the right null space of $\widetilde{\mathbf{H}}_k$. This will automatically eliminate the interference, and the received signal is resumed to:

$$\mathbf{y}_k = \mathbf{H}_k\mathbf{B}_k\mathbf{D}_k\mathbf{d}_k + \mathbf{n}_k. \tag{2.38}$$

It is worth to highlight that for the network configuration used in this work, that is composed by pairs of transmitters and receivers equipped with equal number of antennas, the nullity of the $\widetilde{\mathbf{H}}_k$ matrix is N_R, assuming the linearly independence of the channels. This results in a null space of dimension of $L_k = N_R$, which corresponds to the number of available dimensions to parallelize the streams transmission. In the 3-user case, with two antennas per node, this algorithm allows each pair to send two streams free of interference, while IA is able to send just one. This gain over IA is explained by the full coordination performed by the BD algorithm. Furthermore, in the following analysis it is expected that in terms of sum capacity this algorithms could be seen as an upper bound.

Now the data streams must be parallelized, which can be performed through another SVD. Consider the definition of $\mathbf{H}_{eff,k}$ as:

$$\mathbf{H}_{eff,k} = \mathbf{H}_k\mathbf{B}_k = \mathbf{U}_k\mathbf{\Lambda}_k\mathbf{V}_k^H, \tag{2.39}$$

then the parallelize precoder matrix can be chosen as $\mathbf{V}_k$ and the decoder will be $\mathbf{U}_k^H$. To obtain an optimum transmission, the $\mathbf{V}_k$ matrix can be scaled with a power control matrix, $\mathbf{P}_k^{\frac{1}{2}}$, that can be calculated through the water-filling algorithm with the singular values $\mathbf{\Lambda}_k$.

This whole process on designing the preceoders can be summarized as:

$$\mathbf{M}_k = \mathbf{B}_k\mathbf{D}_k = \left(\widetilde{\mathbf{V}}_k^{(0)}\right)_{(1:L_k)} \mathbf{V}_k\mathbf{P}_k^{\frac{1}{2}}. \tag{2.40}$$

and the reception is performed just by the application of the $\mathbf{U}_k^H$ matrix.

In the simulations of this work the water-filling algorithm was not considered in order to have a fair comparison, since it was used neither by IA nor by the BD algorithms. That is, the power available was the same to all the antennas.

2.5 Simulation framework

First it is important to highlight that the simulation scenarios of this work are always based on cellular networks. So, in order to emulate the current networks, here the 2×2 and 4×4 MIMO antenna configurations are considered. It should be mentioned that, currently, the 4×4 MIMO antenna configuration can be seen as a baseline while the 8×8 MIMO antenna configuration is the maximum accepted for special systems [25]. Moreover, at the 2×2 MIMO case IA is able to handle only three cooperative transmitters (see Section 2.2.2). Since the BD algorithm will also be employed, the simulation framework is composed by a Coordinated Multi-Point (CoMP) cluster composed by three cells, shown in Figure 4.2.

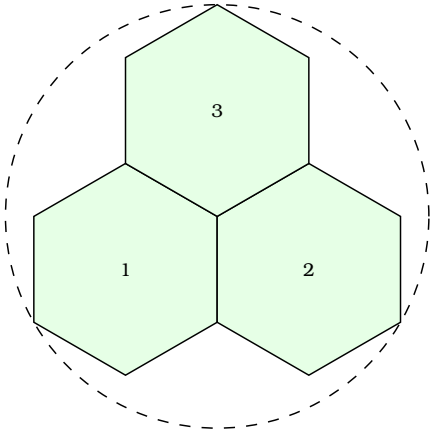

Figure 2.3: Basic simulation scenario composed by a 3-cell cluster.

At this CoMP cluster, there is a BS placed in the center of each cell. Furthermore, each cell contains a receiver/user, that can be placed respecting different distributions. The transmission power available to the transmission of each BS is calculated in order to match a specific value of SNR at the border of the cell. Thus, the location of the users and the SNR parameter can be varied in order to provide different SINR cases. The transmissions are performed using the 4-Phase Shift Keying (4-PSK) modulation scheme with no codification. Finally, a summary of the common parameters used in the simulations are highlighted in Table 2.1

Table 2.1: Simulation parameters of the 3-cell scenario

Parameter	Value
Cell Radius	1 km
Cluster Radius	2 km
Antennas (each Base)	2 or 4
Antennas (each user)	2 or 4
Modulation	4-PSK
Path Loss Model (in dB with d in km)	$128.1 + 37.6 \log_{10}(d)$
Noise Power	$N_0 = -116.4\,\text{dBm}$
Transmission Power	Adjusted to match SNR at the border of the cell

Since this is a CoMP cluster, it is assumed that there is a fast backhaul that enables the data exchange among the base stations. It is important to remember that some IA algorithms, such as the IA Alternating, can be performed on distributed architectures, while others, like the Closed-Form solution, require a CPU. This architecture analysis is left for future work and it is considered that all transmitters have the estimates required to calculate the precoders and receiver matrices, unless otherwise stated. Regarding the external interference, its model is left to be presented in chapter Chapter 4.

As a specific configuration of the simulator, several runs are taken in order to assure a good reliability to the results. Since the transmissions of the symbols are effectively simulated, the

average Bit Error Rate (BER) achieved by the system can be computed in order to grasp the error robustness of the algorithms. Complementary to that, a metric that can translate the maximum rate that the system can achieve is the sum capacity. The SINR of each stream decoded at each receiver can be calculated by (2.2), and then the capacity formula can be applied:

$$C = \log_2 (1 + SINR) . \tag{2.41}$$

Thus, the capacity achieved by all streams in the system is summed to yield the sum capacity, Hence, the evaluation of the algorithms is done in terms of these two metrics, since they provide distinct information regarding system performance.

Chapter 3

Channel Imperfection Analysis

This chapter begins the performance evaluation and the comparison of the previously presented algorithms. Moreover, two kinds of channel imperfection are considered in order to emulate a more realistic scenario. Thus, the influence of correlation between the transmitter antennas and the assumption of imperfect Channel State Information (CSI) knowledge are included on the modeling of the channel coefficients. Next section presents how these imperfections were modeled in this dissertation.

3.1 Imperfection Models

The channel model applied to simulate the correlation among antennas is the Kronecker channel model, which has a simple analytic treatment [26]. The characterization of this model separates the correlation at the transmission and at the reception, which is a quality that fits well with this work's purpose. Then, the Multiple Input Multiple Output (MIMO) channel from transmitter j to receiver k is modeled as:

$$\mathbf{H}_{kj} = \frac{1}{\sqrt{\mathrm{tr}\{\mathbf{R}_r\}}}\mathbf{R}_r^{1/2}\mathbf{H}_{kj}^w\left(\mathbf{R}_t^{1/2}\right)^T \qquad \forall j,k \in \{1,\ldots,K\}, \tag{3.1}$$

where $\mathbf{H}_{kj}^w \sim \mathcal{CN}(\mathbf{0},\mathbf{I})$. The receive and transmit correlation matrices are denoted by $\mathbf{R}_r$ and $\mathbf{R}_t$, respectively. The correlation at the reception is not considered here, then the receive correlation matrix is assumed to be an identity matrix. The transmit correlation matrix has its elements calculated from a single parameter α, and is given by [27]:

$$\mathbf{R}_t(m,n) = |\alpha|^{|m-n|} \quad \text{for } m,n \in \{1,\ldots,N_T\}, \tag{3.2}$$

where N_T is the number of transmit antennas. This model is widely used in the literature and industry and represents the correlation between elements of a uniform linear antenna array, where $\alpha = 0$ and $|\alpha| = 1$ correspond to no correlation and rank 1 channel, respectively [28].

For the imperfect channel modeling, it simply considered the addition of noise to the actual channel matrices. Thus, the channel matrices used at the precoding design stage will be given by [28]:

$$\mathbf{H}_{kj}^w = \sqrt{1-\beta^2}\tilde{\mathbf{H}}_{kj}^w + \beta\mathbf{E}_{kj}, \tag{3.3}$$

where $\mathbf{H}_{kj}^w \sim \mathcal{CN}(\mathbf{0},\mathbf{I})$ is the true Gaussian part of the channel matrix, $\tilde{\mathbf{H}}_{kj}^w \sim \mathcal{CN}(\mathbf{0},\mathbf{I})$ is the imperfect observation of $\mathbf{H}_{kj}^w$ available to the nodes, and $\mathbf{E} \sim \mathcal{CN}(\mathbf{0},\mathbf{I})$ is an i.i.d Gaussian noise term. This way, the β parameter characterizes the strength of the imperfect CSI knowledge,

varying from zero to one. That is, $\beta = 0$ corresponds to perfect channel knowledge and $\beta = 1$ corresponds to no CSI knowledge at the transmitter.

When taking both channel correlation and CSI error into account, the full channel model is then given by

$$\mathbf{H}_{kj}^{w} = \left(\sqrt{1-\beta^2}\tilde{\mathbf{H}}_{kj}^{w} + \beta\mathbf{E}_{kj}\right) \cdot \mathbf{R}_{t}^{1/2}. \tag{3.4}$$

3.2 Channel Imperfection Results

In order to assess the impact of channel imperfections on the performance of the Interference Alignment (IA) algorithms, two variations were considered on the cellular network scenario first presented in Section 2.5. These variations were chosen to provide cases on which the receivers do not perceive too much interference from the unintended transmitters and the other case where this interference is much stronger. Thus, in the first case the three users are placed far from each other respecting a distance of 70% of the cell radius from its respective transmitter, as shown in Figure 3.1(a). In the other case, illustrated in Figure 3.1(b), the users are near to each other respecting the same distance to the center of the cell, so that the pathloss that users experiment in both cases is the same. It is important to say that in this analysis the nodes are equipped with two antennas, hence, when they are employing IA algorithms, each transmitter-receiver pair sends one stream. However, when the Block Diagonalization (BD) scheme is employed the pairs are able to send two streams each.

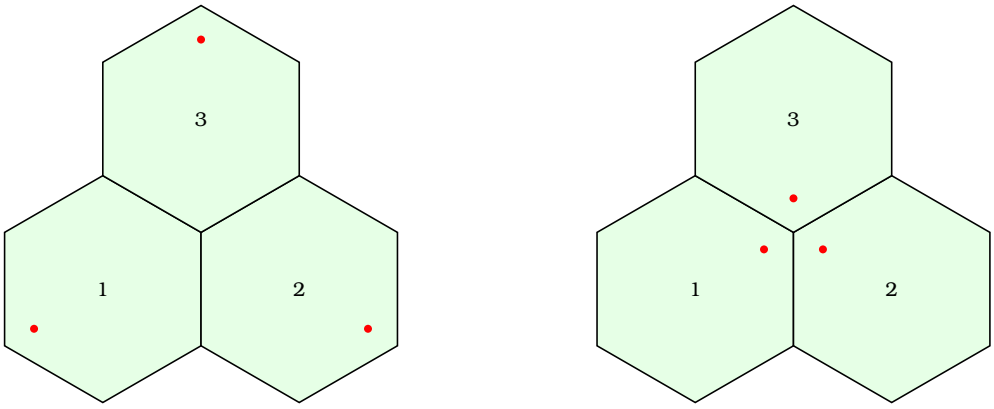

(a) Users far from the cluster center. (b) Users close to the cluster center.

Figure 3.1: Simulation scenarios of channel imperfection analysis. Cluster with 3 cells with one mobile at each cell.

The algorithm comparison starts by showing how their performance, in terms of the sum capacity, behaves when the Signal to Noise Ratio (SNR) is varied, under different cases of channel imperfections. Figures 3.2(a) and 3.2(b) present these performances when the CSI is perfectly known, $\beta = 0$ and the correlation among the antennas is very weak, $\alpha = 0.2$. First, all the algorithms present an almost linear gain with the scaling of the SNR, on both scenarios, which means that all of them were able to mitigate the interference and are just limited by noise. As expected, the BD algorithm achieves the highest sum capacity, at both scenarios, since it can send more streams than the IA-based schemes. Regarding the comparison among the IA algorithms, it can be perceived that those that apply the Zero-Forcing (ZF) filter at the reception, IA closed-form and IA alternating, present a slightly worse performance than the IA Minimum Mean Square Error (MMSE), this happens because their objective is just to accomplish the interference alignment, they do not care about the direct channel. Also, the IA closed-form is better than the alternating due to the choice of the best set of precoders.

Now, Figures 3.2(c) and 3.2(d) present the results that consider errors in the channel

knowledge, more specifically, the case where β is 0.4 and α is 0.2. Thus, this increment on the β parameter caused a great loss in the achieved sum capacity of all algorithms, at both scenarios. An interesting fact is that BD suffered more with the increased error than the IA-based algorithms. This might have happened because the BD process is performed in higher dimensional matrices than IA, then, if an error is inserted on these matrices the effect may be enhanced due to the larger number of entries. The case where the CSI knowledge is perfect, $\beta = 0$, and the correlation among antennas is large, $\alpha = 0.9$, is considered in Figures 3.2(e) and 3.2(f). Similar to the previous case, the performance loss can be noticed among all transmission schemes, however, now the loss is not too significant and all algorithms are affected similarly.

The Bit Error Rate (BER) results of the same set of simulation runs are presented in Figure 3.3. In the cases where the channel imperfections are very weak, Figures 3.3(a) and 3.3(b), the BD algorithm has the worst performance, unlike the sum capacity results. However, this behavior can be also explained by the number of streams this algorithm is able to send. Since this approach performs more parallel transmissions, then its data may be more susceptible to errors. Among the IA algorithms, the IA MMSE again performed better than the others, as expected, because its objective is to minimize the reception errors. The closed-form solution overcame the alternating algorithm due to the choice of the best set of precoders, since maximizing the minimum of the Signal to Interference-plus-Noise Ratios (SINRs) decreases the cases where the streams are more vulnerable to errors. This effect is better perceived in the BER than in the sum capacity, since the latter accounts the SINR inside a log factor.

Cases with stronger channel imperfections are assessed in Figures 3.3(c), 3.3(d), 3.3(e) and 3.3(f). From these results, the imperfect knowledge was shown to have a larger impact on the algorithm performances than the correlation among antennas. Despite the large correlation, the algorithms have their performance just slightly burdened, still achieving good values of BER. On the other hand, the imperfect CSI has a significant effect on the BER results, and none of the algorithms were able to improve their performance by scaling the SNR, when the β value was 0.4.

The previous analysis showed how the algorithms behave in terms of sum capacity and BER. Also, they provided preliminary information on the effect of the channel imperfections on the algorithms' performances. Henceforth, the effect of transmit antenna correlation (α parameter) and CSI estimation error (β parameter) are deeper analyzed. The main objective in this analysis is to grasp the influence of the choice of the α and β values on the described algorithms and how they can provide gains or performance loss in relation to the sum capacity and BER metrics.

The first set of results was acquired from simulations considering 15 dB of SNR at the border of the cells. In Figure 3.4, the α value was varied from 0.2 to 0.9, so that the impact of the correlation among the transmitting antennas can be evaluated, in terms of both performance metrics. It is important to say that the β value is fixed in 0 in this set of simulations. Regarding the sum capacity, it can be perceived that, for both scenarios, all the algorithms present a performance loss when the correlation increases. Although the BD algorithm presented the best performance in all cases, it showed a more accentuated loss at high values of α. When the BER is considered, as well as the sum capacity, the performance gets worse when the correlation is increased, with the BD algorithm presenting the worst performance. Still in this case, the algorithms that presented a slightly accentuated loss are the IA MMSE and the closed-form, which achieved the best results, in terms of BER.

Considering the same network configuration of the correlation analysis, with an SNR of

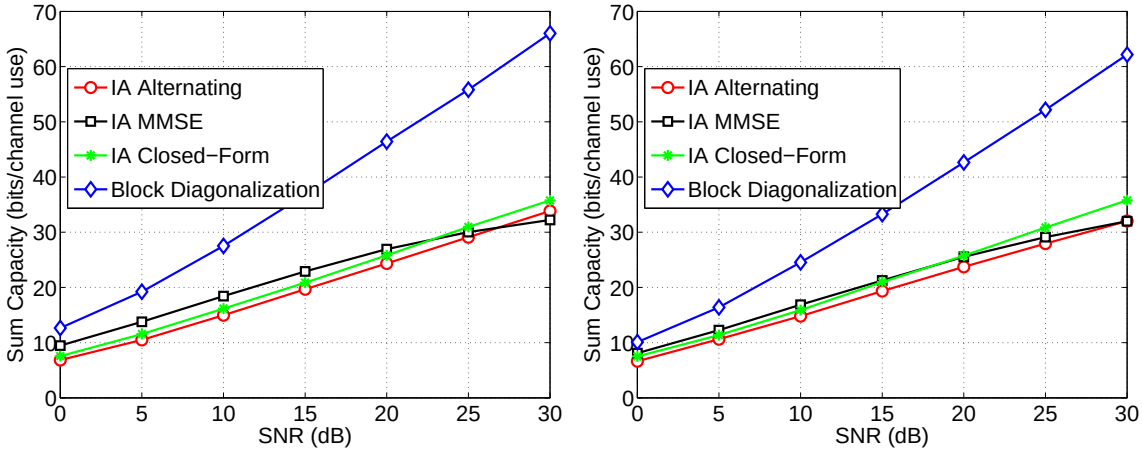

(a) $\alpha = 0.2$ and $\beta = 0$, scenario 1.

(b) $\alpha = 0.2$ and $\beta = 0$, scenario 2.

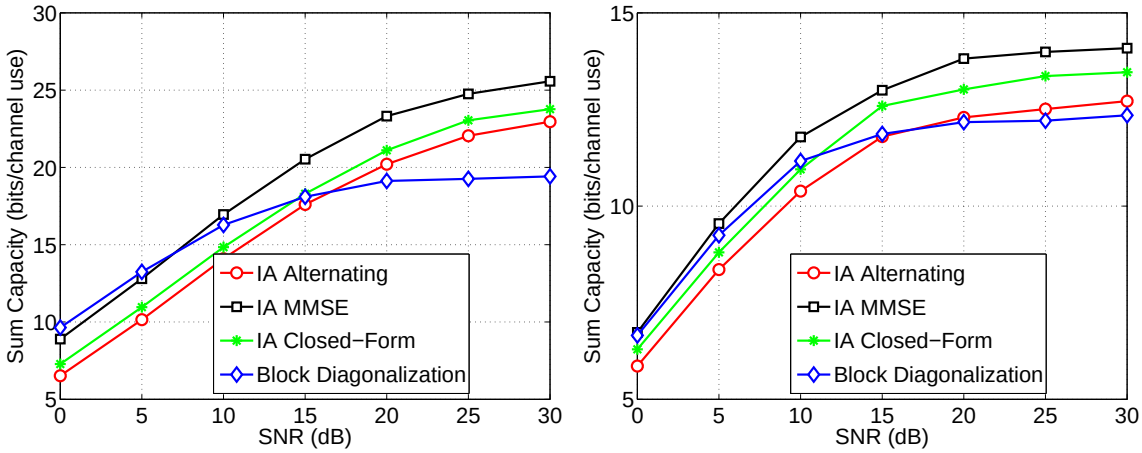

(c) $\alpha = 0.2$ and $\beta = 0.4$, scenario 1.

(d) $\alpha = 0.2$ and $\beta = 0.4$, scenario 2.

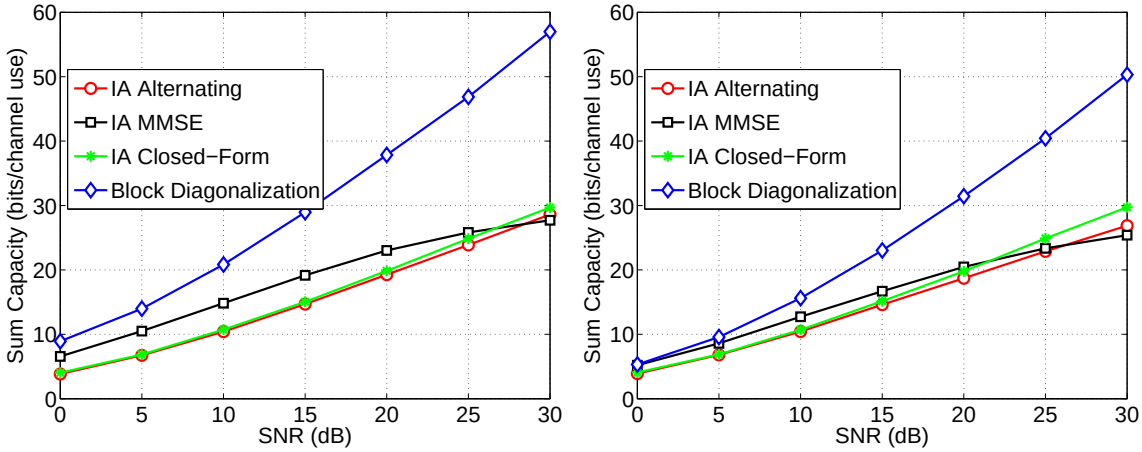

(e) $\alpha = 0.9$ and $\beta = 0$, scenario 1.

(f) $\alpha = 0.9$ and $\beta = 0$, scenario 2.

Figure 3.2: Sum Capacity as a function of the SNR for different combinations of α and β.

15 dB at the cells' edge, Figure 3.5 presents the sum capacities and BERs achieved by all algorithms when the β parameter is varied from 0 to 1, while the α value is fixed in 0.2. Thus, in Figures 3.5(a) and 3.5(b), the large impact of the β parameter on the BD sum capacity is highlighted. The BD algorithm is more affected by this parameter due to the size of matrices that are processed in the precoding design, as already previously discussed. Consequently, IA appears to be more robust to the CSI errors than Joint Processing (JP)-based schemes, since the precoding design, in these schemes, is performed as single transmitter-receiver pairs with

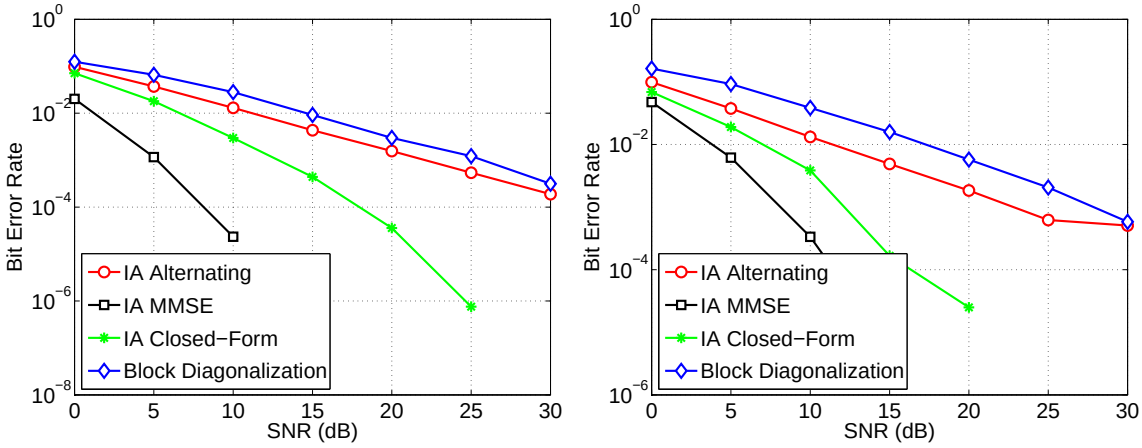

(a) $\alpha = 0.2$ and $\beta = 0$, scenario 1.

(b) $\alpha = 0.2$ and $\beta = 0$, scenario 2.

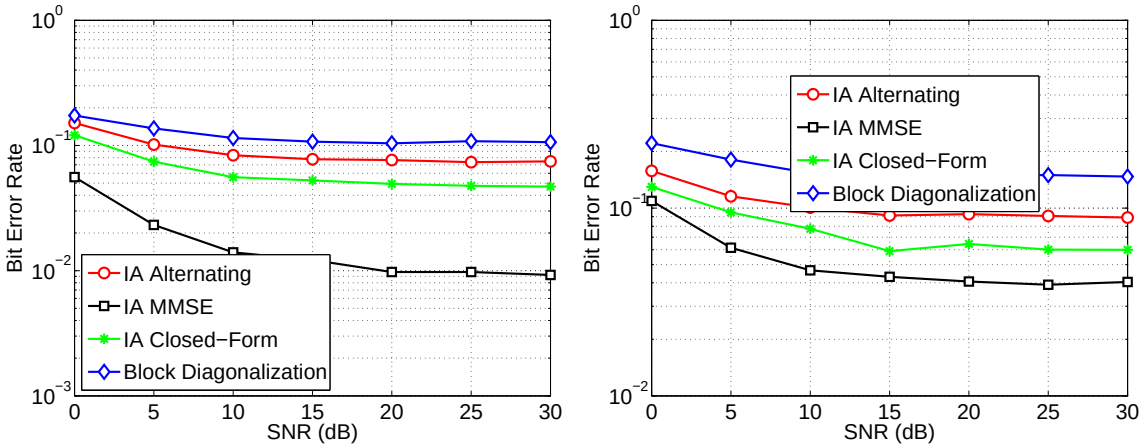

(c) $\alpha = 0.2$ and $\beta = 0.4$, scenario 1.

(d) $\alpha = 0.2$ and $\beta = 0.4$, scenario 2.

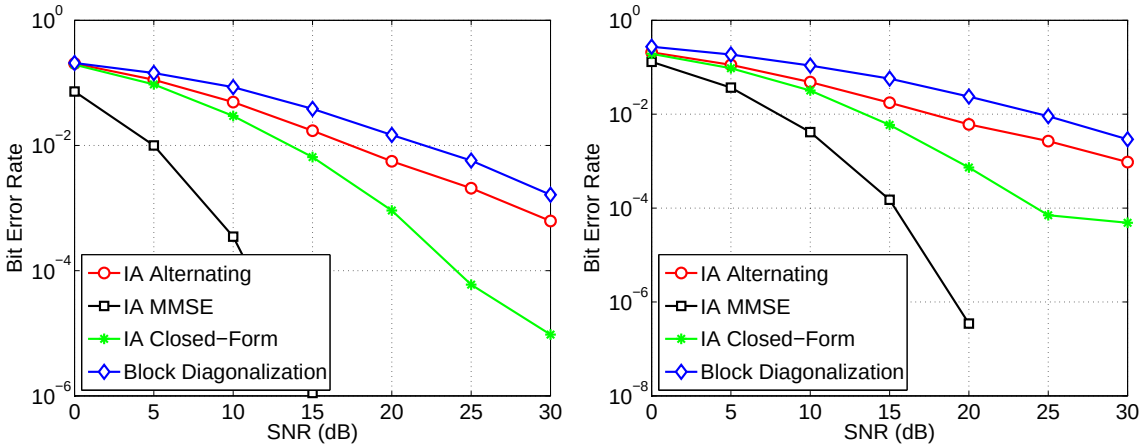

(e) $\alpha = 0.9$ and $\beta = 0$, scenario 1.

(f) $\alpha = 0.9$ and $\beta = 0$, scenario 2.

Figure 3.3: BER as a function of the SNR for different combinations of α and β.

more antennas. The channel estimation error also has a large impact concerning the BER achieved by the algorithms, as it can be seen in Figures 3.5(c) and 3.5(d). However, for low and medium values of β, the IA MMSE and the closed-form are the best ones, followed by the alternating algorithm. When the β is close to 1, the algorithms perform the precoding design with practically random channel matrices, therefore the BER tends to 0.5, which represents random bit decisions.

In order to conclude the evaluation of the impact of channel imperfections, the same set of results, but now considering a low SNR case, is shown in Figures 3.6 and 3.7. From

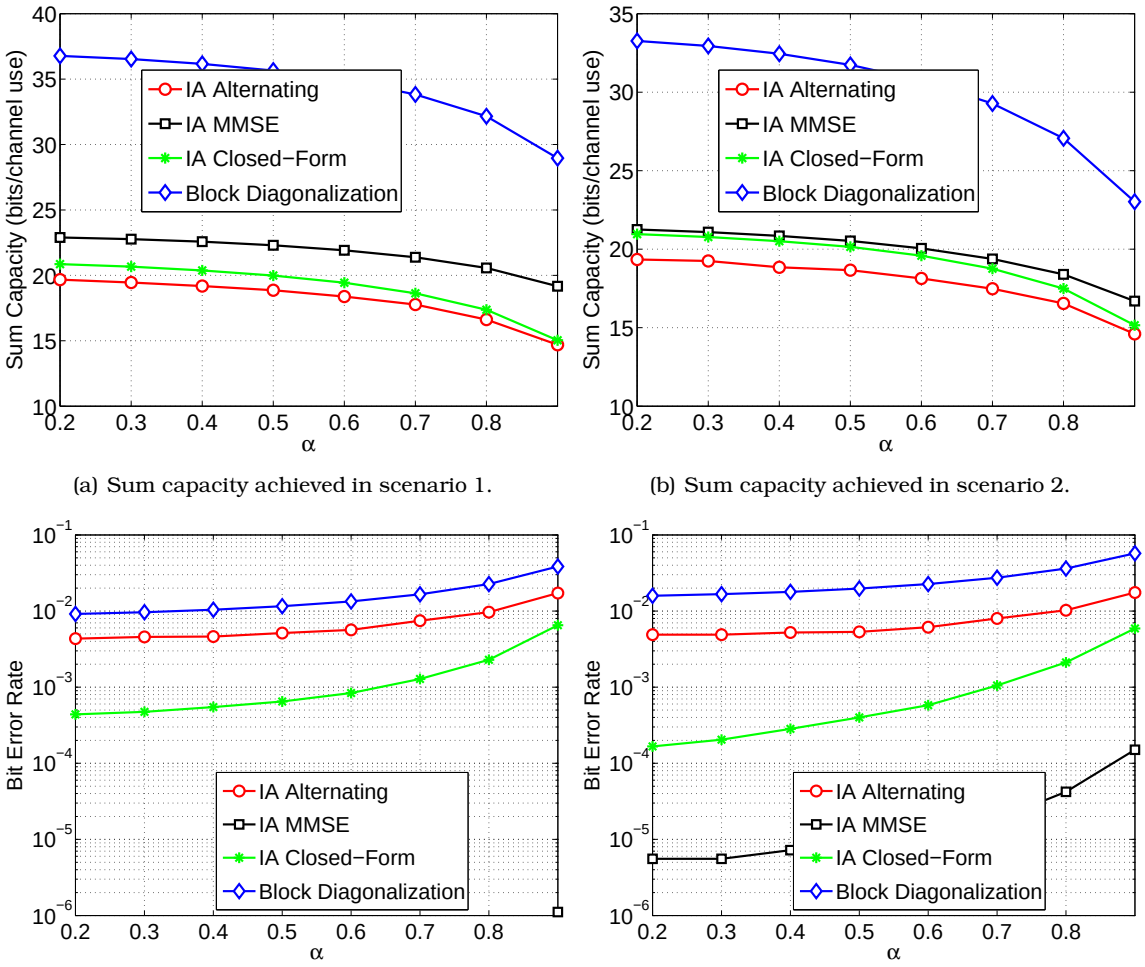

(a) Sum capacity achieved in scenario 1.

(b) Sum capacity achieved in scenario 2.

(c) BER achieved in scenario 1.

(d) BER achieved in scenario 2.

Figure 3.4: Impact of α parameter on the algorithms performance for SNR $= 15$ dB.

the achieved results, the same conclusions of the previous case can be drawn for the case where the SNR at the border of the cells is 0 dB. The correlation affects the performance of the schemes, but the error in the channel knowledge degrades much more the sum capacity and the BER. Moreover, in terms of sum capacity, the BD algorithm presents better performance when the CSI knowledge is good, while the IA algorithms are more robust to channel estimation errors Finally, the IA-based schemes always provide the best BER, especially the IA MMSE algorithm, since its objective is precisely to minimize the reception errors.

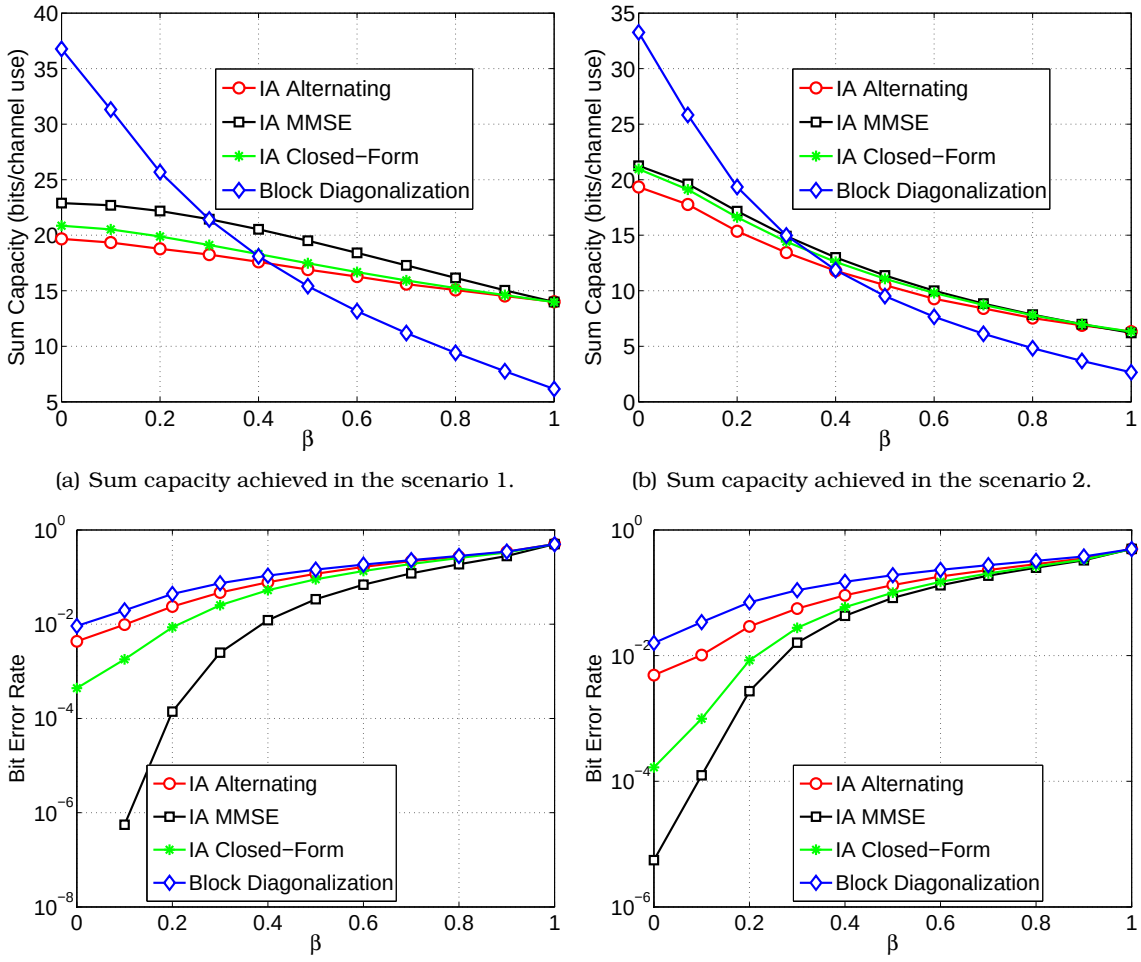

(a) Sum capacity achieved in the scenario 1.

(b) Sum capacity achieved in the scenario 2.

(c) BER achieved in the scenario 1.

(d) BER achieved in the scenario 2.

Figure 3.5: Impact of β parameter on the algorithms performance for SNR $= 15$ dB.

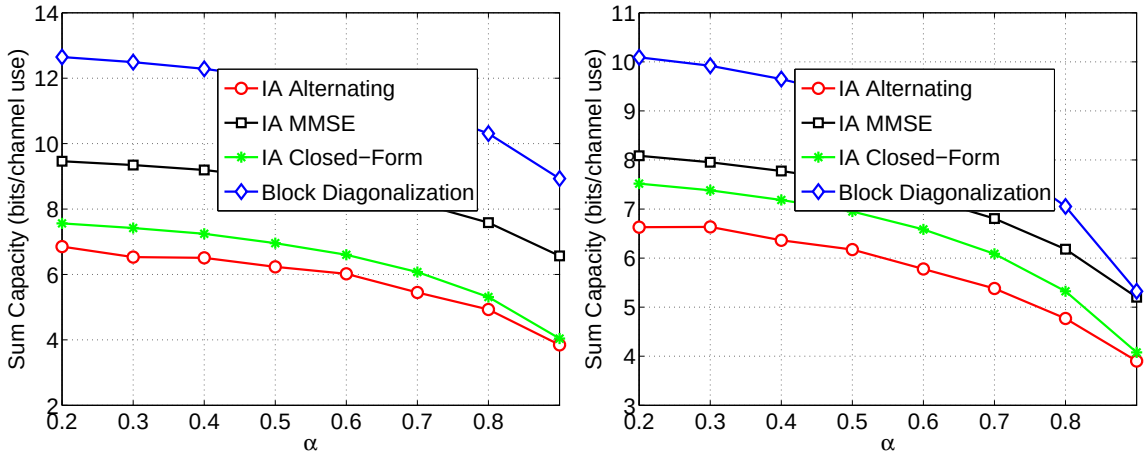

(a) Sum capacity achieved in the scenario 1.

(b) Sum capacity achieved in the scenario 2.

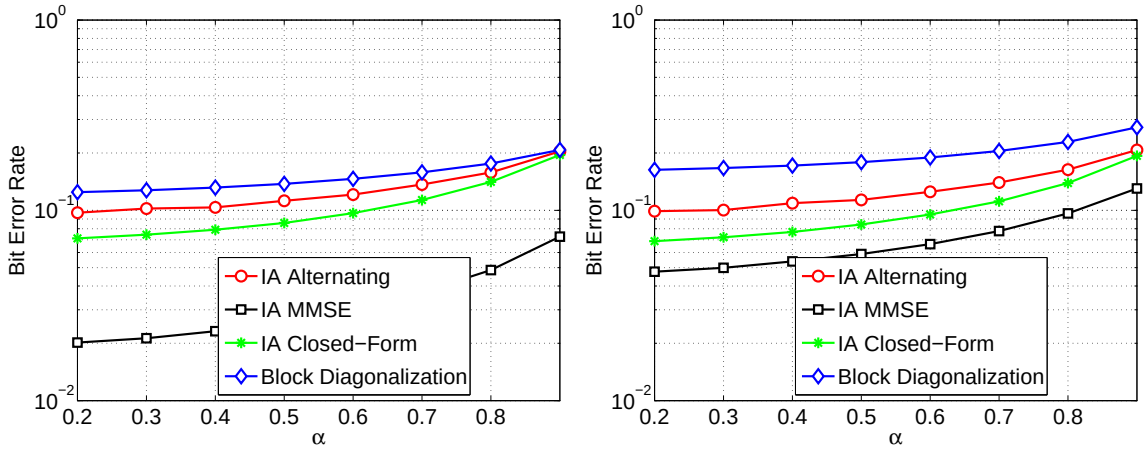

(c) BER achieved in the scenario 1.

(d) BER achieved in the scenario 2.

Figure 3.6: Impact of α parameter on the algorithms performance for SNR $= 0$ dB.

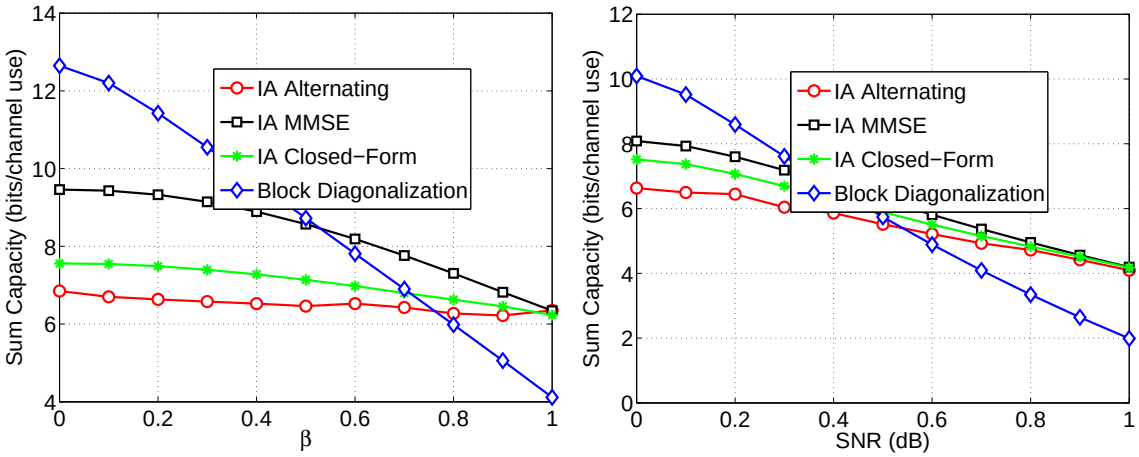

(a) Sum capacity achieved in the scenario 1.

(b) Sum capacity achieved in the scenario 2.

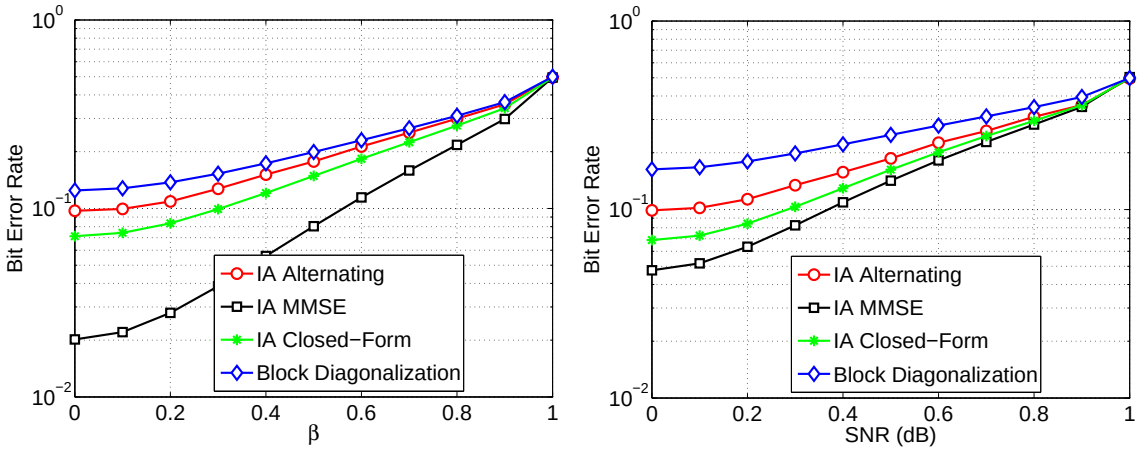

(c) BER achieved in the scenario 1.

(d) BER achieved in the scenario 2.

Figure 3.7: Impact of β parameter on the algorithms performance for SNR $= 0$ dB.

Chapter 4

External Interference Analysis

The feasibility conditions of Interference Alignment (IA) limit the number of cooperating pairs, especially when it is accomplished along the spatial dimension. Three cooperating pairs require at least two antennas per node to perform the communication free of interference. However, at this configuration, if a neighbor transmitter is activated, the cooperation among the four base stations is now not possible. On real cellular networks there are much more than three cells, they actually are composed by dozens of cells. So, at these networks, even if the IA is applied in groups of three, for instance, there will continue to exist some interference. Therefore, it would be a realistic assumption to consider an external interference burdening the cooperating pairs, and thus deserves to be studied. The next sections show how this uncoordinated interference can be included on the simulations.

4.1 External Interference Model

To add the effect of an external interference in the MIMO-Interference Channel (MIMO-IC), presented in Section 2.1, it is just necessary to add a parcel of the incoming signal from outside of the cooperating pairs. Then, the received signal at the i-th receiver is now written as:

$$\mathbf{y}_k = \mathbf{H}_{kk}\mathbf{V}_k\mathbf{d}_k + \sum_{j=1,j\neq k}^{K} \mathbf{H}_{kj}\mathbf{V}_j\mathbf{d}_j + \mathbf{n}_k + \mathbf{e}_k, \tag{4.1}$$

where $\mathbf{e}_k$ is a random vector of colored noise of dimension $N_R \times 1$. Its covariance matrix is $\mathbf{R}_k = \mathbb{E}\{\mathbf{e}_k\mathbf{e}_k^H\}$. Figure 4.1 illustrates a cluster of interfering users burdening the transmissions inside of the Coordinated Multi-Point (CoMP) cluster.

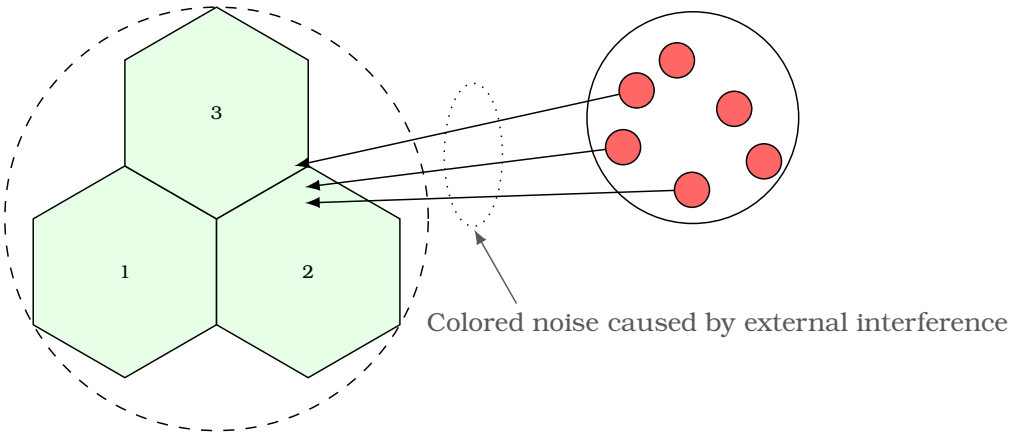

Figure 4.1: Receives inside the cluster perceiving an external interference, modeled as colored noise.

Modeling the external interference as colored noise allows the application of different kinds of external interference in the simulator. If there is just one dominant interferer, then each receiver would perceive it in just one dominant direction. However, if there is a larger number, the perceived interference becomes closer to white noise. This characteristic can be controlled by its covariance matrix. Thus, the rank of the $\mathbf{R}_k$ matrix plays an important role on the system model. If it is intended to add just one dominant interferer in the system, this covariance matrix must have rank one. However, if there are multiple sources of interference with different strengths, then the covariance matrix has to be modeled so that its rank is greater than one and its eigenvalues must follow the power perceived at each receiver.

Once the covariance matrix of the external interference is properly chosen, the colored noise vector must be calculated. Since it is known that the covariance matrix is symmetric, then it can be decomposed as:

$$\mathbf{R} = \mathbf{R}^{1/2}(\mathbf{R}^{1/2})^H, \tag{4.2}$$

therefore, from a generic Additive White Gaussian Noise (AWGN) vector $\mathbf{x}$, the colored noise $\mathbf{y}$ is generated by:

$$\mathbf{y} = \mathbf{R}^{1/2}\mathbf{x}. \tag{4.3}$$

This generated vector has $\mathbf{R}$ as covariance matrix, which can be deducted from:

$$\mathbb{E}\{\mathbf{y}\mathbf{y}^H\} = \mathbb{E}\{\mathbf{R}^{1/2}\mathbf{x}\mathbf{x}^H(\mathbf{R}^{1/2})^H\} \tag{4.4}$$

$$\mathbb{E}\{\mathbf{y}\mathbf{y}^H\} = \mathbf{R}^{1/2}\underbrace{\mathbb{E}\{\mathbf{x}\mathbf{x}^H\}}_{\mathbf{I}}(\mathbf{R}^{1/2})^H = \mathbf{R}. \tag{4.5}$$

This is how the external interference vector is accounted for in the simulator, through the external interference covariance matrix, which has its square root multiplied by an AWGN vector to generate the colored noise samples. The next sections present some improvements that can be performed on the algorithms to take into account this interference.

4.2 Modification on Interference Alignment algorithms

Applying the IA technique for a large number of transmitter-receiver pairs may be impracticable, as discussed in Section 2.2.2. Also, as the number of pairs increases, the number of dimensions required to accomplish IA increases even faster. This is an issue that affects much more IA over the spatial dimension than the other dimensions, such as frequency. This occurs due to the space constraints at the receivers, which in turn limits how many antennas they can have. Since the spatial dimension is indeed the most used in IA, it is fair to consider that the IA groups perceive interference from “outside”. With that in mind, employing the pure IA algorithms in such scenarios could either require a very large number of dimensions to cancel all the interference and/or neglect an external interference source that could destroy the benefit of interference-free transmission, possibly making IA unrealizable in that case.

Although the uncoordinated interference cannot be controlled, the interference from the cooperating pairs can, or more precisely, the interference subspace can be controlled (specifically in the algorithms that employ the alternating framework). Thus, one way to mitigate this external interference is to take into account its covariance matrix to steer, at each receiver, the internal interference to this preferable direction. That is, to consider the external interference when determining the interference subspace at each receiver. This

will, to some extent, allow the (cooperating) transmitters to align their interference at the unintended receivers with the external interference (from the non-cooperating transmitter) that those receivers perceive.

Therefore, the Algorithms 2.2 and 2.3 can naturally be modified to include the covariance matrix of the uncoordinated interference in the step related to updating the interference subspace, while the other steps are performed as usual. In Algorithm 2.2 this corresponds to modifying step 2 when determining the interference subspace, $\mathbf{\Phi}_k$, which is now given by

$$\mathbf{\Phi}_k^{opt} = \nu_{min}^S \left(\sum_{\substack{j=1 \\ j \neq k}}^{K} \mathbf{H}_{kj} \mathbf{V}_j \mathbf{V}_j^H \mathbf{H}_{kj}^H + \mathbf{R}_k \right), \tag{4.6}$$

where $\mathbf{R}_k$ corresponds to the covariance matrix of the external interference seen by user k. In Algorithm 2.3 this corresponds to modifying (2.33) to include $\mathbf{R}_k$ so that the receive filter is now given by:

$$\mathbf{U}_k = \left(\sum_{j=1}^{K} \mathbf{H}_{kj} \mathbf{V}_j \mathbf{V}_j^H \mathbf{H}_{kj}^H + \mathbf{R}_k \right)^{-1} \mathbf{H}_{kk} \mathbf{V}_k. \tag{4.7}$$

These simple modifications were shown to boost the performance of regular IA in [21]. However, note that by taking into account the external interference when determining the interference subspace, a new restriction is imposed into the problem. Because of that, in several cases a perfect interference alignment might not be accomplished anymore, and thus the interference will not be completely eliminated. That is, the complete cancellation of the "internal interference" is compromised in order to be able to later cancel part of the external interference as well. If the external interference is strong, then the modifications in (4.6) and (4.7) will give more emphasis on the external interference and vice-versa. However, if the external interference steers multiple preferable directions, then this approach is less effective, since even though the reserved interference subspace will capture external interference in some of these directions, any interference in other directions (which will be in the desired signal subspace) will have an impact on the desired signal detection. In this work, when the covariance matrix of the external interference is taken into account, the algorithm will be labeled as "enhanced".

Moreover, in [21] it was shown that the alternating minimization algorithm is a lower bound for its correspondent enhanced algorithm. It was also shown that the perfect alignment is almost surely impossible. Therefore, even when the algorithm tries to fit the external interference in the interference subspace, some interference will leak to the desired signal space, disturbing the symbols detection. Thus, aiming to bring the IA algorithm closer to the feasibility, such that less interference leaks into the desired subspace, the number of transmitter streams is reduced. As a consequence, the internal interference may span a smaller subspace and maybe it can be better adapted to the external interference direction(s).

The selection of which stream(s) will not be transmitted must be a careful choice, since IA already suppresses, to a certain extent, some streams to perform transmissions free of interference. So, in order to limit the throughput loss in this work, it is here assumed that the user that perceives the strongest interference will reduce in one its number of streams. Consequently, for the 3-user case, this approach can only be applied when the nodes are equipped with at least four antennas, since for this configuration the pairs are able to send two streams each. This method will be referred to as "modified" IA.

4.2.1 Whitening Block Diagonalization (BD)

As the BD algorithm was chosen as a benchmark in this work, for fairness of comparison it should also be modified to take into account the external interference, as it was the case with the IA algorithm. Hence, the modification on the BD algorithm uses the knowledge of the external interference covariance matrix in order to whiten the external interference and perform a transmission with the block diagonalization method. The procedure of this algorithm is very similar to the conventional BD algorithm, with the main difference being that the block diagonalization is performed in an equivalent channel previously processed with the whitening filter. The algorithm is explained in more details in the following.

Similarly to the conventional BD, the system model from (4.1) can be rewritten as:

$$\mathbf{y}_k = \mathbf{H}_k\mathbf{M}_k\mathbf{d}_k + \mathbf{H}_k\sum_{\substack{j=1\\ j\neq k}}^{K}\mathbf{M}_j\mathbf{d}_j + \mathbf{e}_k + \mathbf{n}_k. \tag{4.8}$$

The first step is to apply a whitening filter, $\mathbf{W}_k = \mathbf{R}_k^{-\frac{1}{2}}$, to the received signal, which yields:

$$\mathbf{r}_k = \mathbf{W}_k\mathbf{H}_k\mathbf{M}_k\mathbf{d}_k + \mathbf{W}_k\mathbf{H}_k\sum_{\substack{j=1\\ j\neq k}}^{K}\mathbf{M}_j\mathbf{d}_j + \underbrace{\mathbf{W}_k\mathbf{z}_k}_{\text{whitened noise}}, \tag{4.9}$$

where $\mathbf{z}_k = \mathbf{e}_k + \mathbf{n}_k$ and $\mathbf{H}_{eq,k} = \mathbf{W}_k\mathbf{H}_k$ is the equivalent channel that will be block diagonalized with the $\mathbf{M}_k$ precoder matrix.

Henceforth, the same steps of the conventional algorithm can be performed, but now considering the effective channel. Thus, the $\mathbf{B}_k$ matrix is designed in a certain way that the interference is canceled, so that its columns span the null space of $\mathbf{W}_l\mathbf{H}_l$ $(\forall l \neq k)$. Then, $\widetilde{\mathbf{H}}_k$ can be defined as:

$$\widetilde{\mathbf{H}}_k = \left[(\mathbf{W}_1\mathbf{H}_1)^T\cdots(\mathbf{W}_{k-1}\mathbf{H}_{k-1})^T \;\; (\mathbf{W}_{k+1}\mathbf{H}_{k+1})^T\cdots(\mathbf{W}_K\mathbf{H}_K)^T\right]^T, \tag{4.10}$$

and its Singular Value Decomposition (SVD) is:

$$\widetilde{\mathbf{H}}_k = \widetilde{\mathbf{U}}_k\left[\widetilde{\mathbf{\Lambda}}_k \;\mathbf{0}\right]\left[\widetilde{\mathbf{V}}_k^{(1)} \;\widetilde{\mathbf{V}}_k^{(0)}\right]^H. \tag{4.11}$$

In order to automatically eliminate the internal interference, $\mathbf{B}_k$ is composed by the N_R columns of $\widetilde{\mathbf{V}}_k^{(0)}$. Thus, the resulting received signal is:

$$\mathbf{r}_k = \mathbf{W}_k\mathbf{H}_k\mathbf{B}_k\mathbf{D}_k\mathbf{d}_k + \mathbf{W}_k\mathbf{z}_k. \tag{4.12}$$

The parallelization of the data transmission can now be accomplished. Then another SVD is applied to $\mathbf{H}_{eff,k}$, defined as:

$$\mathbf{H}_{eff,k} = \mathbf{W}_k\mathbf{H}_k\mathbf{B}_k = \mathbf{U}_k\mathbf{\Lambda}_k\mathbf{V}_k^H, \tag{4.13}$$

then, similar to the conventional BD, the precoder $\mathbf{D}_k$ corresponds to the multiplication of the $\mathbf{V}_k$ matrix by the power control matrix, $\mathbf{P}_k^{\frac{1}{2}}$, while the detection is accomplished by matrix $\mathbf{U}_k^H$.

In summary, the precoder matrix is:

$$\mathbf{M}_k = \mathbf{B}_k\mathbf{D}_k = \left(\widetilde{\mathbf{V}}_k^{(0)}\right)_{(1:N_R)}\mathbf{V}_k\mathbf{P}_k^{\frac{1}{2}}. \tag{4.14}$$

Also, the reception matrix can be written as:

$$\widehat{\mathbf{M}}_k = \mathbf{U}_k^H \mathbf{W}_k. \tag{4.15}$$

As it was the case for all the other algorithms, no power allocation scheme is considered, so the waterfilling step is neglected here. The next section presents how the uncoordinated interference was included in the simulator described in Chapter 2.

4.3 External Interference Analysis

Now it is considered that each receiver is burdened by the presence of a source of external interference. Such interference is assumed to be located at the border of the CoMP cluster, in a position such that the distances to their respective receivers are minimum. Thus, as presented in Section 4.1, each transmission is disturbed by a colored noise modeled through the proper covariance matrix. The power of these interferers can be varied from 0 to 20 dBm, which allows several Signal to Interference-plus-Noise Ratios (SINRs) situations to be modeled. For instance, for a user placed 300 m far from the cluster border, the SINR varies from -22 up to 26 dB for the different values of Signal to Noise Ratios (SNRs).

Furthermore, it is now assumed that the users are randomly placed inside the cells, and two cases are considered: they can be distributed over all the cluster or respecting a distance of 2/3 of the cluster radius, as it can be seen in Figure 4.2. Hence, by knowing the position of each receiver and each interference source, the path loss of the transmitted and interference symbols can be properly calculated.

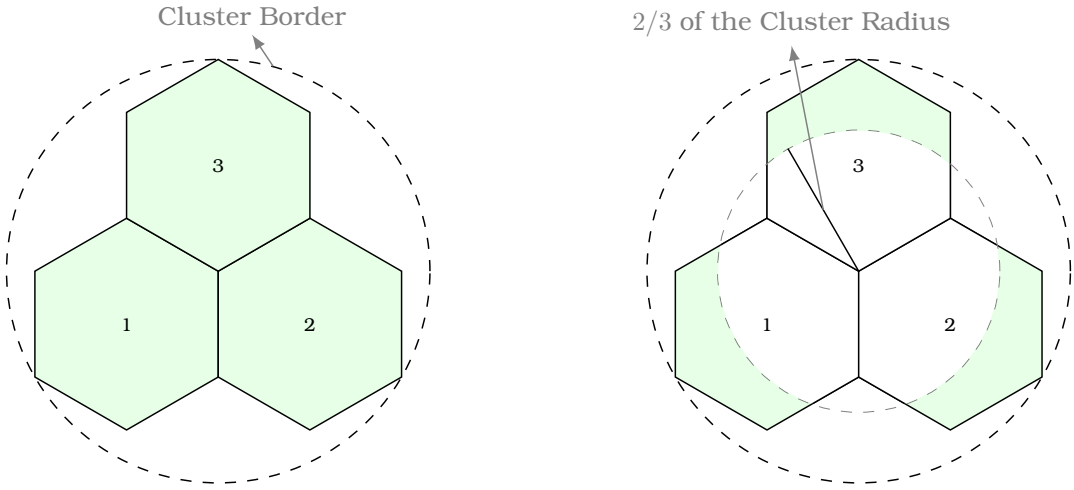

(a) Users distributed over all the cluster.

(b) Users distributed close to the border of the cluster, respecting a distance of 1.3 km from the center.

Figure 4.2: Simulation scenarios of external interference analysis. Cluster with 3 cells with one mobile at each cell.

4.3.1 Two antennas per node case

The external interference analysis is started by considering the same network configuration of the previous chapter, assuming that each node is equipped with two antennas. Therefore, the IA-based algorithms send one stream per transmitter while BD is able to send two streams per pair. Regarding the external interference, it is first assumed that its covariance matrix has rank 1, which emulates the presence of a dominant interferer.

In the first analysis, shown in Figure 4.3, the users were uniformly placed over all cells. In this scenario, the behavior of the sum capacity achieved by each algorithm was evaluated,

with the variation of the external interference level for different SNR values at the border of the cell.

It is possible to verify, especially in low SNR cases, that the external interference has a large impact on the performance of the algorithms that do not try to mitigate the external interference, which are the conventional BD and IA alternating. The IA algorithms that take into account the covariance matrix of the external interference achieved almost the same sum capacity for all values of external interference power. This shows the effectiveness of this approach on mitigating the external interference, despite a perceived loss for high values of external interference, that is probably caused by the maximum achievable Degree of Freedom (DoF). It is worth remembering that perfect alignment is almost surely not possible [21] at this configuration. What the enhanced algorithms do is try to adapt, as much as possible, the interference subspace to the external interference direction. So, in cases in which the external interference power is dominant, performance losses are perceived. Another important observation is that albeit the enhanced IA algorithms send less data streams compared to the BD, they could achieve better sum capacities.

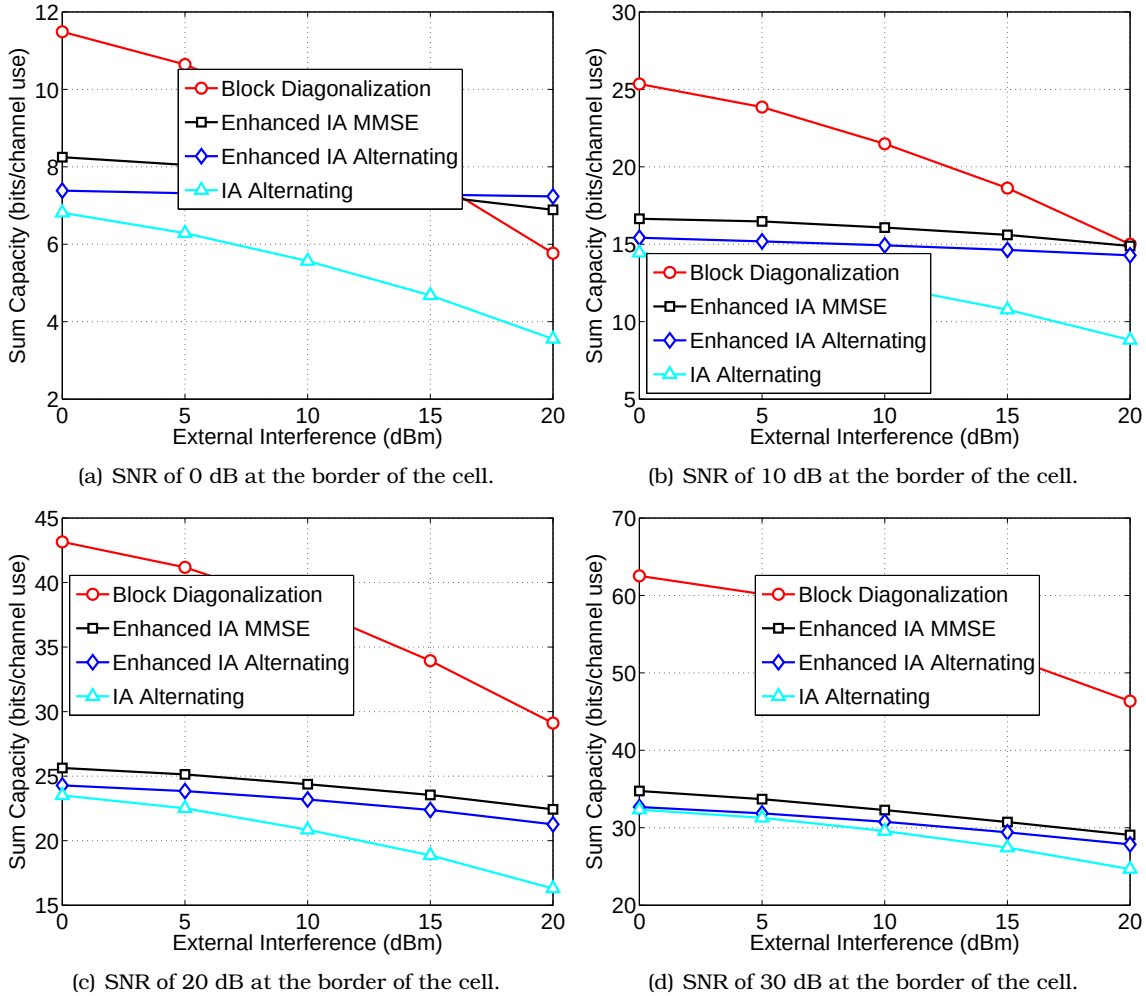

(a) SNR of 0 dB at the border of the cell.

(b) SNR of 10 dB at the border of the cell.

(c) SNR of 20 dB at the border of the cell.

(d) SNR of 30 dB at the border of the cell.

Figure 4.3: Sum Capacity achieved by the algorithms versus External Interference level for different SNR values at the border of the cell.

Continuing with the external interference impact analysis, some figures are now presented that vary the average SNR value at the cell border for different levels of external interference. Additionally, in this case, it was also considered the scenario in which the users are distributed closer to the border of the cluster. This was done because in the regular scenario there are few users that perceive high interference, since most users are closer to the center of the cluster. Figure 4.4 shows the sum capacity results for both scenarios.

In Figures 4.4(a), 4.4(c) and 4.4(e), at the left side, sum capacity results are presented for the scenario in which users are placed over all the cluster, for cases with external interference at the border of the cluster of 0, 10 and 20 dBm, respectively. From these figures it can be verified that, in general, BD performs better than the other algorithms because it is able to send more streams. For the case in which users experience higher external interference, the enhanced IA algorithms perform better than the conventional ones, BD and IA alternating. Moreover, the Minimum Mean Square Error (MMSE)-based algorithm achieves higher sum capacity values than the alternating algorithm, which was already expected, since the alternating algorithm uses a Zero-Forcing (ZF)-based approach.

The sum capacity results for the scenario in which users are closer to the border is presented in Figures 4.4(b), 4.4(d) and 4.4(f), at the right side. In the case of low external interference, the curves have the same behavior as the previous results for the uniform distribution. However, when the external interference level increases, it can be observed that the algorithms that deal with the external interference perform much better than the BD algorithm. Therefore, it is possible to find scenarios in which these enhanced algorithms perform better than BD.

In Figure 4.5 the results related to the Bit Error Rate (BER) metric are presented, also considering both scenarios. It is possible to see that now, BD and conventional IA algorithms achieve the worst result, due to their incapability to mitigate the external interference, with a slight advantage for the IA approach, since it has less streams to eliminate the interference. The use of enhanced algorithms that treat the interference provides a significant gain, especially for the MMSE-based algorithm, because its design criterion is to mimimize the Mean Square Error (MSE) at the reception. Similar to the sum capacity results, the BER curves behavior does not change with the different users' positioning.

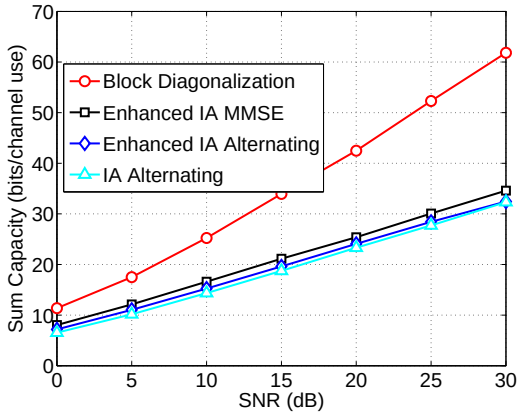

(a) External Interference of 0 dBm. Users distributed over all cells.

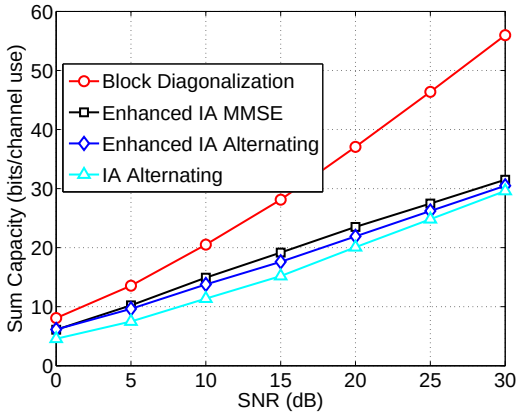

(b) External Interference of 0 dBm. Users after 2/3 of the cluster radius.

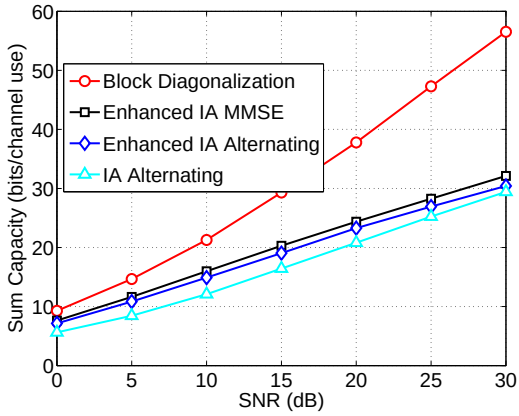

(c) External Interference of 10 dBm. Users distributed over all cells.

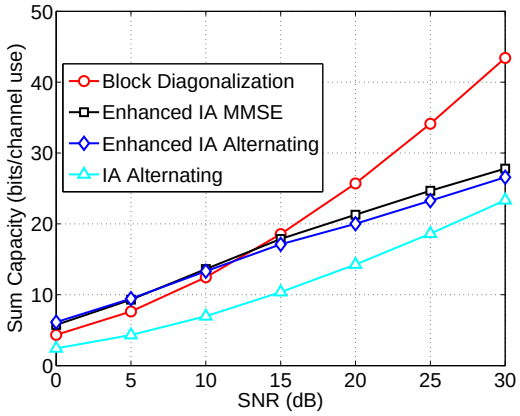

(d) External Interference of 10 dBm. Users after 2/3 of the cluster radius.

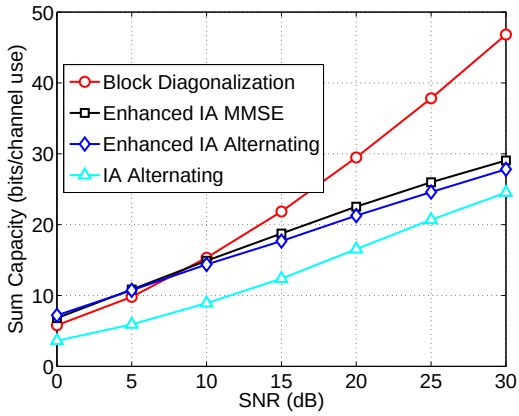

(e) External Interference of 20 dBm. Users distributed over all cells.

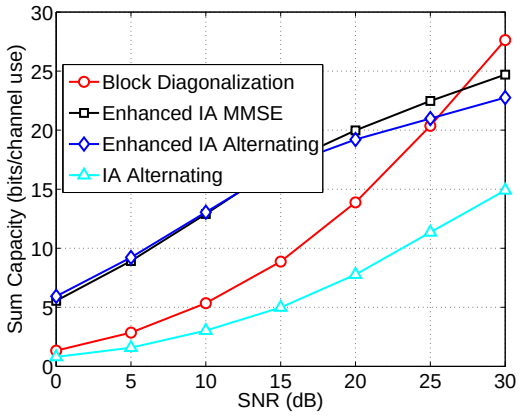

(f) External Interference of 20 dBm. Users after 2/3 of the cluster radius.

Figure 4.4: Sum Capacity versus SNR for different external interference values at the border of the cluster. At the left side, the results relate to the case in which users are distributed over all cells and at the right side, users are distributed respecting a distance of 2/3 of the cluster radius.

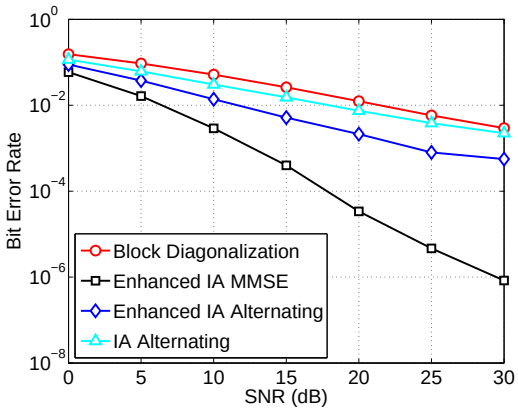

(a) External Interference of 0 dBm. Users distributed over all cells.

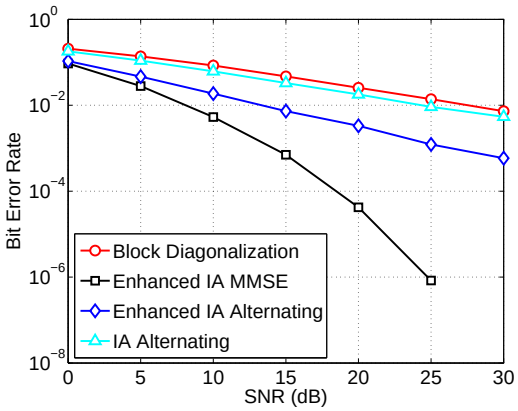

(b) External Interference of 0 dBm. Users after 2/3 of the cluster radius.

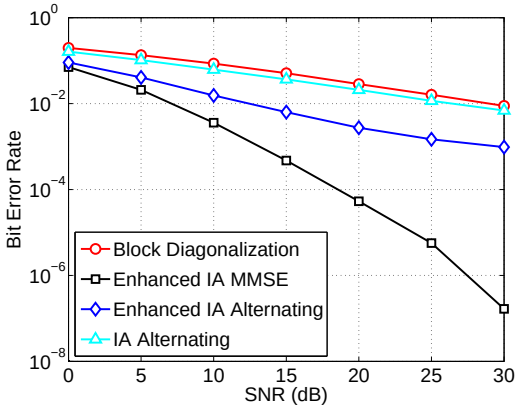

(c) External Interference of 10 dBm. Users distributed over all cells.

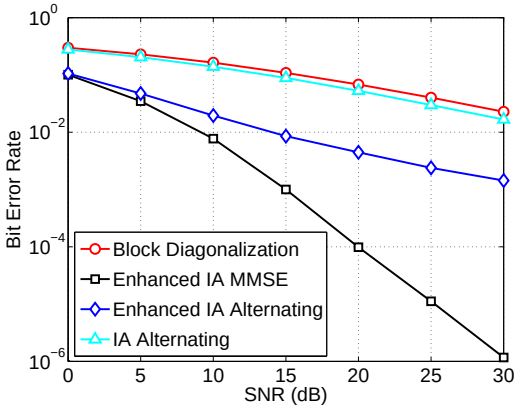

(d) External Interference of 10 dBm. Users after 2/3 of the cluster radius.

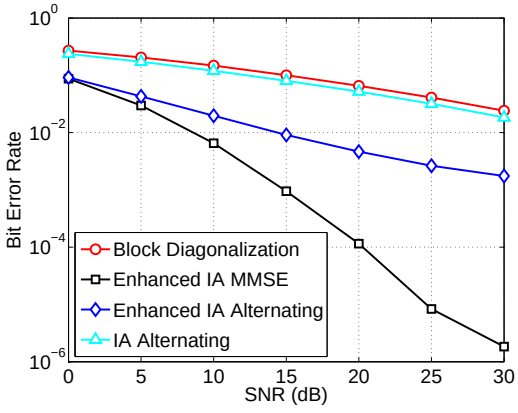

(e) External Interference of 20 dBm. Users distributed over all cells.

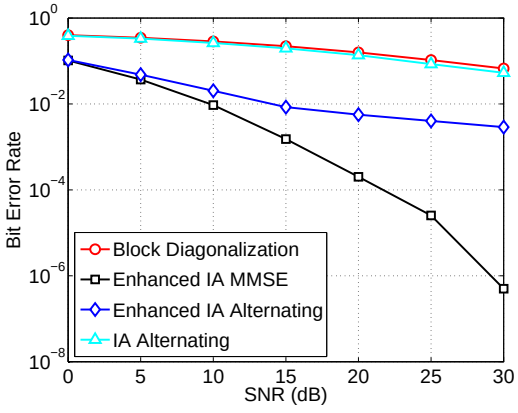

(f) External Interference of 20 dBm. Users after 2/3 of the cluster radius.

Figure 4.5: BER versus SNR for different external interference values at the border of the cluster. At the left side, the results relate to the case in which users are distributed over all cells and at the right side, users are distributed respecting a distance of 2/3 of the cluster radius.

4.3.2 Four antennas per node case

For the sake of having more variations of external interference, a cellular scenario with nodes equipped with four antennas is now considered. Hence, the number of dominant directions of the external interference (the rank of the external interference covariance matrix) can be varied up to four. Now the BD whitening algorithm is introduced in the analysis, as well as the modified IA. For this antenna configuration the BD-based algorithms are able to transmit up to four streams per user while IA is able to transmit two streams per user. Also, the modified IA (see Section 4.2) will transmit a total of five streams. That is, two users can receive two streams and the user that perceives the strongest level of external interference receives just one data stream. At this analysis, the IA MMSE was neglected for te sake of simplicity. Moreover, as the enhanced alternating is an upper bound of the conventional alternating [21], therefore only the enhanced and the modified alternating were considered. Finally, to capture cases of significant external interference, the scenario where the users are placed close to the border of the cluster was also simulated, where the external interference is stronger.

In the first set of results the external interference was considered with a single dominant direction. The sum capacity achieved by the algorithms in this scenario are presented in Figures 4.6(a), 4.6(c), 4.6(e). It can be noticed that for low values of external interference (Figure 4.6(a)) the two BD-based algorithms achieve similar performance for all SNRs values, with a slightly gain for the whitening BD algorithm. As the external interference level increases, from Figures 4.6(c) and 4.6(e), it can be seen that the BD algorithm that explicitly handles the external interference outperforms the other algorithms by a larger gap, in special the conventional BD, that does not mitigate the uncoordinated interference. Regarding the IA algorithms, it is important to remember that they transmit less streams than the BD algorithms, but IA does not require that every base station know the signal to be transmitted to every user, thus demanding less from the backhaul than BD. That explains why the IA algorithms usually obtain a sum capacity lower than the BD algorithms.

Sum capacity is only one side of the coin. In Figures 4.6(b), 4.6(d) and 4.6(f) the BER achieved by the algorithms is presented and it can be noticed that the IA algorithms provide a lower BER than the BD algorithms. Another point that can be observed in Figure 4.6 corresponds to the discussion in Section 4.2. In summary, the enhanced IA imposes the additional restriction of taking the external interference into account when determining the interference subspace, which for this antenna configuration and number of users makes the IA “unfeasible”. That is, the enhanced IA does not have sufficient resolvable dimensions (DoFs) to eliminate the interference (internal and external) anymore. If the number of transmitted streams of only one user was reduced, as it is the case for the modified IA, the scenario gets close to the feasibility and improving the superposition of the interference subspace with the external interference. This behavior is evidenced in the BER curves, although from the sum capacity curves we can see that enhanced IA is still able to provide a higher throughput.

The next step is to increase the rank of the external interference covariance matrix, where Figure 4.7 illustrates the results obtained with a rank-2 external interference. Similar conclusions can be drawn to those ones obtained from the case with rank-1 interference. The whitening BD provides the best performance regarding the sum capacity result, followed by the conventional BD, when the interference level is low. As the external interference power increases, the performance loss in the conventional BD is very accentuated. Regarding the IA algorithms, the increase on the dimension of the external interference moves the enhanced IA

further away from alignment feasibility. This can be attenuated by the modified IA, where a stream of a single user is sacrificed, which moves it again closer to alignment feasibility. In fact, the modified IA algorithm is able to achieve a sum rate very similar to the enhanced IA, but with a lower (better) BER.

Continuing the analyses, Figure 4.8 illustrates the results when the external interference equally spans all the available dimensions, so the covariance matrix is full rank now. Since the external interference already spans all the dimensions, this scenario is specially suitable for the whitening approach. That is, since interference cannot be canceled, then we should at least whiten it. Nevertheless, the impact of the external interference is larger than in the previous scenarios. For instance, in Figure 4.8(e) the whitening BD achieves at most 60 bits/channel use, while in other scenarios it reaches more than 80 bits/channel use. In general, the comparison among the algorithms is equal to the case where the external interference has covariance matrix of rank 2. So, the enhanced and modified Alternating performed similarly, in terms of sum capacity, and the modified one achieved better BERs.

Finally, Figure 4.9 presents the sum rate capacity achieved by each algorithm for different values of external interference, with different ranks of covariance matrix, at an SNR at the border of the cell fixed with the value of 15 dB. We can see that the rank of the external interference changes how effectively the algorithms are handling it. More specifically, the IA approaches provide very good resistance to external interference with rank-1 and somewhat even for rank-2 covariance matrices. The BD approaches provide less resistance to the external interference, but can still achieve more capacity for all simulated external interference levels, when the external interference is handled, since all the transmitters have a deeper cooperation in BD than in IA algorithms.

When the external interference spans all dimensions, as in Figure 4.9(c), then no algorithm is able to cancel any part of the interference, but it is still possible to obtain some gain at least by whitening the external interference.

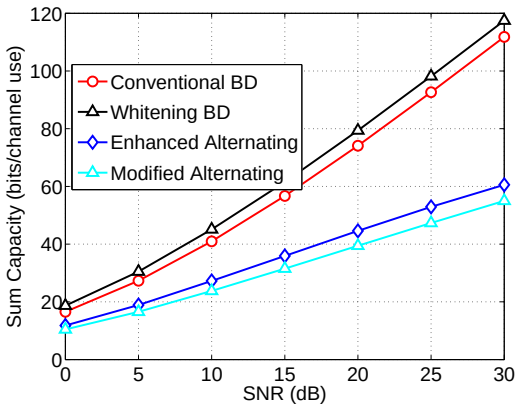

(a) Sum Capacity results. External Interference of 0 dBm.

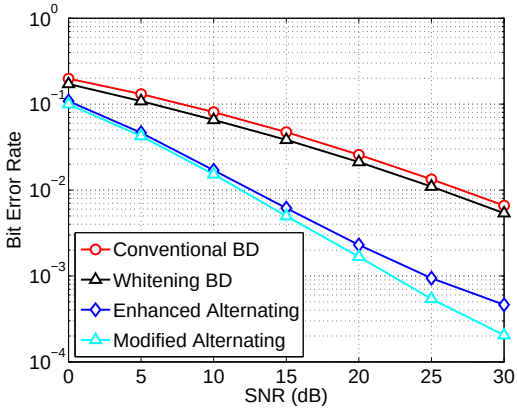

(b) BER results. External Interference of 0 dBm.

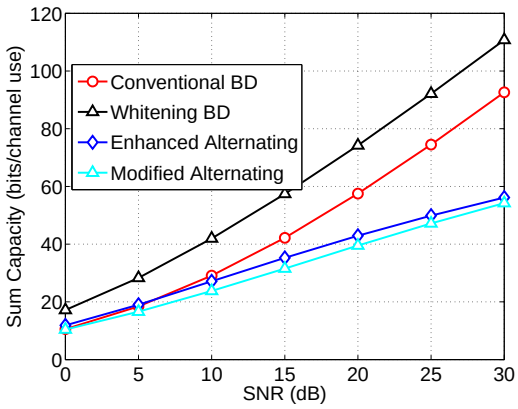

(c) Sum Capacity results. External Interference of 10 dBm.

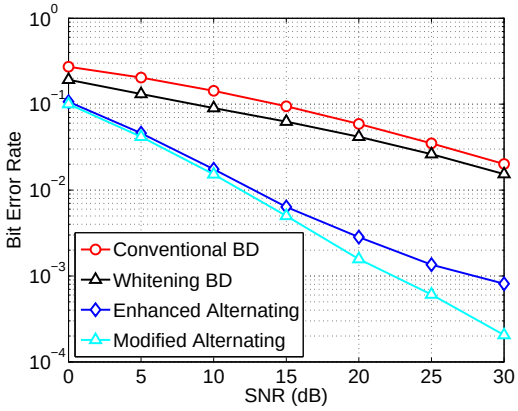

(d) BER results. External Interference of 10 dBm.

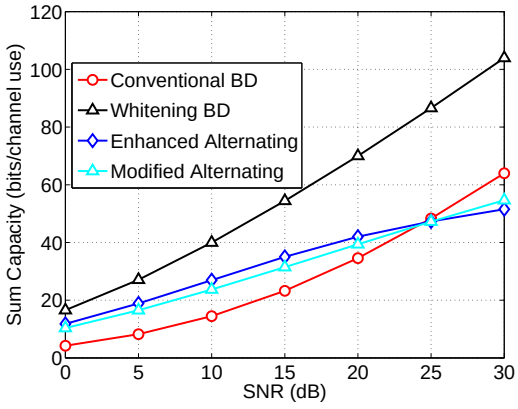

(e) Sum Capacity results. External Interference of 20 dBm.

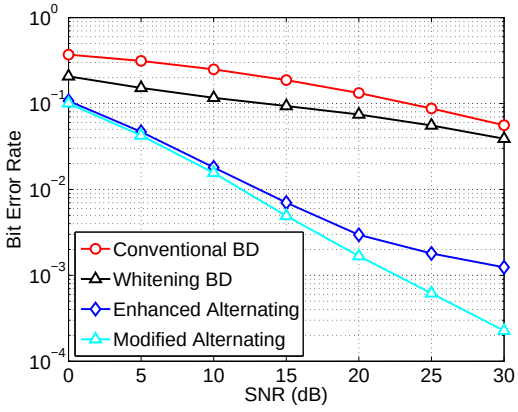

(f) BER results. External Interference of 20 dBm.

Figure 4.6: Simulation with a Rank-1 external interference and nodes equipped with 4 antennas. The left side presents the Sum Capacity versus SNR while the right side presents the BER versus SNR, both for different external interference values at the border of the cluster.

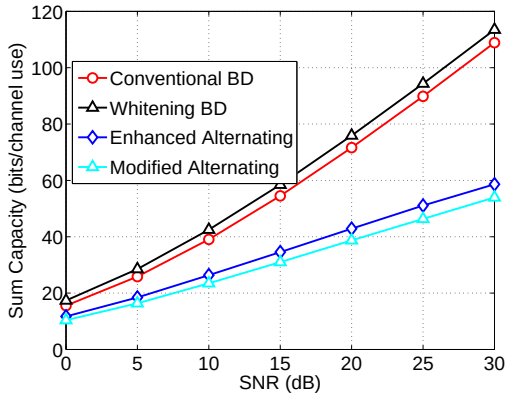

(a) Sum Capacity results. External Interference of 0 dBm.

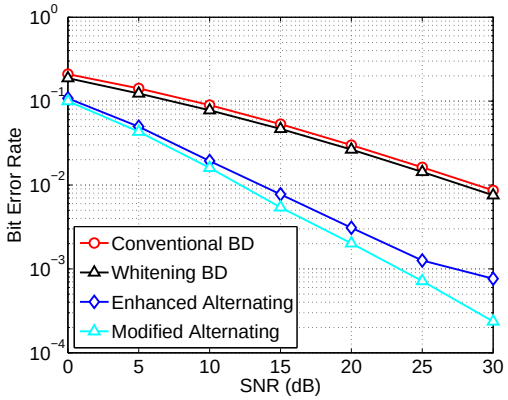

(b) BER results. External Interference of 0 dBm.

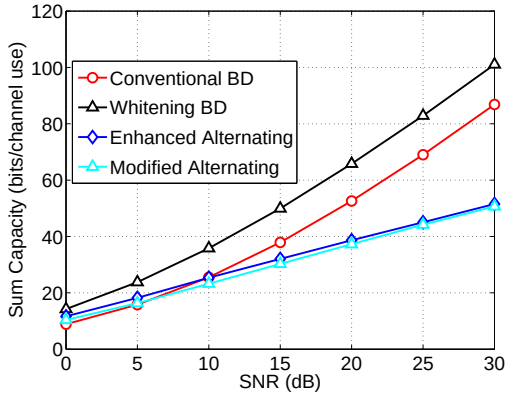

(c) Sum Capacity results. External Interference of 10 dBm.

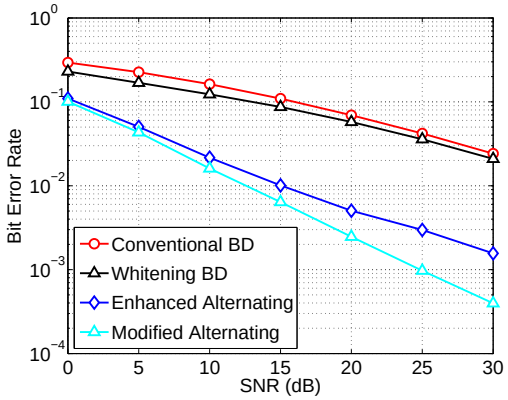

(d) BER results. External Interference of 10 dBm.

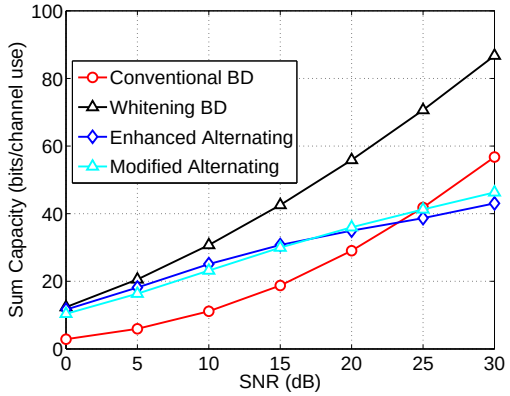

(e) Sum Capacity results. External Interference of 20 dBm.

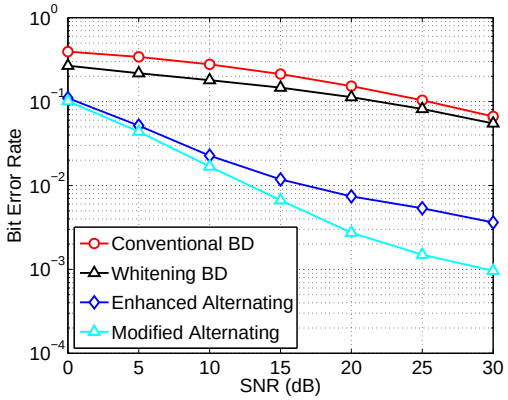

(f) BER results. External Interference of 20 dBm.

Figure 4.7: Simulation with a Rank-2 external interference and nodes equipped with 4 antennas. The left side presents the Sum Capacity versus SNR while the right side presents the BER versus SNR, both for different external interference values at the border of the cluster.

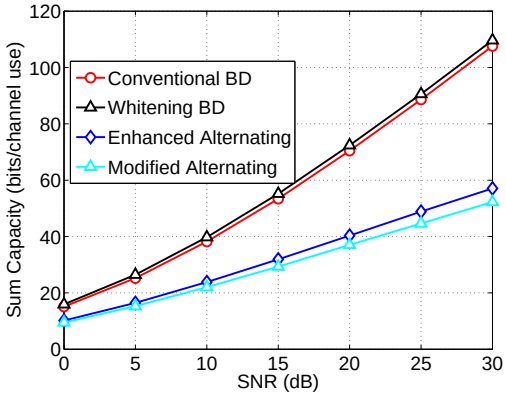

(a) Sum Capacity results. External Interference of 0 dBm.

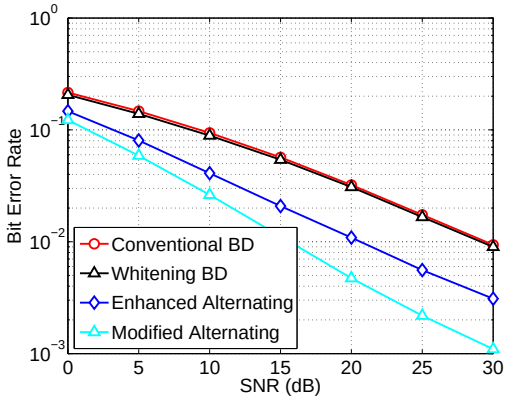

(b) BER results. External Interference of 0 dBm.

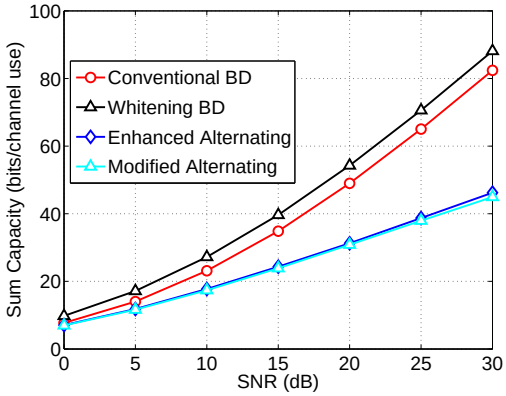

(c) Sum Capacity results. External Interference of 10 dBm.

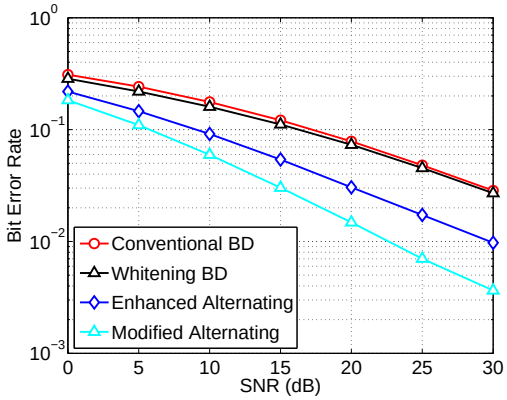

(d) BER results. External Interference of 10 dBm.

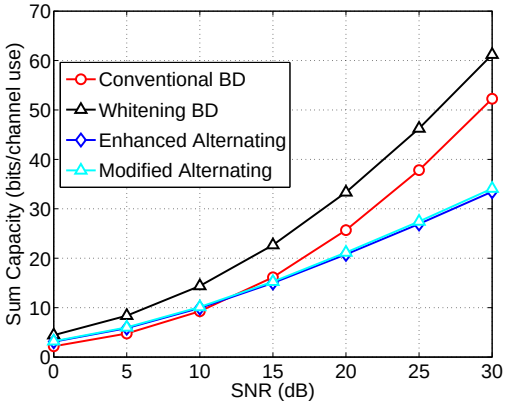

(e) Sum Capacity results. External Interference of 20 dBm.

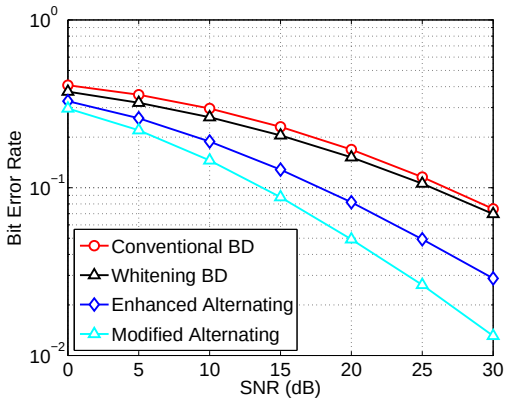

(f) BER results. External Interference of 20 dBm.

Figure 4.8: Simulation with a Rank-4 external interference and nodes equipped with 4 antennas. The left side presents the Sum Capacity versus SNR while the right side presents the BER versus SNR, both for different external interference values at the border of the cluster.

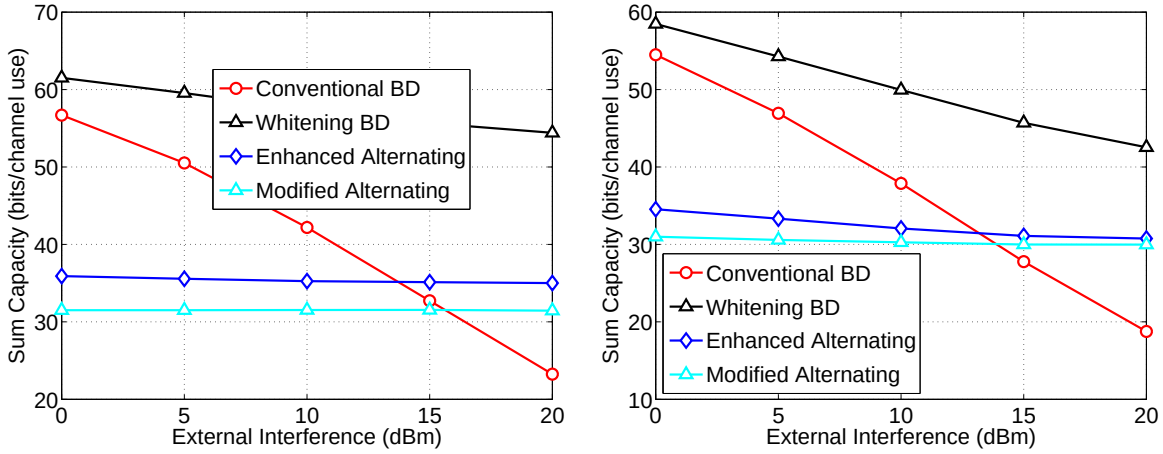

(a) Rank-1 covariance matrix of the external interference.

(b) Rank-2 covariance matrix of the external interference.

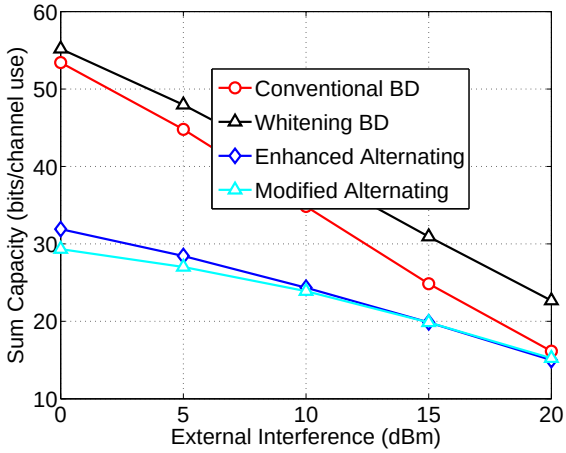

(c) Rank-4 covariance matrix of the external interference.

Figure 4.9: Sum Capacity achieved by IA and BD algorithms as a function of the interference level at the border of the cluster, with the external interference modeled with covariance matrices of different ranks.

4.4 Jakes model

In a practical system, the characteristics of the channel are not static and perfectly known all the time, due to the channel variations and bursty traffic, for instance. This also applies to external interference as well. Hence, another valuable investigation is to grasp how each algorithm behaves with the consideration of the channel variation and how much robust they are to a delayed channel estimation. Therefore, simulations considering a Rayleigh fading channel generated by the Jakes Model [29] are performed in this section.

4.4.1 Channel Variation Modeling

Similarly to the channel coefficients, the external interference must also be modeled in terms of its temporal variation. Thus, the Jakes' model was also used to compute the external interference. The received channel from Equation (4.1) can be rewritten as:

$$\mathbf{y}_i = \sum_{j=1}^{K} \mathbf{H}_{ij}\mathbf{F}_j\mathbf{d}_j + \underbrace{\mathbf{H}_{iE}\mathbf{F}_E\mathbf{d}_E}_{\mathbf{e}_i} + \mathbf{n}_i, \tag{4.16}$$

where the index E represents the external interference source.

Here, the channel variation was modeled by the Jakes Model, such that each element in $\mathbf{H}_{ij}$ and $\mathbf{H}_{iE}$ is equivalent to the sum of several complex sinusoids corresponding to the multipaths. In other words, each element "h" in $\mathbf{H}_{ij}$ and $\mathbf{H}_{iE}$ can be mathematically represented as below:

$$h(t) = \frac{1}{\sqrt{L}} \sum_{l=0}^{L-1} \exp\left(j(2\pi f_D \cos(\phi_l)t + \varphi_l)\right), \tag{4.17}$$

where L is the number of channel multipaths and f_D is the maximum Doppler shift, given by $f_D = \frac{v f_c}{c}$ (v is the mobile terminal speed, f_c is the carrier frequency and c is the speed of light), and ϕ_l and φ_l are random variables uniformly distributed in the interval $[0, 2\pi)$.

The precoders of the external user are randomly chosen (constrained to have a unitary norm such that $\mathbf{F}_E^H\mathbf{F}_E = \mathbf{I}$) and varied at the same rate as the regular precoder. Therefore, the instantaneous covariance matrix of external interference can be calculated by:

$$\mathbf{R}_k = \mathbf{H}_{kE}\mathbf{F}_E\mathbf{F}_E^H\mathbf{H}_{kE}^H. \tag{4.18}$$

Note that the covariance matrix, $\mathbf{R}_k$, does not necessarily have unitary norm.

4.4.2 Simulation Results with Jakes Model

Now the channel variations are included in the simulator through the application of the Jakes' model. In order to capture the average performance of the cellular scenario, the simulation was performed through several snapshots, where in each snapshot users were positioned differently and the time variation was evaluated for 100 Transmission Time Intervals (TTIs). In the beginning of each TTI, the precoders are calculated, based on the estimated channels from the last TTI, and used for all symbols transmitted during this TTI. In each TTI 14 symbols are transmitted and in order to simplify the simulation, the channel is kept constant during one TTI, but the channel variation from one TTI to the next is equivalent to the variation after the transmission of 14 symbols. Note that, with this simulation structure, as the channel varies the transmissions will be accomplished with outdated channel estimates. So, if the channel variations are very fast, then the precoders will be designed with an outdated Channel State Information (CSI). This is how the impact of a

delayed CSI is considered in this work. The channel parameters are presented in Table 4.4.2.

Table 4.1: Jakes' channel parameters.

Carrier frequency (f_D)	2 GHz
Number of multipaths (L)	20
Mobile speed	Changeable
TTI	1 ms
Symbols per TTI	14 symbols
Rate	14 kSymbols/s

To study the impact of the channel variation and the delayed CSI in the IA algorithms performances, a network configuration was considered in which the nodes are equipped with four antennas. The presence of the external interference is simulated in the same manner of the previous analysis, where the interferer source is located in the CoMP cluster border, with power varying from 0 to 20 dBm and allowing the variation in the rank of its covariance matrix. The users are also randomly located close to the border of the cells, respecting a distance of 2/3 of the cluster radius. Still similar to the previous analysis, the IA algorithms considered in this study are just the enhanced and modified alternating. For benchmarking purposes, the conventional and the whitening BD were considered.

The first presented result considers the external interference generated by just one dominant source (rank-1 covariance matrix). Aiming to grasp the impact of the channel variations and the delayed CSI, the analysis can start with the scenario where the external interference level is low, so Figures 4.10(a), 4.10(c), 4.10(e) show the sum capacity results when the external interference power is 0 dBm at the border of the cluster. Then, for this scenario it can be perceived that there is a significant performance loss among all algorithms, given by the delayed CSI knowledge. Regarding the BD-based algorithms, it can be perceived that as the mobile speed increases, the conventional BD tends to outperform the whitening BD. This happens because the estimated external interference covariance matrix is delayed, as well as the channel coefficients. As a result the whitening algorithm is burdened by two sources of error. Concerning the IA algorithms, they have a very similar behavior when the users speeds are varied. Moreover, the BD-based algorithms have a larger absolute performance loss in comparison to the IA technique, however the relative performance loss is not too great when the two techniques are compared. For example, in the SNR 20 dB case, the whitening BD achieves almost 120 bits/channel use when the mobile is stopped and 22 bits/channel use when the mobile speed is 60 km/h. At the same case, the enhanced IA performance varies from 60 to 15 bit/channel use. Thus, the sum capacity of the BD-based algorithm decreased in almost 100 bits/channel use, while the IA lost only 45 bits/channel use. Finally, the percentage losses were around 80 and 75%, for the BD and IA-based algorithms, respectively.

Now looking at the case with a significant amount of external interference, shown in Figures 4.10(b), 4.10(d), 4.10(f), the same impact of the delayed CSI on the algorithms can be perceived. Moreover, the conventional BD presents the same interesting behavior: when the users' speed increases, the impact of the channel variations has a smaller effect on it than in the other algorithms. This behavior is highlighted in Figure 4.10(f), where this algorithm achieves the best performance for a value of 30 dB of SNR. This is explained because it does not use the external interference estimates. Also, for low values of SNR, the IA based algorithms present performances very close to the whitening BD algorithm, showing cases where it can be better the application of the IA technique.

Figure 4.11 highlights the impact of the channel variation on the algorithms. It presents in the same plot the performance achieved when the users are stopped (with updated channel)

and are moving with a speed of 60 km/h (with outdated channel). So several cases of external interference are considered in this set of simulations, where the ranks of the covariance matrices are one or four, and the power is varied from 0 to 20 dBm. Then, it can be concluded that the BD-based algorithms have a large performance loss when the channel variation is very strong, regardless of the interference scenario. This corroborates with the results presented in Chapter 3, showing that BD is more sensitive to CSI errors than the IA-based algorithms.

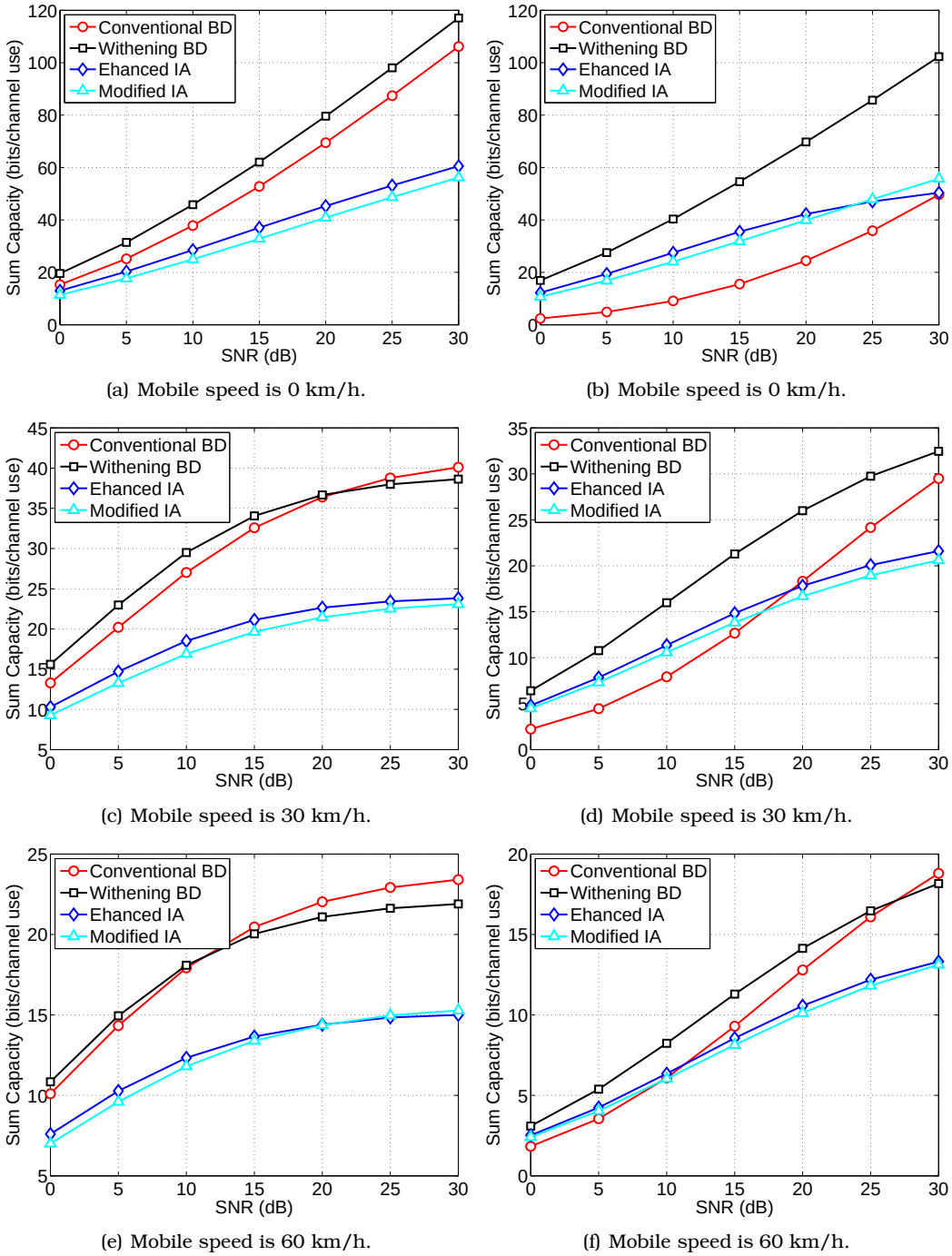

(a) Mobile speed is 0 km/h.

(b) Mobile speed is 0 km/h.

(c) Mobile speed is 30 km/h.

(d) Mobile speed is 30 km/h.

(e) Mobile speed is 60 km/h.

(f) Mobile speed is 60 km/h.

Figure 4.10: Comparison of Sum Capacity achieved by IA, BD with users placed closer to the edge of the cluster for different values of mobile speed. At the left side, the results concern the interference of 0 dBm at the cluster edge, while at the right side, the results are obtained considering 20 dBm of external interference.

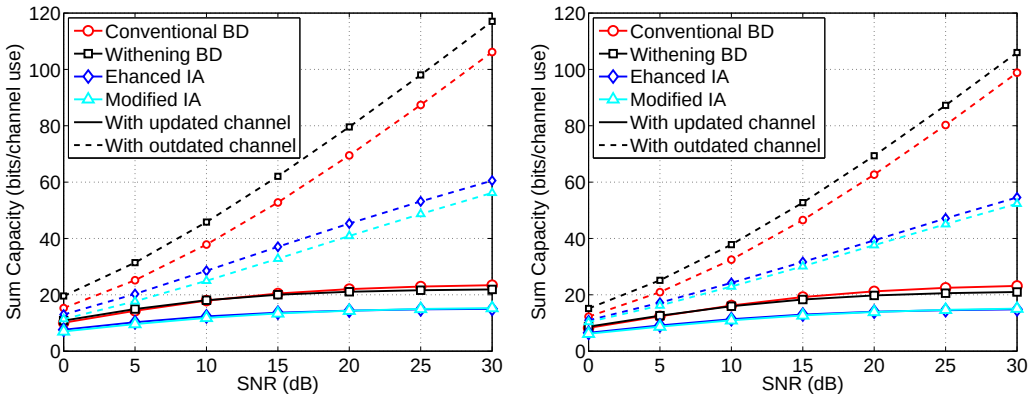

(a) External Interference of 0 dBm at the cluster edge.

(b) External Interference of 0 dBm at the cluster edge.

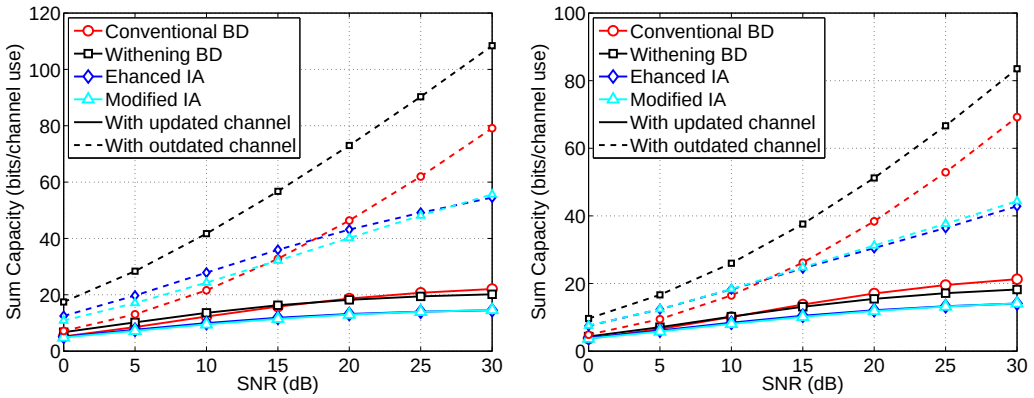

(c) External Interference of 10 dBm at the cluster edge.

(d) External Interference of 10 dBm at the cluster edge.

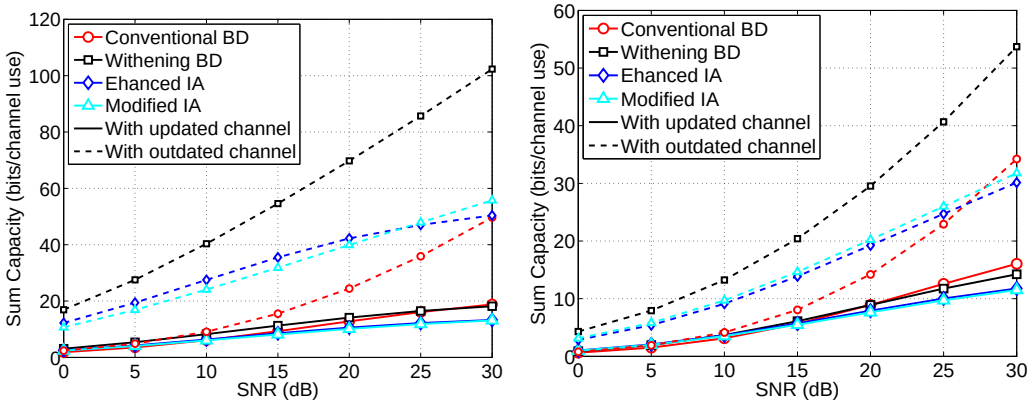

(e) External Interference of 20 dBm at the cluster edge.

(f) External Interference of 20 dBm at the cluster edge.

Figure 4.11: Sum Capacity achieved by IA, BD with users placed closer to the edge of the cluster for different values of external interference. At the left side the external interference was modeled with a rank-1 covariance matrix, while at the right side it was modeled with rank-4 covariance matrix. Considering the outdated channel with the solid lines and updated with dashed lines.

Chapter 5

System Level Interference Alignment

The previous analyses could clarify how Interference Alignment (IA) is burdened when some realistic conditions are considered, such as the channel imperfections and the presence of an external interference. However, through all the previous analyses the dilemma between sending less streams with a reliable link (applying IA) or to achieve higher rates with less reliable transmissions (applying a Joint Processing (JP) scheme) holds. A reasonable step towards solving this dilemma is to actually perform the packet transmissions in accordance to the current features of wireless networks. Following this line, some recent works have focused on evaluating the systemic performance of IA [23, 30]. But, the employment of this technique in real networks raises several implementation issues that have not been deeply discussed yet. Consequently, the achievable performance gains of IA are somewhat unclear yet. With the purpose of performing a systemic analysis of the IA technique, and comparing it against well-established transmission technologies, this work has resorted to a system level cellular network simulator.

As well as the previous simulator, the one implemented here has a similar Coordinated Multi-Point (CoMP) infrastructure, but considering a larger number of cells. This network architecture was maintained since JP schemes will also be used for comparison. Differently from the previous chapters, at this simulator transmissions that do not perform any cooperation will also be employed. These transmissions do not try to mitigate the incoming interference, thus it can be seen as a lower bound of IA. Moreover, different scheduler policies are assessed by the simulator in this chapter. In the next sections, more details about the scenario, transmission schemes and other issues about the simulator are addressed.

5.1 Simulation Scenario

The simulated network is composed by seven neighbor CoMP-cells with a wrap-around approach to avoid the border effects. Every CoMP-cell is comprised by seven conventional cells, which are respectively formed by three Transmission Points (TPs). Thus, through the sectorization scheme, each conventional cell is divided into three hexagonal sectors with $334\ m$ of diameter. Hence, the antenna radiation pattern of the TP antennas is assumed to be $120°$ of beamwidth. The User Equipments (UEs) that are placed inside the sectors are equipped with two antennas each, as well as the TPs. Finally, the described scenario composed by 147 TPs is presented in Figure 5.1.

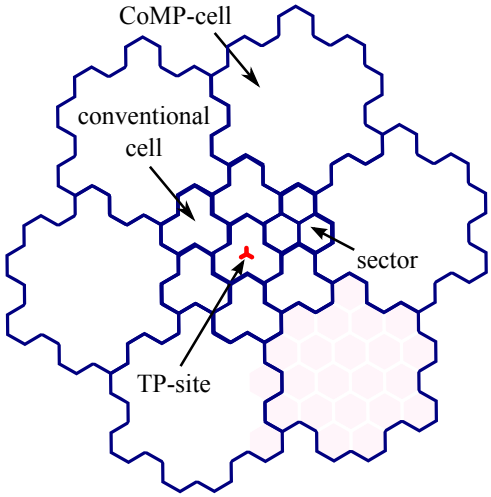

Figure 5.1: Multicell scenario composed by seven CoMP-cells.

This work focused on the downlink of this system, which employs Orthogonal Frequency Division Multiple Access (OFDMA) with equal power allocated among the subcarriers. These subcarriers are grouped in blocks of 12 adjacent subcarriers as Physical Resource Blocks (PRBs) [31], each of which are assigned to one or more ⟨TP, UE⟩ pairs within each CoMP-cell.

The channel coherence bandwidth is assumed to be larger than the PRB bandwidth. The channel gain is composed of average pathloss, shadowing, antenna gain and small-scale fading. The pathloss is given by $PL = 35.7 + 38\log_{10}(d)$ to emulate an urban micro environment [32]. Shadowing, which is assumed to be equal among the different UEs within a same cell, is modeled by a log-normal distribution of zero-mean and standard deviation $\sigma_{\text{sh}} = 8dB$. The Spatial Channel Model was used to simulate the small-scale fading, so that the spatial correlation can be properly accounted for.

Before the transmission simulation, a link adaptation mechanism is employed. Using estimations of Signal to Interference-plus-Noise Ratio (SINR) in each UE, it tries to find which Modulation and Coding Scheme (MCS) will provide a reliable transmission with the maximum throughput. Aligned with Long Term Evolution (LTE), a set of fifteen MCSs is available, each composed by a combination of modulation schemes — say 4-, 16- and 64-Quadrature Amplitude Modulation (QAM) — and coding rates between 1/13 and 1. Furthermore, The transmit power per PRB for each TP is calculated to guarantee an Signal to Noise Ratio (SNR) at the edge of the sector, such that it would be possible to transmit with the lowest MCS. Finally, the link budget is calculated in accordance with Table 5.1, where the simulation parameters are summarized.

Table 5.1: Simulation parameters of the multicell scenario.

Parameter	Value
Number of CoMP-cells	7
Number of sites per CoMP-cell	7
Number of antennas per UE	2
Number of antennas per TP	2
Antennas radiation pattern	120^o
Maximal diameter of cell	334 m
Carrier frequency	2.0 GHz
Subcarrier spacing	15 kHz
Number of PRBs	6
Number of subcarriers per PRB	12
Channel profile	SCM [32]
Shadowing standard deviation	8 dB
Required SNR at the cell border	-6.2 dB
Snapshot duration	1 s
Effective TTI duration	1 ms
Number of symbols per TTI	14
UE speed	3 km/h

Therefore, at this scenario several transmission strategies can be employed to exploit the coordination. Those ones that are more relevant for the current investigations are described in the next subsections.

5.1.1 Full Joint Processing

The Full Joint Processing (FJP) strategy attempts to establish a CoMP transmission concerning the suppression of the interference, including the interference between the streams of a same UE. The Minimum Mean Square Error (MMSE) precoding was chosen since it may be more suitable to overcome the ill-conditioned channel matrices that the Spatial Channel Model (SCM) may impose. The MMSE precoder is designed as [33]:

$$\mathbf{M}_{\mathcal{G}} = \mathbf{H}_{\mathcal{G}}{}^{\mathrm{H}} \left(\mathbf{H}_{\mathcal{G}} \mathbf{H}_{\mathcal{G}}{}^{\mathrm{H}} + \frac{\sigma_{\eta}^{2}}{P_{\mathrm{PRB}}} \mathbf{I} \right)^{-1}, \tag{5.1}$$

where the $\mathbf{M}_{\mathcal{G}}$ and $\mathbf{H}_{\mathcal{G}}$ are respectively the precoder and aggregated channel matrix of the whole CoMP-cell. So, at the $\mathbf{H}_{\mathcal{G}}$ matrix, the channel between all TPs and UEs of that particular CoMP-cell are included.

The power allocation must respect the constraint on the maximum per-cell power P_{PRB} available at each TP. At the same time, the power ratio among elements of each column of the matrix $\mathbf{M}_{\mathcal{G}}$ cannot be changed in order to preserve the properties of the spatial precoding. Considering the precoding matrix $\mathbf{M}_{\mathcal{G}} \in \mathbb{C}^{M \times L}$, and hypothetically the cell i^{*} is responsible for the highest power consumption, then, the whole $\mathbf{M}_{\mathcal{G}}$ matrix must be scaled so that the squared norm of the row $\mathbf{M}_{i^{*}}$ with highest norm becomes equal to $\sqrt{P_{\mathrm{PRB}}}$ [34]:

$$\mathbf{M}_{\mathcal{G}} = \frac{\mathbf{M}_{\mathcal{G}}}{||\mathbf{M}_{i^{*}}||_{\mathrm{F}}}. \tag{5.2}$$

Despite the fact that FJP does not take advantage of all available power, in practice it is a very attractive transmission strategy that leads to reasonable spectral efficiency results.

5.1.2 Conventional

The simplest transmission strategy herein investigated is the one referred to as *conventional*. The conventional transmission strategy assumes no coordination among the TPs; each sector choses one of its UEs and, thereby, the associated TP transmits to it. The interference between the two streams of a same UE is dealt through MMSE processing, which is given by (5.1).

5.1.3 Interference Alignment

As mentioned in Section 2.2.2, the spatial interference alignment is affected by some important limitations, such as the number of pairs that are able to cooperate. Based on the assumption that there are at most two antennas per node (whether TP or UE), the amount of pairs that will apply IA can be determined. Exclusively to the **2x2** scenario, the systemic IA must comprise three TP-UE pairs.

For this reason, each CoMP-cell is divided into two subregions: core and periphery. The core of a CoMP-cell is formed by combining three adjacent sectors, whereas all the other sectors surrounding it comprise the periphery. Both subregions are highlighted in Figure 5.2 for a hypothetic combination, wherein the core is defined by the three-sectors area.

While an IA algorithm is applied within the core, the conventional scheme is adopted for the peripheral sectors in accordance with the description given in Section 5.1.2. Due to the directionality of the transmission antennas, the effectiveness of the interference alignment

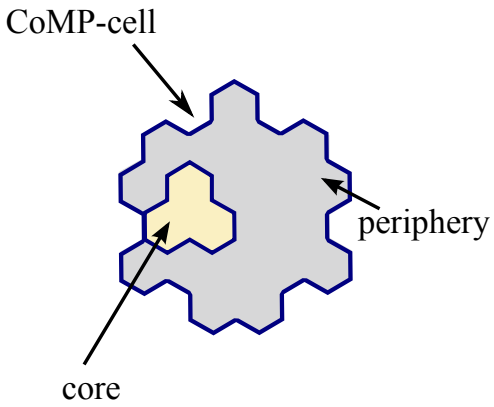

Figure 5.2: CoMP-cell with its subregions for a hypothetic combination: core and periphery.

within the core as well as the influence of external interference are tightly dependent on the sectors chosen for combining. Therefore, three particular combinations of core-periphery subregions are considered for simulation, named simply as A, B, and C. They are illustrated in Figure 5.3.

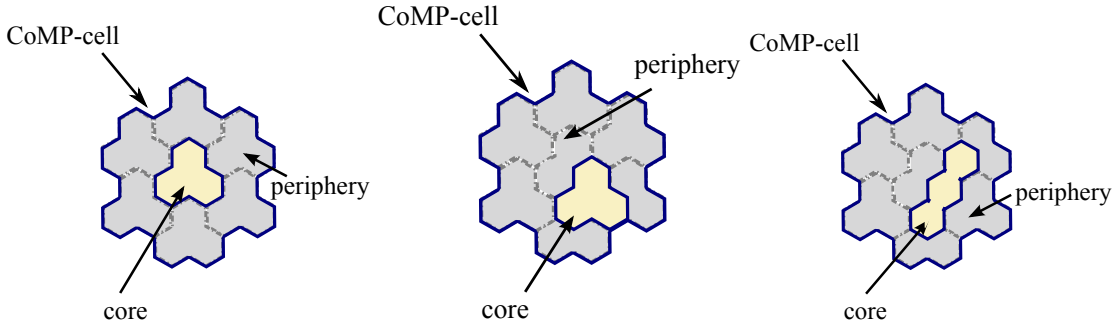

Figure 5.3: CoMP-cell with its subregions core and periphery for three different combinations.

Henceforth, all the IA algorithms presented in Section 2.3 can be properly employed, each preserving its characteristics as previously discussed. Furthermore, as a matter of simplicity, the following analyses of the IA-based Algorithms 2.1, 2.2 and 2.3, presented in Section 2.3, are respectively referred to as IA closed-form, IA alternating and IA MMSE.

5.1.4 Partial Joint Processing

The Partial Joint Processing (PJP) is designed especially to support the analyses of the interference alignment scenario as described in Section 5.1.3. Thus, PJP is applied in scenarios very similar to IA, in which core and periphery subregions are defined just as illustrated in Figure 5.3. The main difference lies in the type of transmission employed within the core. Now the joint processing takes place in a form similar to that described in Section 5.1.1, but properly tailored to the three combining sectors composing the core.

It is essential to highlight that when the conventional and the JP transmissions are employed, two streams per TPs are sent. On the other hand, when IA schemes are performed, they are just able to send one stream per TP, due to the network configuration. Finally, a random scheduler policy was applied for the following analysis, while other schemes are just addressed in Section 5.3.

5.2 Results and Analyses

In this section some results obtained from several simulation campaigns of the earlier described transmission strategies are presented, especially looking at the behavior of the IA-based schemes. The simulation events are organized in snapshots, during which path loss and shadowing are assumed to remain constant for all links, while the temporal variations of

fast fading are considered. The dynamics of fast fading can be captured by assuring that each snapshot takes at least 1 s, which is longer than 10 times the channel coherence time for the considered parameters. In order to capture the impact of long-term propagation effects on the system performance, several snapshots (say, from 4 to 8) are simulated, so that, confidence intervals at a 90% level can be obtained based on Student's t-distribution.

Throughout this section, the schemes' performances are evaluated mainly through the *UE throughput* measures. These measures are taken along the snapshot lifetime, and based on them several aspects can be analyzed. The average throughput can be obtained over either all UEs or just over those ones inside the core area, which are presented as function of the offered load. The offered load herein means the number of UEs physically present in a sector, regardless of whether they are scheduled or not. Since the transmission scheme limits the number of UEs that can be simultaneously scheduled, the increase of offered load also increases the proportion of those users that are scheduled. Therefore, the larger the offered load, the smaller the throughput averaged over all UEs. Furthermore, the transmission strategies that allow coordination with three TPs have their average UE throughput diluted in the conventional performance. It is important to highlight that this analysis considers that all UEs are randomly chosen inside of each sector.

As mentioned before, at the previous sections some comparisons among IA and JP algorithms were performed, albeit in a more simplistic scenario. Their investigations showed that the JP transmission provides a better performance when the Shannon capacity metric is considered. On the other hand, regarding the Bit Error Rate (BER) results, the IA algorithms outperform the JP schemes. This previous analysis brings an important dilemma: the choice of sending less streams, but with a more reliable transmission (using IA schemes), instead of trying to achieve higher rates (using JP). To deal with this dilemma, we are supposed to account for how much information is effectively transmitted. At this point, the system throughput proves to be very suitable.

The analysis begins in terms of the average throughput of UEs. This set of results shows only combination A to allow for a clearer comparison; the results of the other combinations are later presented separately. This way, Figure 5.4 presents the average throughput as a function of the offered load achieved by each of the discussed algorithms. In Figure 5.4(a), the achieved throughput is related to the system performance, where all UEs are accounted. Therefore, the FJP scheme achieves the highest performance for all load values, as expected. Comparing now the remaining transmissions schemes, PJP presented a performance slightly higher than the others. The conventional and the IA MMSE achieved almost the same performances. Lastly, the IA algorithms that apply the Zero-Forcing (ZF) criterion at the reception, IA alternating and IA closed-form, achieved the worst results. This unsatisfactory performance happens in part due to the channel correlation that may degrade more those schemes that use ZF criteria. But it also happens because these algorithms may neglect their own performance to mitigate the interference of just two neighbor TPs, when there are several other sources interfering with the transmissions. So, the pure IA objective is not optimal in this case.

A better separation between the algorithm performances can be noticed in terms of the results regarding the UEs inside the core area, presented in Figure 5.4(b). In this case the results are not diluted within the peripheral UEs. As expected, the JP based schemes perform better than the conventional and the IA MMSE, which, in a similar way, perform better if compared with the IA algorithms that use the ZF criterion. In this case, FJP still provides the best performance, but the gain in comparison to the other techniques is not too large as it was in the set of results that considers all the UEs of the system. The reason is that FJP

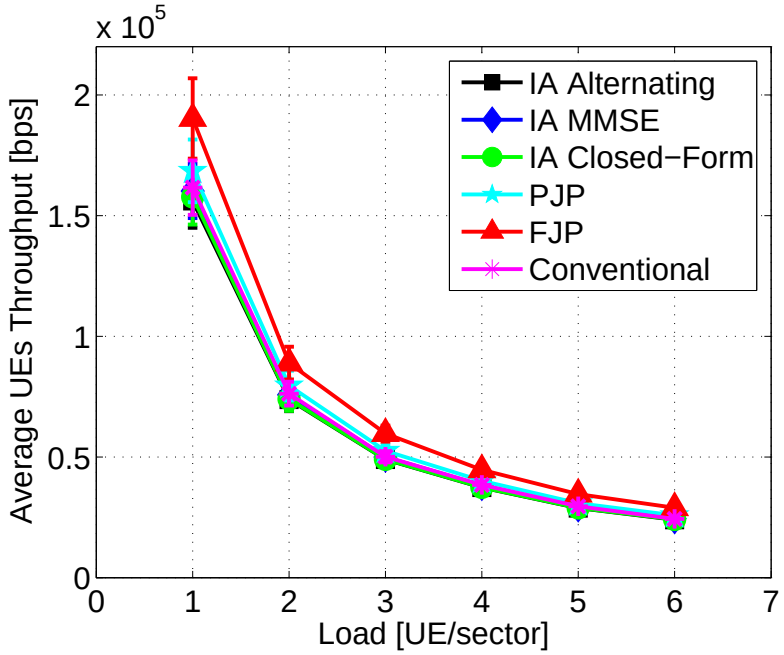

(a) Average throughput calculated considering all UEs.

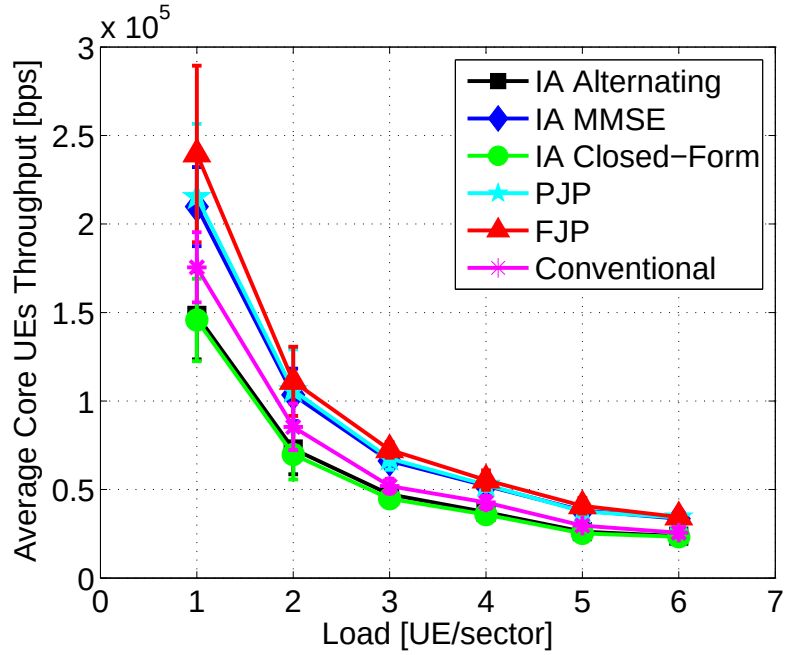

(b) Average throughput calculated considering the core UEs.

Figure 5.4: Average throughput of the UEs when each algorithm is applied.

is conceived with a view to the whole CoMP-cell. This means that the performance of each separated cell is not optimized, since this technique optimizes the overall system performance. Thus, when just three sectors are chosen, the whole performance is not represented.

Furthermore, both the IA-MMSE algorithm and the PJP tend to have a similar performance on the core sectors, although the IA-based scheme sends one stream per TP less than the JP transmission. This behavior represents the above mentioned trade-off. However, when the whole system is analyzed, the PJP scheme performs slightly better than IA-MMSE. As a matter of fact, since commonly the JP-based schemes do not use all the power available in all coordinated sectors, PJP causes a little less interference in the neighbor sectors than IA-MMSE. To illustrate this, it can be inferred from the simulation results that the IA-based algorithms and conventional tend to spend about 26% more energy than PJP.

Different arrangements of the sectors composing the core area are supposed to provide

different performances, since different combinations of sectors are established and therefrom different efficiency in terms of both cooperation and robustness to interference may be perceived. Figure 5.5 presents the results considering only the throughput of the UEs that are inside the core in each combination presented in Section 5.1.3. As it can be perceived, combination A always has a much better performance than the other ones, followed by combination C. This result was not the one expected, since combination B tends to offer a higher interference among the core sectors. Hence, it was expected that eliminating a more severe interference the performance gain could be higher, what did not happen. Nevertheless, it is known that the presented coordinated algorithms are somehow altruistic, in the sense that they neglect their own performance in order to avoid the interference. Therefore, there is a suspicion that such altruistic behavior is responsible for the performance loss, since the precoders of those schemes redirect part of the power in order to mitigate the interference. Still, this suspicion must be further investigated in depth.

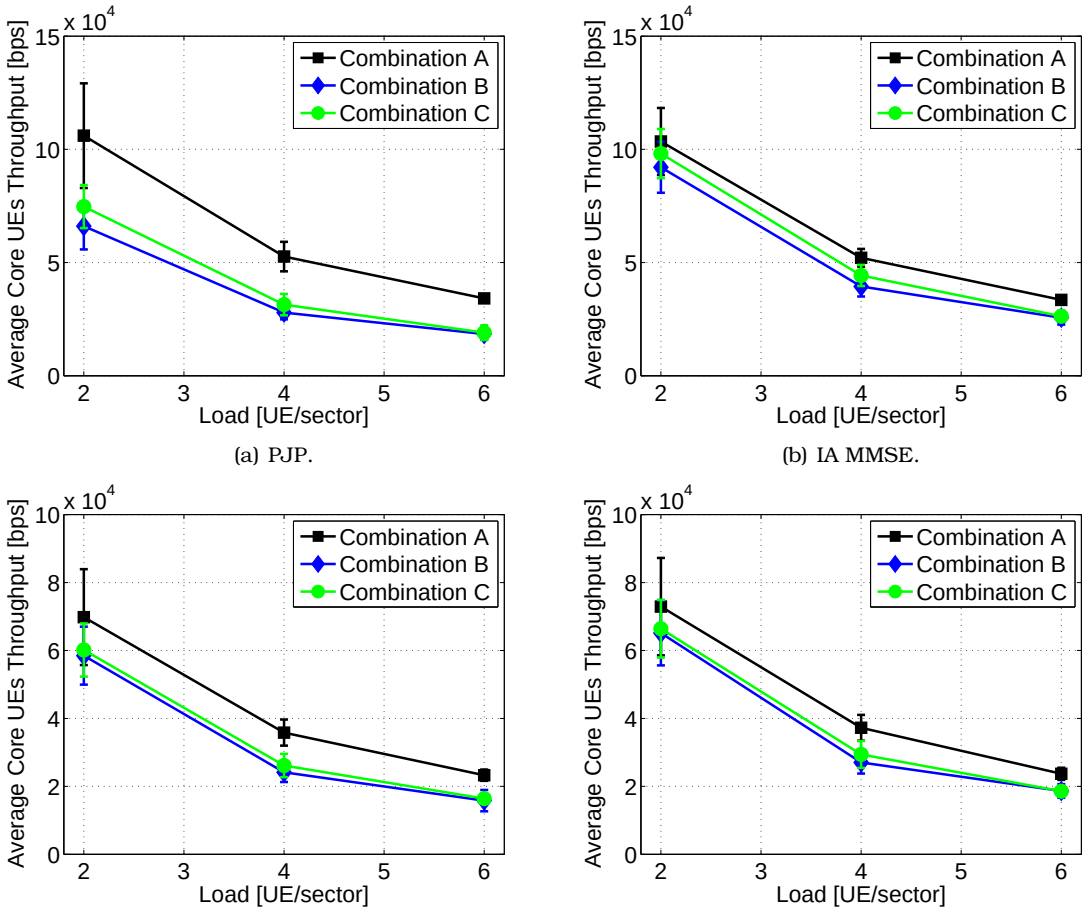

(a) PJP. (b) IA MMSE.

(c) IA Closed-Form. (d) IA Alternating.

Figure 5.5: Average throughput of the core UEs when each algorithm is applied for different combinations of sectors performing the cooperation.

The average throughput analysis of this scenario is concluded by showing the performance achieved considering all UEs present in the network. Remember that, similarly to the previous results, those ones are diluted by the conventional transmissions. From Figure 5.6, the same conclusion deduced before can be taken, but now the results of combination B and C are more similar with a trend of gain for combination C. This analysis shows that the geometry of the core region does not generate more interference in the periphery, therefore causing no influence on the conventional UEs performance.

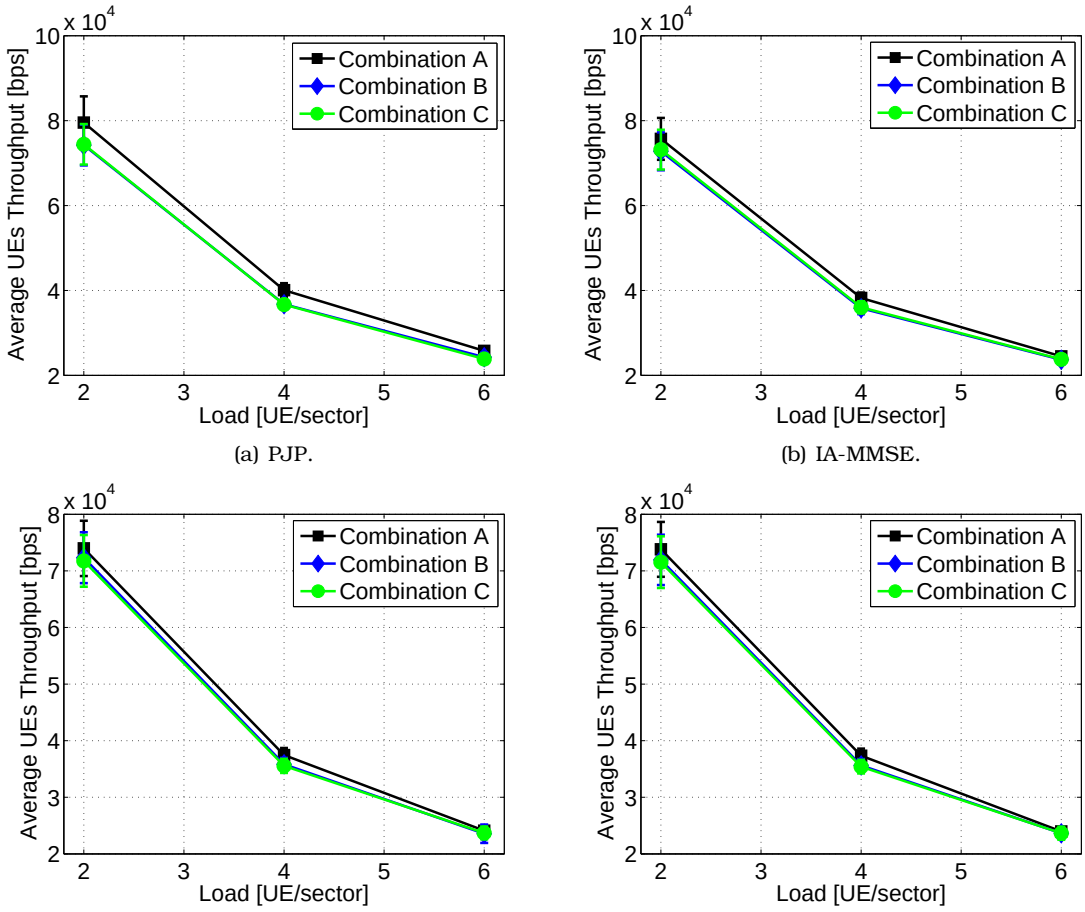

(a) PJP.

(b) IA-MMSE.

(c) IA-ZF.

(d) IA-Alt.

Figure 5.6: Average throughput of UEs when each algorithm is applied for different combinations of sectors performing the cooperation.

5.3 Scheduler Analysis

The schedulers are responsible for choosing the UEs that will communicate with the TPs. There are different approaches for performing this choice, some of them just care about the TP-UE performance, while others are more altruistic and aim to improve the overall system performance. There are also those concerned about the fairness in the network. Hence, the choice of the scheduler plays an important role not only on the system performance but also on the management policies.

Despite its importance, this topic has been poorly addressed in the IA literature. The previous works either neglected the existence of a scheduler or considered a random one, similar to the herein presented results. So, in order to give the first step to evaluate the IA technique considering different scheduling policies, different approaches are addressed in this section.

Besides the random approach applied in the previous results, a max gain scheduler is considered, regardless of the transmission scheme that is employed. This algorithm chooses the UE inside of each sector that presents the highest channel gain. Most of the time, the max gain scheduler will choose those UEs close to the TPs, neglecting the UEs at the border, which may improve the system performance. On the other hand, the random scheduler can just assure that all the UEs have the same probability to be selected. Thus, both approaches can be seen as opposites.

However, there are some approaches designed specifically to aid a kind of transmission. For instance, choosing a set of UEs that are spatially separable can aid the precoding design

of the JP-based transmission schemes. Thus, when PJP is applied, a scheduler based on successive projections [35] can be additionally considered. At this approach, the channel vector of a subset of UEs is successively projected onto the null space of the channels of the UEs already scheduled, so that, at the end, it yields a subset of UEs whose channel vectors are very close to mutual orthogonality.

Regarding a proper scheduler to the IA transmission schemes, this work resorted to the chordal and Fubini-Study distances, which are a good way to measure the quality of the alignment between two subspaces [36, 37]. These distances can be employed to measure the angle between spaces. The chordal distance between two matrices $\mathbf{A}$ and $\mathbf{B}$ is defined as:

$$d_{cd}(\mathbf{A},\mathbf{B}) = \frac{1}{\sqrt{2}}||\mathbb{O}(\mathbf{A})\mathbb{O}(\mathbf{A})^H - \mathbb{O}(\mathbf{B})\mathbb{O}(\mathbf{B})^H||_F, \tag{5.3}$$

while the Fubini-Study distance is given by [37]:

$$d_{fs}(\mathbf{A},\mathbf{B}) = \arccos|\det(\mathbb{O}(\mathbf{A})^H\mathbb{O}(\mathbf{B}))|, \tag{5.4}$$

where $\mathbb{O}(\mathbf{A})$ is defined as a matrix which consists of the orthonormal basis vector that spans the column space of $\mathbf{A}$ and $||\cdot||_F$ denotes the Frobenius norm.

With this in mind, these distances can be employed to aid the IA by choosing the UEs that present the shortest distances between the incoming interferences, in other words, those with the most aligned interference. Therefore, the schedulers developed in [38], based on these distance-based metrics, can be applied when the IA transmission schemes are employed in this analysis. It is important to highlight that these distances are not related to the strength of the channel, which means that the schedulers based on them do not use the information of pathloss and channel gain, for instance.

Summarizing the schedulers used in this analysis, when the conventional transmission scheme is applied, just the random and the max gain schedulers can be employed, since the conventional sectors do not cooperate. For PJP the successive projections scheduler can be used, besides the random and the max gain schedulers. Finally, the IA schemes, represented here just by the IA MMSE, can also be aided by the schedulers based on the chordal and Fubini-Study distances.

Figure 5.7 aggregates the average throughput performance of the core UEs when the different combinations of schedulers and transmission schemes are applied. Therefore, at a first glance, the opposite performance of the random and the max gain schedulers can be perceived. All transmission schemes reached the highest performance when combined with the max gain schedulers, and the worst when the random approach is applied. Regarding the PJP transmissions in Figure 5.7(c), the successive projection could boost its performance, however it could not reach the max gain result.

Still on the same figure, but now regarding the schedulers based on the subspaces distances, in Figure 5.7(a) they were shown to achieve similar performances to the random one. As they only care about the angles between the interfering signals, hence a UE at the border will be scheduled with the same chance of the UE very close to the TP. Also, the main "weakness" of the IA algorithms is that they do not care about the direct channel gain, which is not tackled by this kind of scheduler. So, this policy does not add any gain to the algorithms performances and they act like a random scheduler when applied in this system.

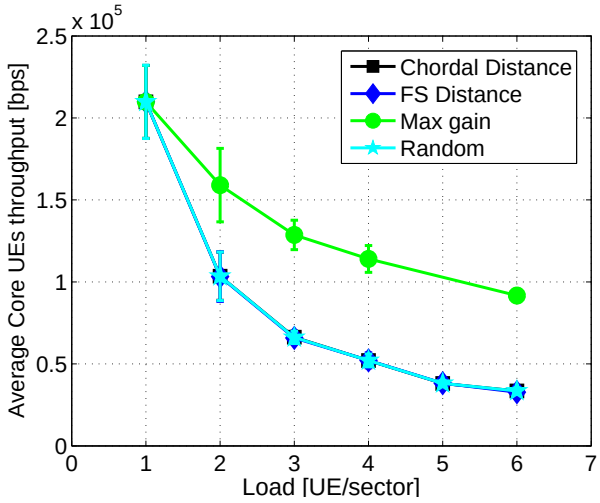

(a) IA-MMSE.

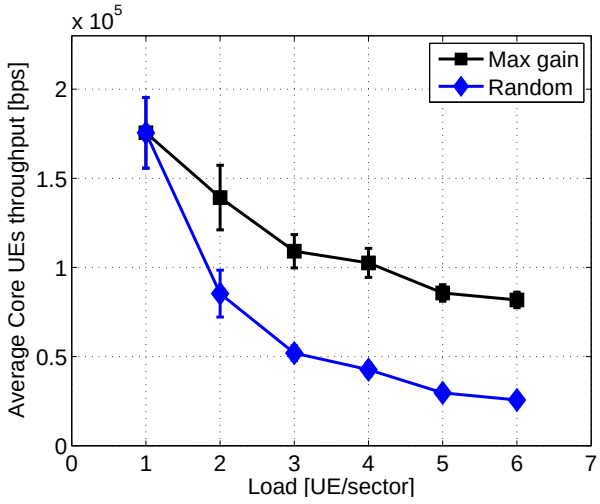

(b) Conventional.

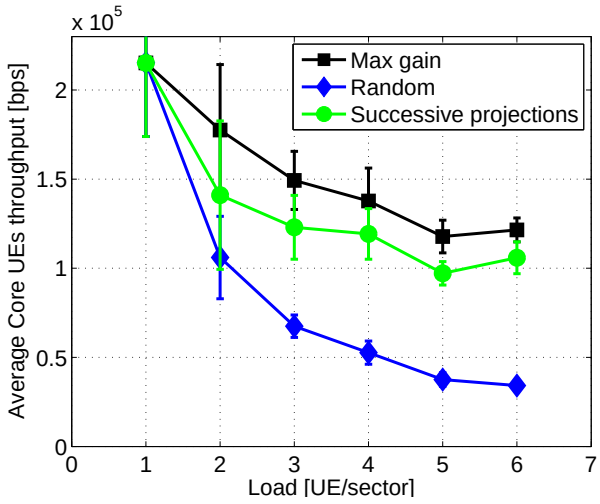

(c) PJP.

Figure 5.7: Average throughput achieved by users in the core of the CoMP cell versus the load of the system for different schedulers and transmission schemes.

Chapter 6

Conclusions and Future Work

The main objective of this work was to assess the Interference Alignment (IA) technique in order to grasp the actual gains that this technique could provide on current cellular networks. To accomplish this goal, three different algorithms were studied and had their performances compared with Joint Processing (JP)-based schemes. These schemes were chosen as benchmark because they also perform some cooperation among the transmitters to avoid the interference. The three IA algorithms were the closed-form solution, the alternating IA and the IA MMSE. The first one can be applied just in a particular network configuration, while the other two are more flexible. Furthermore, the Minimum Mean Square Error (MMSE) one relaxes a little the constraint of the perfect alignment. Therefore, throughout the whole work the technique evaluation was taken based on the performance of these algorithms on different simulation scenarios.

Initially these algorithms were simulated in a scenario composed by one Coordinated Multi-Point (CoMP) cluster comprised by three conventional cells. This framework was chosen since the Block Diagonalization (BD) algorithm, a JP-based scheme chosen for comparison, requires not only the knowledge of the channel coefficients of the network, but also the data that will be sent to all users. Therefore, from this main scenario and under different users' placement, some channel imperfections were considered, which yielded several simulation cases. Finally, the algorithms' performance were analyzed via sum capacity and Bit Error Rate (BER) results.

Thus, the impact on the performance of the algorithms, regarding the correlation among the transmitter antennas and the imperfect Channel State Information (CSI), was analyzed. Regarding the correlation, both sum capacity and BER results showed that as the correlation increases, all algorithms have their performance decreased, with the IA MMSE being slightly more robust than the others. Nevertheless, when the imperfect CSI is considered, the IA algorithms were shown to be more robust than BD. Further results showed that in some cases IA could overcome BD, in terms of sum capacity, even with BD sending more streams. Another interesting behavior that can be observed from this set of results is that there is a dilemma between using IA for a more reliable transmission or applying BD to send more information.

Since the current cellular networks are composed by dozens of cells, the previous scenario is somehow limited. Thus, the presence of uncoordinated interference burdening the CoMP cell was included in another set of simulations. Several cases of interference were considered by modeling it through a colored noise generated with the proper covariance matrix. Then,

the iterative IA and the BD algorithms are able to take into account this covariance matrix to improve their performance, with the price of compromising IA feasibility. Besides considering the external interference, the IA alternating was also modified to send less streams, what approximates the algorithm closer to the feasibility again.

Thus, all the algorithms, with modifications or not, had their performances assessed in the scenario with the presence of the external interference. The first set of results considered that the interference perceived by each user came from a dominant interference. It was shown that both IA and BD suffered a significant performance loss, regardless of the analyzed metric. Also, the modifications on both algorithms were able to mitigate part of the interference and could boost their performance. It is important to highlight that, similarly to the previous analysis, IA is better with regard to BER while BD achieves the highest sum capacities.

When the rank of the external interference covariance matrix was increased, emulating interference caused from multiple sources, the IA and BD conventional algorithms were even more disturbed. Furthermore, those algorithms that try to mitigate the external interference as well, showed to be less effective, but they still could provide performance gains. Considering a covariance matrix of rank-4, the extreme case, is a good illustration of this. All algorithms presented performances losses with the increasing level of interference.

A way to combine both channel imperfection and the external interference was developed in Section 4.4. The simulations were conducted considering the same scenario, but now the channel matrices were generated through the Jakes' model. So, besides the channel time variation, and the external interference, a delayed CSI could be considered. Therefore, the results in the section corroborate the previous analysis. The IA is more robust to a imperfect CSI than BD. The modification on the algorithms are able to boost their performance in the presence of the external interference. And more important, the dilemma between IA and BD remained.

Aiming to solve this dilemma a more elaborated simulator was considered. The cellular network was composed by 147 Transmission Points (TPs) and the evaluation of the technique was performed via the throughput, metric that translates the amount of data that is being effectively decoded at the reception. For this framework, the same IA algorithms presented in Chapter 2 were employed. However, for benchmarking purposes, an MMSE transmission scheme based on the JP approach was applied, and a conventional transmission, that does not try to mitigate the interference inside its own cell.

The system level simulations showed that the IA MMSE can be an alternative between the non-cooperation and the full cooperation, since it presented an intermediary performance between the conventional transmission and Partial Joint Processing (PJP). Nevertheless, the other IA algorithms, the closed-form and the alternating, presented the worst performance. Also, different arrangements of sectors were assessed to see if some technique could take any benefit from it. But what could be perceived is that all algorithms achieved the best performance when the set of sectors chosen to cooperate are from the same TP. This happens since, in the presence of strong interference, the algorithms may neglect their own performance to avoid interference.

Concluding the work, an analysis of different scheduler policies for IA was begun. In addition to the random and the max gain schedulers, the successive projections approach was considered for the JP based schemes. While for IA transmission two subspace distances approaches were implemented. Results showed that when the max gain was employed all the algorithms could achieve the highest throughput. Furthermore, the subspaces distances were not able to aid the IA algorithms and did not show any performance gain in comparison

to the random one, due to these metrics not being related to the channel gain, but only with the angles between the interferers.

Hence, this work tried to provide useful insights on how the IA technique could really perform under realistic conditions. Although the herein discussed investigations let some unresolved points, the obtained results unfolded several possibilities for future work. Thus, the next steps that can be taken are described below:

External interference Using the covariance matrix of the external interference in the precoding design showed to be very effective. However, it was not assessed in the system level simulator, which is important not only by its performance evaluation, but it also brings up several implementation issues. Since the transmissions performed in the system are not necessarily synchronized, then the external interference may change in the middle of a transmission. So, how to gather reliable estimations of interference? How the algorithms will be affected by imperfect estimations? These are important questions to be addressed.

Scheduling This work gave a kick-off on the evaluation of some scheduling policies that tried to aid the IA technique. Nevertheless, none of than could provide any gain. Hence, modifying these policies to take into account not only the angles between the subspaces, but also the channel gain, could provide some performance gain. So, as the results presented here could be seen just as preliminary evaluations, this topic deserves to be deeper investigated.

Extended scenario Still related to the system level simulator, it can be desirable to pursue some variations and extensions of the current scenario. Several possibilities are allowed here, replicating the IA group, in such a manner that all the cells of the system would be applying the IA technique, can be one of them. Form the cooperation groups dynamically or exploiting other combinations of sectors could also be considered. Thus, the simulator must be modified to include some features in order to simulate these extended scenarios.

Frequency domain The limitation of aligning the interference just within three pairs has been reflected throughout the whole work. In fact, it is inherent to the manner how IA is exploited in the spatial dimension. To allow more transmitters to enter in the cooperation, it would be necessary to have more antennas at each node of the network. With this in mind, the application of the IA concept in the frequency domain can be very fruitful, since the frequency domain is more adaptable than the spatial domain.

Bibliography

[1] C. E. Shannon, "Communication in the presence of noise." *Proceedings of the Institute of Radio Engineers*, vol. 37, pp. 10–21, Jan. 1949.

[2] C. Suh, M. Ho, and D. Tse, "Downlink interference alignment," *IEEE Transactions on Communications*, vol. 59, no. 9, pp. 2616–2626, Sept. 2011.

[3] V. R. Cadambe and S. A. Jafar, "Interference Alignment and Spatial Degrees of Freedom for the K User Interference Channel," in *IEEE International Conference on Communications (ICC)*, May 2008, pp. 971–975.

[4] A. Goldsmith. Cambridge University Press, 2005.

[5] G. J. Foschini and M. J. Gans, "On limits of wireless communications when using multiple antennas," *Wireless Pers. Commun.*, vol. 6, no. 3, pp. 311–335, 1998.

[6] V. R. Cadambe and S. A. Jafar, "Interference Alignment and Degrees of Freedom of the K User Interference Channel," *IEEE Transactions on Information Theory*, vol. 54, no. 8, pp. 3425–3441, Aug 2008. [Online]. Available: http://ieeexplore.ieee.org/lpdocs/epic03/wrapper.htm?arnumber=4567443

[7] A. Ghasemi, A. S. Motahari, and A. K. Khandani, "Interference Alignment for the K User MIMO Interference Channel," *Arxiv preprint*, vol. abs/0909.4, p. 19, Sept. 2009. [Online]. Available: http://arxiv.org/abs/0909.4604

[8] M. Maddah-ali, A. S. Motahari, and A. K. Khandani, "Signaling over MIMO Multi-Base Systems: Combination of Multi-Access and Broadcast Schemes," in *IEEE International Symposium on Information Theory*, Jul. 2006, pp. 2104–2108. [Online]. Available: http://ieeexplore.ieee.org/lpdocs/epic03/wrapper.htm?arnumber=4036340

[9] T. Gou and S. A. Jafar, "Degrees of freedom of the K user $M \times N$ MIMO interference channel," *Arxiv preprint*, vol. abs/0809.0099, pp. 1–28, Aug. 2008. [Online]. Available: http://arxiv.org/abs/0809.0099

[10] S. W. Peters and R. W. Heath, "Interference Alignment via Alternating Minimization," in *Proc. IEEE International Conference on Acoustics, Speech and Signal Processing (ICASSP)*, Apr. 2009, pp. 2445–2448.

[11] K. Gomadam, V. Cadambe, and S. Jafar, "Approaching the capacity of wireless networks through distributed interference alignment," in *IEEE Global Telecommunications Conference (GLOBECOM)*, Dec. 2008, pp. 1–6.

[12] D. Schmidt, C. Shi, R. Berry, M. Honig, and W. Utschick, "Minimum mean squared error interference alignment," in *Signals, Systems and Computers, 2009 Conference Record of the Forty-Third Asilomar Conference on*, 2009, pp. 1106–1110.

[13] C. Shi, D. A. Schmidt, R. A. Berry, M. L. Honig, and W. Utschick, "Distributed interference pricing for the MIMO interference channel," in *Proceedings of the 2009 IEEE international conference on Communications*, ser. ICC'09. Piscataway, NJ, USA: IEEE Press, 2009, pp. 1796–1800. [Online]. Available: http://dl.acm.org/citation.cfm?id=1817271.1817605

[14] Z. Ho and D. Gesbert, "Balancing egoism and altruism on interference channel: The MIMO case," in *Communications (ICC), 2010 IEEE International Conference on*, 2010, pp. 1–5.

[15] H. Shen, B. Li, and Y. Luo, "Precoding design using interference alignment for the network mimo," in *Personal, Indoor and Mobile Radio Communications, 2009 IEEE 20th International Symposium on*, 2009, pp. 2519–2523.

[16] C. Suh and D. Tse, "Interference alignment for cellular networks," in *Communication, Control, and Computing, 2008 46th Annual Allerton Conference on*, 2008, pp. 1037–1044.

[17] J. Sun, Y. Liu, and G. Zhu, "On the degrees of freedom of the cellular network," in *IEEE International Conference on Communications (ICC)*, May 2010, pp. 1–5.

[18] S. Gollakota, S. D. Perli, and D. Katabi, "Interference alignment and cancellation," in *Proceedings of the ACM SIGCOMM 2009 conference on Data communication*, ser. SIGCOMM '09. New York, NY, USA: ACM, 2009, pp. 159–170. [Online]. Available: http://doi.acm.org/10.1145/1592568.1592588

[19] C. Yetis, T. Gou, S. Jafar, and A. Kayran, "Feasibility conditions for interference alignment," in *Proc. IEEE Global Telecommunications Conference (GLOBECOM)*, Dec. 2009, pp. 1–6.

[20] H. Shen, B. Li, M. Tao, and Y. Luo, "The New Interference Alignment Scheme for the MIMO Interference Channel," in *Proc. IEEE Wireless Communication and Networking Conference (WCNC)*. IEEE, Apr. 2010, pp. 1–6.

[21] S. W. Peters and R. W. Heath, "Cooperative algorithms for MIMO interference channels," *IEEE Transactions on Vehicular Technology*, vol. 60, no. 1, pp. 206–218, Jan. 2011.

[22] R. Brandt, H. Asplund, and M. Bengtsson, "Interference alignment in frequency; a measurement based performance analysis," in *Proc. International Conference on Systems, Signals and Image Processing (IWSSIP)*, Apr. 2012, pp. 227–230.

[23] D. Aziz, F. Boccardi, and A. Weber, "System-level performance study of interference alignment in cellular systems with base-station coordination," in *Proc. IEEE International Symposium on Personal Indoor and Mobile Radio Communications (PIMRC)*, Sept. 2012, pp. 1155–1160.

[24] Q. H. Spencer, A. L. Swindlehurst, and M. Haardt, "Zero-forcing methods for downlink spatial multiplexing in multiuser MIMO channels," *IEEE Transactions on Signal Processing*, vol. 52, pp. 461–471, Feb. 2004.

[25] I. F. Akyildiz, D. M. Gutierrez-Estevez, and E. C. Reyes, "The evolution to 4G cellular systems: LTE-Advanced," *Phys. Commun.*, vol. 3, no. 4, pp. 217–244, Dec. 2010. [Online]. Available: http://dx.doi.org/10.1016/j.phycom.2010.08.001

[26] H. Özcelik, N. Czink, and E. Bonek, "What makes a good MIMO channel model?" in *IEEE Vehicular Technology Conference (VTC)*, no. 61, Jun. 2005, pp. 156–160.

[27] TSG-RAN Working Group 4, "LTE channel models for concept evaluation in RAN1," 3GPP, Tech. Rep. R4-0.60101, Feb. 2007.

[28] B. N. Makouei, J. G. Andrews, and R. W. Heath, "MIMO Interference Alignment Over Correlated Channels With Imperfect CSI," *IEEE Transactions on Signal Processing*, vol. 59, no. 6, pp. 2783–2794, Jun. 2011.

[29] W. C. Jakes, *Microwave Mobile Communications*. New York: Wiley, 1974.

[30] R. Mungara, G. George, and A. Lozano, "System-level performance of distributed cooperation," in *Annual Conference on Signals, Systems and Computers (ASILOMAR)*, Nov. 2012, pp. 1561–1565.

[31] 3GPP, "Physical layer aspects for evolved universal terrestrial radio access (UTRA)," Third Generation Partnership Project, Tech. Rep. TR 25.814 V7.1.0, Sep. 2006.

[32] 3GPP, "Spatial channel model for MIMO simulations," 3GPP, Tech. Rep. TR 25.996 V6.1.0, Sep. 2003.

[33] G. Li, X. Zhang, X. Liu, and D. Yang, "Joint combiner and precoding in MU-MIMO downlink systems with limited feedback," in *Proc. IEEE Vehicular Technology Conf.*, Sept. 2011, pp. 1–4.

[34] R. Batista, T. Maciel, Y. Silva, and F. Cavalcanti, "Impact evaluation of imperfect CSI on the performance of downlink CoMP systems," in *Simpósio Brasileiro de Telecomunicações*, Brazil, Sept. 2011, pp. 1–5.

[35] T. Yoo, N. Jindal, and A. Goldsmith, "Finite-rate feedback mimo broadcast channels with a large number of users," in *IEEE International Symposium on Information Theory*, Jul. 2006, pp. 1214 –1218.

[36] J. Klotz and A. Sezgin, "Antenna selection criteria for interference alignment," in *IEEE 21st International Symposium on Personal Indoor and Mobile Radio Communications (PIMRC)*, Sep. 2010, pp. 527–531.

[37] D. Love and R. Heath, "Limited feedback unitary precoding for spatial multiplexing systems," *IEEE Transactions on Information Theory*, vol. 51, no. 8, pp. 2967–2976, Aug. 2005.

[38] C. Bandeira, D. Moreira, P. Normando, W. Freitas Jr., Y. Silva, and F. Cavalcanti, "Performance of joint antenna and user selection schemes for interference alignment in MIMO interference channels," in *Proc. IEEE Vehicular Technology Conf.*, Jun. 2013.